THE UNIVERSITY OF CALGARY

ARMA DECONVOLUTION

by

Derek F. Evoy

A THESIS

SUBMITTED TO THE FACULTY OF GRADUATE STUDIES

IN PARTIAL FULFILLMENT OF THE REQUIREMENTS FOR THE

DEGREE OF MASTER OF ENGINEERING

DEPARTMENT OF ELECTRICAL ENGINEERING

CALGARY, ALBERTA

APRIL, 1987

ISBN Ø-315-35949-8

THE UNIVERSITY OF CALGARY

2500 University Drive N.W., Calgary, Alberta, Canada T2N 1N4

Faculty of
GRADUATE STUDIES

Telephone (403) 220-5417

May 20, 1987

To Whom It May Concern:

Numerical values on the axes of certain graphs in the text are illegible. This is not a problem since it is comparison of the shapes of the graphs that is important, not the specific values.

Yours truly,

D.F. Evoy

DFE/hjb

THE UNIVERSITY OF CALGARY

FACULTY OF GRADUATE STUDIES

The undersigned certify that they have read, and recommend to the Faculty of Graduate Studies for acceptance, a thesis entitled, "ARMA Deconvolution" submitted by Derek F. Evoy in partial fulfillment of the requirements for the degree of Master of Engineering.

Dr. S. T. Nichols
(Supervisor & Chairman)
Electrical Engineering

Dr. L. P. Dennis
Seis-Pro Consultants Ltd.

Dr. R. B. Streets
Electrical Engineering

Dr. W. C. Chan
Electrical Engineering

DATE: 87-04-27

ABSTRACT

Theoretical motivation for the preferred representation of seismic data by ARMA (p,q) models is developed. Reverberations are shown to be AR (p) whereas absorptive earth filtering effects are shown to be MA (q).

Modelling techniques are applied to both real and synthetic seismic data. The resultant spectral fits to periodograms are contrasted, as are deconvolution results. ARMA (p,q) models are found to provide superior spectral fits compared with AR (p) models where the seismic spectrum rolls off into noise, but only marginally improved fits through high signal frequencies. The consequence is that ARMA (p,q) deconvolutions boost noise without significantly improving signal when compared with AR (p) techniques. At high orders all techniques except Levinson Transient Error ARMA (p,q) and Levinson AR (p) tend to introduce spikes to the spectrum. Levinson AR (p) remains the deconvolution of choice.

Oversampling is found to necessitate high model orders and result in overfitting to spectral roll off and noise. Improvements in estimation at lower model orders are achieved on decimated and decimated and demodulated data.

ACKNOWLEDGMENTS

Dr. S. T. Nichols provided guidance and ideas throughout the development of this work. Dr. M. J. E. Salami and other students of the Department of Electrical Engineering were generous with providing help and computer programs to effect the modelling.

Petro-Canada provided data and were understanding in allowing time to pursue this work.

Ms. Thelma Cameron typed the thesis and implemented changes with characteristic efficiency and remarkably good humour.

TABLE OF CONTENTS

LIST OF TABLES

LIST OF FIGURES

LIST OF SYMBOLS

A	area
A_i	amplitude of incident wave
A_r	amplitude of reflected wave
A_t	amplitude of transmitted wave
AR (p)	autoregressive (order p)
ARMA (p,q)	autoregressive moving average (order p,q)
a_k	set of AR (p) coefficients; estimated set of AR (p) coefficients
b_k	set of MA (q) coefficients; estimated set of MA (q) coefficients
c_k	modified MA (q) coefficients
d_k, $\tilde{d}_k$	displacement due to downgoing wave
$e(n)$	error (residual)
$e_N(n)$	transfer function of N layered earth
F	force
$g(n)$	inverse filter
$h(n)$	impulse response
K	modulus of elasticity
k_1, k_2	wave number
M_k, $\mathcal{M}_k$	communication matrix
MA (q)	moving average (order q)
MLSE	minimum least squares error
N	length of data sequence

n	sampled time
$n(t)$, $n(n)$	noise continuous, sampled
q_i	reflection coefficient position
$R_x(k)$	autocorrelation of x(n)
$R_x^+(k)$	causal autocorrelation of x(n)
$R_{xy}(k)$	cross correlation of x(n) and y(n)
$r(t)$, $r(n)$	reflection coefficient series continous, sampled
r_{12}, r_k	reflection coefficient
$S_x(k)$	power spectrum of x(n)
$S_x^+(k)$	causal power spectrum of x(n)
$S_x^-(k)$	anti-causal power spectrum of x(n)
SVD	singular value decomposition
$s(t)$, $s(n)$	seismic trace continuous, sampled
t_{12}, t_k	transmission coefficient
u	displacement from rest position
u_k, $\tilde{u}_k$	displacement due to upgoing wave
v	velocity of compressional wave propagation
$w(t)$, $w(n)$	seismic wavelet continuous, sampled
$X(f)$	Fourier transform of x(n)
$X(z)$	Z transform of x(n)
x	length
Δx	change in x
$x(t)$, $x(n)$	time series continuous, sampled
Z	impedance

$\delta(n)$	kronecker delta
$\varepsilon(n)$	white noise sequence
λ	number of reflection coefficients
ρ	variance of noise, density
$\sigma_x(n)$	variance of x(n)
*	convolution

Chapter 1. Introduction

The application of the techniques of time series analysis to the processing of seismic data revolutionized the petroleum exploration industry during the 1960's [1]. The consequent improvement in the resolution and reliability of the seismic method established it as the primary tool for hydrocarbon exploration. Very few exploratory wells are drilled now without prior seismic confirmation [2] and the geophysical (seismic) industry has grown to become a major user of computer power [3].

Perhaps the greatest contribution of time series analysis to the processing of seismic data is the theory of inverse filtering, or deconvolution, and the related field of wavelet estimation. The object of the seismic method is to provide unambiguous information on the position and relative hardness of reflectors in the subsurface by echo ranging. The distribution of reflector positions and relative hardnesses in the subsurface is described as the reflectivity sequence of the earth and it provides information on the geometry and composition of the various rock types in the subsurface. Unfortunately, the seismic data recorded in the field do not

depict the desired reflectivity sequence but rather are considered to be the convolution of the reflectivity sequence with a seismic "wavelet" which comprises the effects of source characteristics, earth filtering, reverberation, and the like [4]. Deconvolution uses an estimate of this wavelet to design an inverse filter which is convolved with the recorded seismic data to yield just the desired reflectivity response. The procedure greatly increases the resolution and interpretability of seismic data.

Because the seismic wavelet in effect filters the reflectivity response, and deconvolution undoes the effect of the wavelet filter, the theory and practise of deconvolution evolved in concert with the field of spectral analysis. Consequently deconvolution has traditionally been motivated from the point of view of maximizing spectral expansion, or whitening the spectrum. Modern methods of spectral estimation, however, suggest a more reasoned and satisfying approach to deconvolution.

In recent years a variety of parameter modelling techniques have been applied in the estimation of a power spectral density [5, 6]. These techniques represent the power spectral density of a stochastic time series in terms of the

magnitude squared of a characteristic rational function of polynomials. The coefficients of the polynomials are also the multipliers in a model recursive equation which describes the time series itself as a linear combination of the past values of the time series, and the past and present values of a hypothetical white noise excitation series. In other words, the techniques model a given time series as the response of a causal time invarient linear system - whose transfer function is a characteristic rational function of polynomials - to a white noise excitation. Consequently specification of the coefficients in estimating the power spectral density function provides an analytic characterization of the time series.

As mentioned earlier seismic data is considered to be the convolution of a reflectivity sequence and a seismic wavelet. If the reflectivity sequence can be considered to be random, or white, and the wavelet can be considered to be causal and time invariant then the seismic data can be modelled as the response of a white noise input to a filter whose impulse response is the wavelet. Estimation of the power spectral density of the seismic data by modelling techniques, therefore, explicitly specifies the seismic wavelet in analytic form and it is then straightforward to calculate the inverse wavelet (by interchanging poles and zeroes in the rational

polynomial description of the wavelet) for deconvolution. The techniques, therefore, give not only analytical descriptions of the inverse wavelets but also intuitively satisfying motivation for their application to deconvolution.

The most general of the rational function models is the auto-regressive-moving-average or ARMA (p,q) model with a p^{th} order denominator polynomial (the auto-regressive part) and a q^{th} order numerator polynomial (the moving-average part). The power spectral density functions of seismic wavelets are particularly well described by ARMA (p,q) models; the absorptive earth filtering effects are represented by the moving-average components in the numerator polynomial and the reverberations affecting wavelet shape are represented by the auto-regressive components in the denominator polynomial. Furthermore, although the roots of the auto-regressive, denominator polynomial (the poles of the wavelet) must lie inside the unit circle to ensure a stable inverse, the roots of the moving-average, numerator polynomial (the zeroes of the wavelet) may be reflected out of the unit circle in any combination to yield a finite number of possible phase possibilities other than minimum phase using all-pass networks. Traditional techniques are usually restricted by the assumption of minimum phase.

Despite the obvious advantages only a few deconvolution techniques employing rational function models have been recorded in the geophysical literature to date, other than Levinson, and those few have used auto-regressive, or AR (p), models rather than the more general and preferred ARMA (p,q) models. One reason for this apparent lack of enthusiasm is industry inertia fostered by the success of traditional methods. More serious reasons are that modelling techniques are sensitive to the specification of model type and model order, are computationally less efficient than traditional methods (particularly in the case of ARMA (p,q) models) and are more adversely affected by noise in the data. These disadvantages, however, must be considered in trade-off against the obvious merits of the application of ARMA (p,q) models.

In this thesis the application of ARMA (p,q) models to the deconvolution of seismic signals is considered. The related topic of estimating seismic wavelets is also discussed. Chapter 2 provides a brief overview of the seismic reflection method, reviews the development of the seismic time series model from wave theory, demonstrating the ARMA (p,q) nature of the seismic process, and establishes the importance of wavelet estimation and deconvolution in seismic data processing.

In Chapter 3 traditional wavelet estimation and deconvolution techniques are reviewed and a few of the AR (p) modelling techniques are described. The wavelet estimation techniques range from purely deterministic to purely statistical; the assumptions and strengths and weaknesses of each technique are discussed. Chapter 4 introduces linear modelling techniques and further develops the motivation for the preferred application of ARMA (p,q) models to the estimation of seismic wavelets and the deconvolution of seismic data. Several techniques for determining the parameters of ARMA (p,q) models from time series are then described; in particular the Box-Jenkins method [7], the Cadzow "high-performance" method, [8], the method of Gutowski, Robinson, and Trietel - the GRT method [9], and the recently developed method of Salami [10, 66]. The strengths and weaknesses of each method are examined. Chapter 5 presents the results of ARMA (p,q) modelling in seismic wavelet estimation and deconvolution. Chapter 6 provides conclusions.

Chapter 2. The Reflection Seismic Method

2.1. Introduction

The reflection seismic method consists of recording the earth response to a controlled disturbance as a function of time. Both the disturbance and the response recording transducers are located at, or very near, the earth's surface and the transit times (from initiation of disturbance) and amplitudes of the responses provide information on the relative hardness and position of reflectors in the subsurface. The reflectors correspond to the interfaces between differing rock types in the subsurface. Where the seismic reflection method differs from the seemingly analogous techniques of sonar and radar echo ranging is in the complicated nature of the target and the target response. Subsurface reflectors do not completely reflect the imposed disturbances and consequently the recorded response comprises a complex superposition of reflected and multiply transmitted and re-reflected signals. The purpose of seismic data processing is to enhance the primary reflection information in the recorded signal such that reflection transit times and amplitudes can be measured unambiguously, and diminish the contribution of reverberatory effects and other forms of noise.

2.2 Data Acquisition

Seismic reflection data is obtained by initiating a controlled source of pressure (seismic) waves at, or near, the earth's surface and recording the earth response with respect to time at transducers positioned on the earth's surface. The standard source of pressure waves is dynamite exploded in a 10 - 100 foot deep hole; dropped weights and vibrators at the surface can also be used but are less common. The transducers, or geophones, consist of a magnet suspended in a coil. The housing of the magnet and coil is buried or otherwise affixed to the earth with a long spike. When the earth responds to the reflected pressure waves the resultant displacement of the housing causes the magnet to move within the coil and induces a voltage which is proportional to the velocity of the earth's motion. This output voltage is amplified, sampled, and recorded time sequentially on tape.

For a variety of reasons a technique known as "CDP" shooting is now standard for seismic reflection data acquisition. The CDP method repeatedly samples the same reflector location by in effect taking a series of recordings with the shots and geophones in a variety of positions symmetric about the

reflector location along a straight line. This is accomplished by laying out many geophones along the straight line of survey, shooting and recording, then moving the shot location and the geophones an incremental distance along the line of survey and repeating the procedure. Because the method results in the repeated sampling of the same reflector locations, called common depth points, the technique is known as the CDP method. Figure 2.1 illustrates the CDP method of seismic reflection data acquisition.

The obvious advantage of the CDP method is that the records of shot-trace pairs which sample the same common depth point can be summed to increase signal to noise ratio where the noise is random and uncorrelated between records. A second advantage is that the time delay between records for the same CDP, due to the increased travel time between the further offset shot and receiver pairs, can be related to the average velocity of seismic wave propagation down to the subject CDP and back.

2.3 Reflection Theory

In most areas with hydrocarbon potential the subsurface of the earth is composed of large sub-parallel sheets of

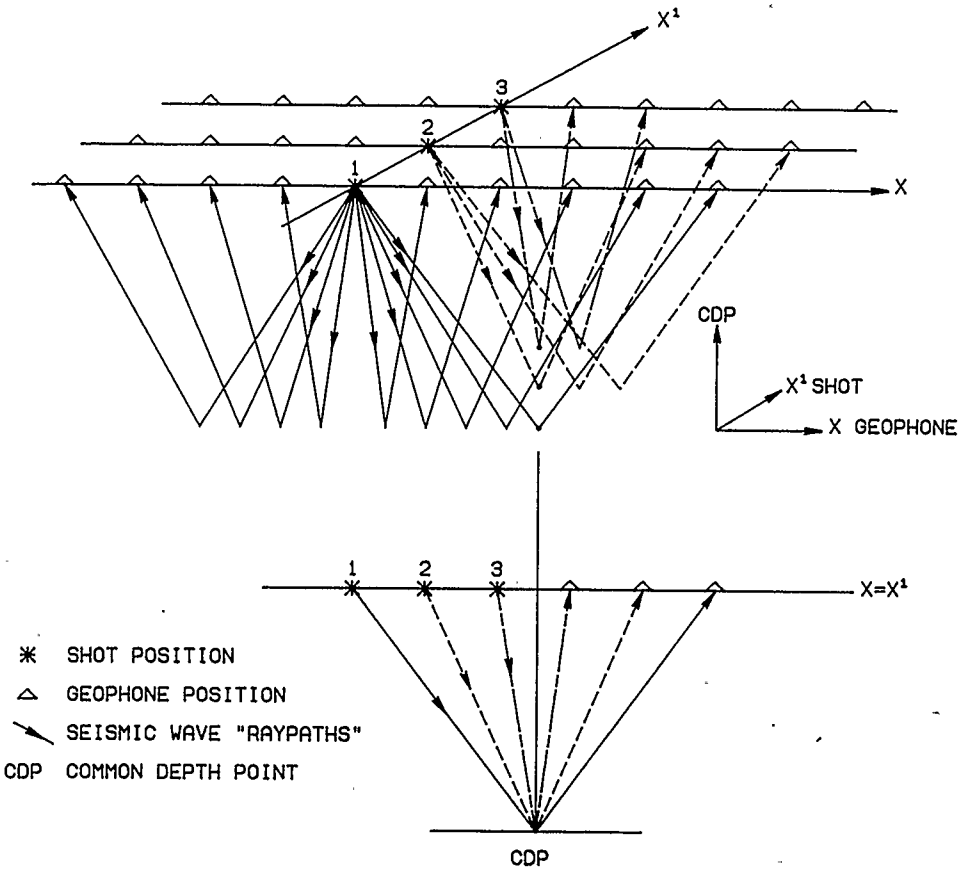

Figure 2.1 GEOMETRY OF CDP SEISMIC DATA AQUISITION. SHOTS AND GEOPHONES ARE POSITIONED ALONG THE SAME LINE OF PROFILE ($X=X^1$). SEPARATION IS DEPICTED FOR CLARITY IN UPPER DIAGRAM.

different sedimentary rock types. The velocity of seismic waves is generally different in each different rock type and consequently waves incident on the boundary between different rock types will be partially reflected and partially transmitted in accordance with the results of elastic wave theory.

There are two types of distortion which can be described for a given block of material: volumetric strain caused by compressive stress and rotational strain caused by shear stress. Conventional seismic acquisition techniques discriminate against shear stress waves and hence only compressive stress waves are of interest.

2.3.1 Elastic Wave Theory

Hooke's law for perfectly elastic material states that the strain a material undergoes is proportional to the stresses applied to the material. Considering, without loss of generality, one dimensional strain in x, the strain is the fractional change in x or $\Delta x/x$; the stress is defined as the applied force per unit area, F/A so

$$K \frac{\Delta x}{x} = \frac{F}{A}$$

where the constant of proportionality, K, is the modulus of elasticity. It turns out that the velocity of compressional wave propagation is related to K; in the one dimensional case for example

$$v = \frac{K}{\rho}$$

where ρ is the density of the material.

Continuing with the one dimensional case undergoing strain, let Δx be the portion of material under consideration and Δu be the incremental quantity of the material compression or dilation resulting from the force F; the strain is therefore $\Delta u/\Delta x$. The mass of material under consideration is $\rho A \Delta x$ where A is a unit area of cross section given to the one dimensional material. Newton's second law of motion requires that force equals mass times acceleration or F = ma. Denoting displacement from rest position as u, acceleration is given by $\partial^2 u/\partial^2 t$ so the applied force is

$$F = \rho A \Delta x \frac{\partial^2 u}{\partial^2 u}$$

The elastic force of the material itself is given by Hooke's law at position x

$$F = KA \frac{\Delta u}{\Delta x}; \text{ or } \quad F = KA \frac{\partial u}{\partial x}$$

in the limit as $\Delta x \to o$.

At x + dx an incremented elastic force F + dF is exercised.

$$F + dF = F + \frac{\partial F}{\partial x} dx = KA \frac{\partial u}{\partial x} + KA \frac{\partial^2 u}{\partial x^2} dx$$

The elastic force acting on the material element dx is therefore the difference of the forces exercised at x and x + dx or

$$F = KA \frac{\partial^2 u}{\partial x^2} dx$$

Equating the two forces

$$\rho \frac{\partial^2 u}{\partial t^2} = K \frac{\partial^2 u}{\partial x^2} \quad \text{or} \quad \frac{\partial^2 u}{\partial x^2} = \frac{1}{v^2} \frac{\partial^2 u}{\partial t^2}$$

which is the familiar one dimensional wave equation where v is the velocity of wave propagation and

$$v = \frac{K}{\rho}$$

as noted earlier.

D'Alembert's solution to the wave equation is

$$u(x,t) = F(x-vt) + G(x+vt)$$

which describes waves of fixed shape travelling in opposite directions; that is, one toward and one away from the source of disturbance. Considering only the wave travelling outward from the source

$$u(x,t) = F(x-vt)$$

and assuming, again without loss of generality, a monotonic wave of the form

$$u(x,t) = A_i \exp(j2\pi(k_1 x - wt))$$

impinging on a boundary between two materials (1 and 2) at perpendicular incidence, part of the wave energy will be reflected

$$A_r \exp(j2\pi(-k_1 x - wt))$$

and part will be transmitted.

$$A_t \exp(j2\pi(k_2 x - wt))$$

Under the restrictions that displacement must be continuous across the boundary and that the net stress on the boundary is zero it follows that

$$A_r + A_t = A_i$$

and

$$\rho_1 v_1 A_r - \rho_2 v_2 A_t = - \rho_1 v_1 A_i$$

respectively, so that

$$r_{12} = \frac{A_r}{A_i} = \frac{\rho_2 v_2 - \rho_1 v_1}{\rho_2 v_2 + \rho_1 v_1}$$

which is the definition of the reflection coefficient r_{12} where the subscript 1 pertains to properties of material 1 and subscript 2 pertains to properties of material 2.

Similarly the transmission coefficient t_{12} can be defined as

$$t_{12} = \frac{A_t}{A_i} = \frac{2\rho_1 v_1}{\rho_2 v_2 + \rho_1 v_1}$$

The above derivations yield reflection and transmission coefficients for particle displacement. It can be shown that the same coefficient definitions result for particle velocity and particle acceleration [11].

Certain useful relationships between coefficients will be exploited in subsequent development and so are explicitly stated here as follows:

$$r_{12} = -r_{21}$$

$$t_{12} = 1 + r_{12} \; ; \; t_{21} = 1 + r_{21} = 1 - r_{12} \qquad 2.1$$

$$t_{12}t_{21} = 1 - r_{12}^2 \; ; \; t_{12}t_{21} - r_{12}r_{21} = 1$$

Obviously the reflection and transmission coefficients can be generalized to waves impinging on the boundary between any two materials k and k + 1. For notational convenience only the alpha subscript is written and a prime is used to indicate an upgoing wave at the boundary of k + 1 and k, as:

$$r_k = r_{k,k+1} \; ; \; r'_k = r_{k+1,k}$$

$$t_k = t_{k,k+1} \; ; \; t'_k = t_{k+1,k}$$

More complete and comprehensive discussions of wave theory abound in the literature [2, 12 - 15] but the simplistic one dimensional case provides sufficient conceptual background for this report.

2.3.2 The Convolutional Model

Seismic wave propagation is well described by classical wave theory. Diffractions, scattering phenomena, and "wavefront healing" can all be modelled using classical theory. But even under very restrictive conditions numerical calculations

of the differential and integral equations arising from the general expressions for spherical wave propagation in inhomogeneous media are very involved and solution of the inverse problem, that of determining earth properties from the output recorded reflection data, is computationally infeasible.

An alternative description of seismic reflection was developed in the 1950's and formalized through the 1960's employing then recently developed statistical communication theory [4, 16 - 19]. Under the restriction of normal incidence D'Alembert's solution provides that each interface transmits a scaled replica of the impinging waveform and reflects the complementary scaled replica of the waveform. Since the recording transducers are at the surface, only ultimately reflected signals are recorded. Furthermore the depth relationships of the interfaces can be mapped into time relationships using velocity information and the interfaces can therefore be represented as a time series of reflection coefficients. Consequently seismic reflection data can be represented as the superposition of identically shaped waveforms scaled and spaced in accordance with the amplitude and separation of reflection coefficients on a time axis. Equivalently, seismic reflection data can be represented as the convolution of a constant waveform with a time series of reflection coefficients.

Two serious assumptions are evoked in this description: firstly that the recorded seismic data is normal incidence, secondly that the seismic waveform is time invariant. A third assumption not resulting directly from the model formulation but important in computational work is that noise in the system is uncorrelated and additive. With these assumptions the model can be written as

$$s(t) = w(t) * r(t) + n(t) \qquad 2.2$$

where s(t) denotes the recorded seismic trace, w(t) the seismic wavelet, r(t) the reflection coefficient series, and n(t) the noise. The asterisk denotes the convolution operator. Since all subsequent development will assume sampled data a standardized notation using integer valued n as the discrete time index will be employed such that 2.2 can be written as

$$s(n) = w(n) * \grave{r}(n) + n(n) \qquad 2.3$$

Ironically, Norman Ricker developed a deterministic wave theory description of seismic data in the early 1940's which invoked reflection coefficients and wavelets but which fell just short of explicitly stating the convolutional model and therefore missed the all-important next step - deconvolution. Ricker's work will be discussed in Chapter 4.

The convolutional model, expressed in the filter theory notation of equation 2.3, immediately suggests deconvolution; inverse filtering out the wavelet to yield unadulterated reflection coefficient information. That is, designing a filter g(n) such that

$$g(n) * w(n) = \delta(n)$$

where the kronecker delta

$$\delta(n) = \begin{cases} 1 & n=0 \\ 0 & n\neq 0 \end{cases}$$

Convolving s(n) with the inverse filter g(n) gives

$$\begin{aligned} s(n) * g(n) &= [w(n) * r(n) + n(n)] * g(n) \\ &= w(n) * g(n) * r(n) + n(n) * g(n) \\ &= r(n) + n'(n) \end{aligned}$$

A variety of techniques for estimating g(n) and performing deconvolution are described in Chapter 3. It should be noted that deconvolution and wavelet estimation are essentially different specifications of the same basic problem and as such the various techniques of deconvolution and wavelet estimation have evolved hand in hand [20].

In the next section it will be shown that the convolutional model is complicated by reverberations in a layered system.

2.3.3 Wave Propagation in Layered Media

As waves travel outward from the source and encounter each of the interfaces between differing layers of material, part of the wave is reflected and part is transmitted. The reflected waves travel back toward the surface and are themselves reflected in part and transmitted in part by each of the interfaces encountered on their path until they are eventually recorded at the earth's surface. Energy which transmits directly to an interface and reflects directly back is termed primary reflection energy. Energy which reflects from more than one interface is termed multiple reflection energy.

The complex process of primary and multiple reflection in a layered system is particularly well described in terms of communication theory [1, 11, 21, 22]. Displacement at any interface can be described by a z-transform of the waves impinging on that interface [21] and, under certain plausible assumptions, the "earth transfer function" can be expressed as a rational function of polynomials in a complex variable,

where the numerator polynomial represents the transfer function for primary reflections and the denominator polynomial represents the transfer function for multiple reflections [36, 1]. This important result forms the basis for the ARMA (p,q) description of seismic data advocated in Chapter 4.

Following Treitel and Robinson [21] assume a horizontally stratified elastic earth subject to plane harmonic compressional motion at normal incidence. Let each layer be homogeneous and isotropic with material of velocity v_k and density ρ_k comprising the kth layer so that the reflection and transmission coefficients at the interface of the kth and k + 1 layers are r_k and t_k respectively.

Further, let the travel time through each layer be constant such that, for convenience, the one-way vertical travel time through any given layer is one unit of time. The model can be generalized to layers of varying travel time by assigning identical velocities and densities to contiguous layers as required.

Letting $d_{k,k+2m-1}$ denote the displacement at the top of the kth layer due to downgoing waves at time k + 2m - 1, and introducing z^{-1} as a unit delay operator, the displacement at the top of the kth layer can be described by a z-transform summing the appropriate displacements for all time, that is:

$$D_k(z) = \sum_{m=o}^{\infty} d_{k,k+2m-1} \; z^{-(k+2m-1)}$$

Similarly the displacement at the bottom of the kth layer can be described by the z-transform:

$$\tilde{D}_k(z) = \sum_{m=o}^{\infty} \tilde{d}_{k,k+2m} \; z^{-(k+2m)}$$

where $\tilde{D}_k(z)$ is related to $D_k(z)$ by a unit delay and a z-transform characteristic of the layer $A_k(z)$, so

$$\tilde{D}_k(z) = z^{-1} A_k(z) D_k(z)$$

In the absorption free case $A(z) = 1$ so that

$$\tilde{D}_k(z) = z^{-1} D_k(z) \qquad 2.4$$

The displacements resulting from upgoing waves can be similarly described. For upgoing waves at the top of layer k the z-transform description of resulting displacement is

$$U_k(z) = \sum_{m=o}^{\infty} u_{k,k+2m+1} \; z^{-(k+2m+1)}$$

For upgoing waves at the bottom of layer k the z-transform is

$$\tilde{U}_k(z) = \sum_{m=o}^{\infty} u_{k,k+2m+1} \, z^{-k+2m}$$

and, assuming no absorption,

$$U_k(z) = z^{-1} \tilde{U}_k(z) \qquad 2.5$$

Figure 2.2 illustrates the waves d_k, $\tilde{d}_k$, u_k and $\tilde{u}_k$ in the layered system. Figure 2.3 depicts the relationship of all four waves at the k, k + 1 interface at time j.

Recognizing from Figure 2.3 that each wave is a composite of reflected and transmitted waves and recalling the relationships between reflection and transmission coefficients described in equations 2.1, the interaction at the k, k + 1 interface at time j can be described by the two equations,

$$\tilde{t}_k d_{k,j} = d_{k+1,j} + r_k u_{k+1,j}$$

$$\tilde{t}_k u_{k,j} = r_k d_{k+1,j} + u_{k+1,j} \qquad 2.6$$

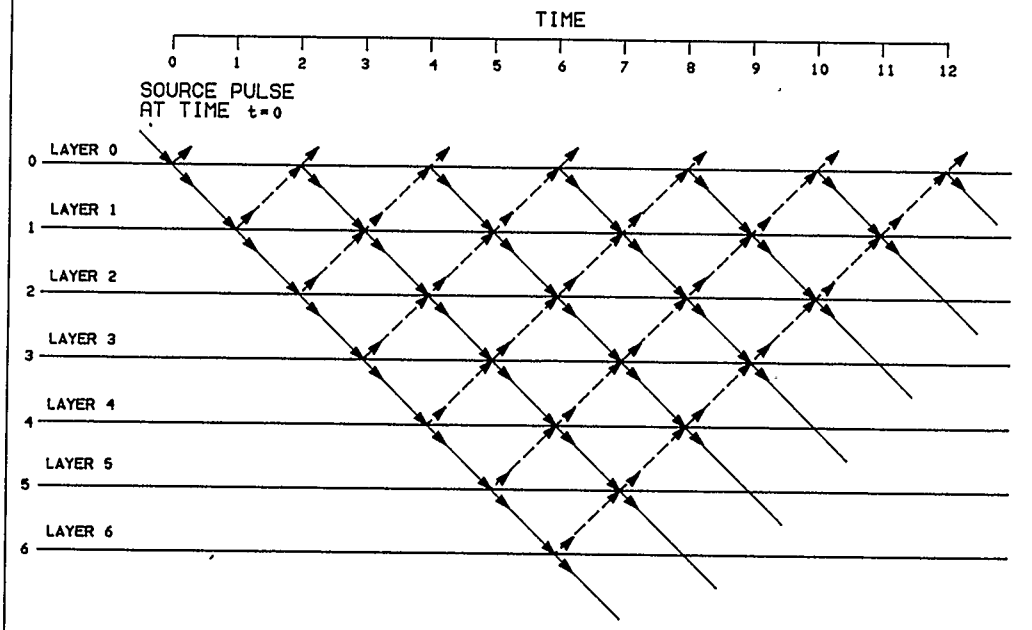

Figure 2.2 WAVE PROPAGATION IN N LAYER SYSTEM

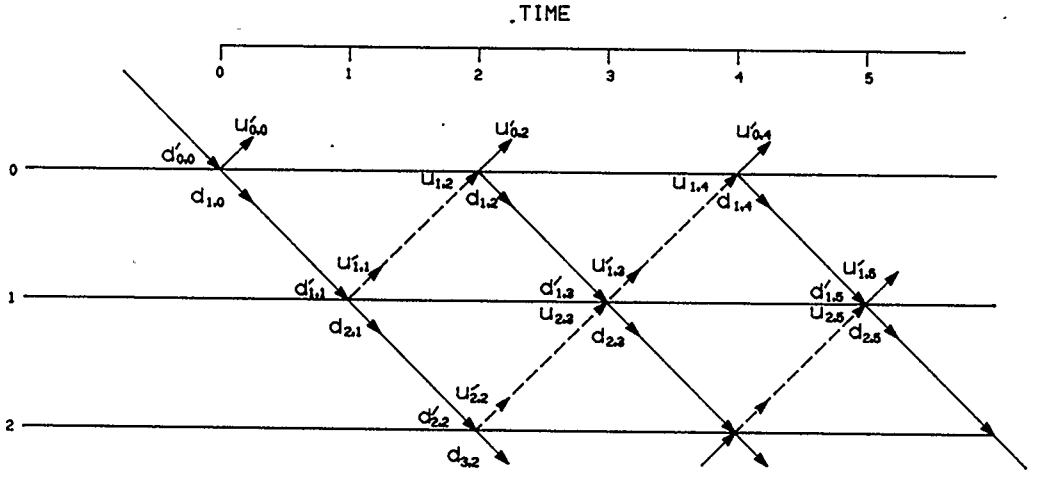

Figure 2.3 DISPLACEMENT RELATIONSHIPS DUE TO UPGOING AND DOWNGOING WAVES

Incorporating delays and summing over time index $j = k+2m$, $m = 0,1,2,\ldots$, equations 2.6 can be reformulated in terms of the z-transforms noted earlier, as

$$\tilde{t}_k D_k(z) = D_{k+1}(z) + r_k U_{k+1}(z)$$

$$\tilde{t}_k U_k(z) = r_k D_{k+1}(z) + U_{k+1}(z) \qquad 2.7$$

Assuming no absorption, so that the transforms for the tops and bottoms of the layers are related by a unit time delay, as described in equations 2.4 and 2.5, equations 2.7 become

$$t_k D_k(z) = z D_{k+1}(z) + r_k z^{-1} U_{k+1}(z)$$

$$t_k U_k(z) = r_k z D_{k+1}(z) + z^{-1} U_{k+1}(z)$$

These may be rewritten in matrix notation as

$$\begin{bmatrix} D_k(z) \\ U_k(z) \end{bmatrix} = M_k \begin{bmatrix} D_{k+1}(z) \\ U_{k+1}(z) \end{bmatrix} \qquad 2.8$$

where M_k is a matrix described by

$$M_k = \frac{1}{t_k} \begin{bmatrix} z & r_k z^{-1} \\ r_k z & z^{-1} \end{bmatrix} \qquad 2.9$$

M_k is termed the "communication matrix" [21, 22] or "scattering matrix" [11].

The communication matrix M_k is defined for k = 1,2,3.... At the interface between 0 and 1 there are no delayed waves in the composite so the communication matrix M_o becomes

$$M_o = \frac{1}{t_o} \begin{bmatrix} 1 & r_o \\ r_o & 1 \end{bmatrix}$$

By successive substitution the communication matrix yields a chain matrix description of wave propagation through the layered system so that

$$\begin{bmatrix} D_o(z) \\ U_o(z) \end{bmatrix} = M_o M_1 M_2 \cdots M_n \begin{bmatrix} D_{n+1}(z) \\ U_{n+1}(z) \end{bmatrix} \qquad 2.10$$

For a system of N + 1 layers, with layer N + 1 an infinite half space, there will be no upgoing energy impinging on interface N, therefore, $U_{N+1}(z) = 0$; furthermore

$D_o(z)$ is generally assumed to be a unit spike, consequently equations 2.10 can be rewritten [22] as

$$\begin{bmatrix} 1 \\ U_o(z) \end{bmatrix} = M_o M_1 M_2 \ldots . M_N \begin{bmatrix} D_{N+1}(z) \\ 0 \end{bmatrix} \qquad 2.11$$

Silvia and Robinson [1] recognize that the seismic method records upward travelling energy at the top of the first layer, that is $U_1(z)$. In order to take advantage of the assumptions employed in equation 2.11 they also reformulate the communication matrix equation 2.8 in the form

$$\begin{bmatrix} U_{k+1}(z) \\ D_{k+1}(z) \end{bmatrix} = M_k \begin{bmatrix} U_k(z) \\ D_k(z) \end{bmatrix}$$

where

$$M_k = \frac{z}{t'_k} \begin{bmatrix} 1 & r'_k z^{-2} \\ r'_k & z^{-2} \end{bmatrix} \qquad 2.12$$

Comparing M_k in 2.12 with M_k in 2.9 only the "directions" of the coefficients have changed, which is as expected.

Employing M_k in a chain matrix equation for $U_1(z)$ under the assumptions $U_{N+1}(z) = 0$, $D_1(z) = 1 + r'_o U_1(z)$ yields

$$\begin{bmatrix} 0 \\ D_{N+1}(z) \end{bmatrix} = M_N M_{N-1} \cdots M_1 \begin{bmatrix} U_1(z) \\ 1+r'_o U_1(z) \end{bmatrix}$$

Separating out the multipliers and defining the product terms of the chain matrices as follows:

$$\frac{z^n M_n M_{n-1} \cdots M_1}{(t'_1 t'_2 \cdots t'_N)^{-1}} = \begin{bmatrix} m_{11}^N(z) & m_{12}^N(z) \\ m_{21}^N(z) & m_{22}^N(z) \end{bmatrix} = \begin{bmatrix} m_{11}^N(z) & z^{-2N} m_{21}^N(z^{-1}) \\ m_{21}^N(z) & z^{-2N} m_{11}^N(z^{-1}) \end{bmatrix} \quad 2.14$$

the following equation can be extracted from 2.13

$$0 = \frac{z^N}{t'_1 t'_2 \cdots t'_N} \left[m_{11}^N(z) U_1(z) + z^{-2N} m_{21}^N(z^{-1})(1+r'_o U_1(z)) \right]$$

or

$$U_1(z) = \frac{-z^{-2N} m_{21}^N(z^{-1})}{m_{11}^N(z) - r_o z^{-2N} m_{21}^N(z^{-1})}$$

Since $U_1(z)$ is the z-transform of the response at the geophones of the N layered system excited by a unit impulse, it follows that the transfer function of the N layered earth is $E_N(z) = U_1(z)$ [1]. This result provides the earth

response in the convolutional model which relates the seismic wavelet $w(n) \leftrightarrow W(z)$ to the seismic trace $s(n) \leftrightarrow S(z)$ so that

$$s(n) = w(n) * e_N(n)$$

$$S(z) = W(z) \cdot E_N(z) \qquad 2.15$$

The double arrow $\leftrightarrow$ denotes transform equivalence.

Provided the N layered earth model is a bounded time-invariant system, its transfer function can be expressed as a rational function of polynomials in a complex variable [1]. That is

$$E_N(z) = \frac{B_N(z)}{A_N(z)} = \frac{\sum_{n=1}^{N} b_n z^{-n}}{\sum_{n=0}^{N} a_n z^{-n}} \qquad 2.16$$

where

$$B_N(z) = -z^{-2N}\, m_{21}^{N}(z)$$

$$A_N(z) = m_{11}^{N}(z) - r_o z^{-2N} m_{21}^{N}(z^{-1})$$

Recursion formulae can be written for the product terms by substitution of 2.12 in equations 2.14 [1] yielding

$$m_{11}^{n}(z) = m_{11}^{n-1}(z) - r_n z^{-2} m_{21}^{n-1}(z)$$

$$m_{21}^{n}(z) = r_n m_{11}^{n-1}(z) + z^{-2} m_{21}^{n-1}(z) \qquad n = 2,3,\ldots N$$

Using the recursion formulae under the assumption of small reflection coefficients, $A_N(Z)$ can be expressed as

$$A_N(z) = \sum_{n=o}^{N} a_n z^{-n} \simeq 1 + \phi_1^N z^{-1} + \phi_2^N z^{-2} + \ldots + \phi_N^N z^{-N}$$

where

$$\phi_m^N = \sum_{n=o}^{N} r_n r_{n+m} \; ; \; m \geq 1, \; N \geq 1$$

Similarly, $B_N(z)$ can be expressed as

$$B_N(z) = \sum_{n=1}^{N} b_n z^{-n} \simeq r_1 z^{-1} + r_2 z^{-2} + \ldots + r_N z^{-N}$$

$B_N(z)$ is recognized as the z-transform of the reflection coefficient series of the earth, r(n), corresponding to the generating function for primary reflections. $A_N(z)$ is therefore the z-transform of the reverberation series which is the generating function for all multiple energy in the N layered system.

Recognition of $B_N(z)$ as the z-transform of the reflection coefficient series highlights a disrepancy between the convolutional models of equations 2.3 and 2.15 rewritten here as

$$s(n) = w(n) * r(n) \qquad 2.3$$

and

$$s(n) = w(n) * e_N(n) \qquad 2.15$$

respectively.

Taking z-transforms and substituting $r(n) \leftrightarrow R(z)$ for $b_N(n) \leftrightarrow B_N(z)$ in equation 2.16, yields

$$S(z) = W(z)R(z) \qquad 2.17$$

$$S(z) = W(z) \frac{R(z)}{A_N(z)}$$

Obviously, $A_N(z) \neq 1$ except in an idealized non-reverberatory system since for the layered system described above $A_N(z)$ is the z-transform of the entire multiple reflection sequence.

Consequently, the wavelets $w(n) \leftrightarrow W(z)$ in equation 2.17 must differ such that

$$S(z) = W(z)R(z) \qquad 2.18$$

$$S(z) = W'(z) \frac{R(z)}{A_N(z)}$$

where

$$W(z) = \frac{W'(z)}{A_N(z)} \qquad 2.19$$

Equation 2.19 requires that the wavelet employed in the convolutional model of seismic data must incorporate all multiple reflection information if deconvolution is to recover the true reflection coefficient series. This result is not widely recognized in the geophysical literature although it was stated by Robinson as early as 1954 [16, 1]. Industry

practice generally fails to distinguish between wavelets W(z) and W'(z) in equations 2.18 [23] and therefore allows implicit bastardization of the "true" reflection coefficient such that

$$R(z) = \frac{R'(z)}{A_N(z)}$$

where R'(z) ⇔ r'(n) represents the true reflection coefficient series and R(z), in the industry accepted convolutional model, incorporates all multiple reflected energy. Under the industry model, then, deconvolution cannot yield the true reflection coefficient series; instead deconvolution is applied only as "wave shaping" to inverse filter out the smearing affect of the seismic wavelet. Other techniques are deployed to rid the "deconvolved" data of multiple reflections. Deconvolution and the rational model description of seismic data will be explored further in Chapters 3 and 4 respectively.

2.4 Data Processing

The CDP method of seismic acquisition described earlier yields multichannel data records with each trace containing reflection information from a different point in the subsurface. Adjacent records overlap in subsurface sampling and the degree of overlap, the number of times each subsurface point is included in different records, is called the multiplicity or "fold". To achieve the desired output for interpretation, the appropriate channels from different records which include information from the same subsurface point must be collected ("gathered"), corrected by time shifts to equate to normal incidence, and summed ("stacked"). Much of seismic data processing, therefore, is concerned with multichannel techniques employed to compensate for the geometry of acquisition.

More pertinent to this report are the single channel techniques of scaling, filtering, and deconvolution applied in seismic processing.

Scaling compensates for such effects as spherical divergence and absorptive energy loss. The principal purpose of scaling is to make the information on the seismic trace, which otherwise decays rapidly with time, more visible to the seismic

interpreter. Scaling is typically accomplished by application of data adaptive multipliers, which normalize energy within a given window to some preset value, or by analytic time variant multipliers which boost each data sample by some function of its time sample value.

Arguments persist regarding the validity of scaling to pre-process data for input to subsequent processes. Relevant to deconvolution are concerns that scaling destroys the supposed minimum phase character of seismic data but that not scaling leaves the data time variant.

Filtering is applied to reduce unwanted noise on seismic data. Since there is seldom a discrete frequency cut-off separating signal and noise, filter selection requires interpretive judgment of the trade-off between tolerable signal to noise levels and desired temporal resolution. Filtering is seldom applied prior to deconvolution but again arguments can be made both for and against pre-filtering. Clearly deconvolutions should be designed on signal rather than noise, but the previously mentioned trade-off against resolution still applies.

Deconvolution is applied to seismic data to inverse filter out the effects of "earth filtering" and yield unambiguous

temporally distinct reflection coefficients comprising the reflectivity series of the subsurface. The rationale for deconvolution was described earlier in discussion of the convolutional model. Notwithstanding all of the weaknesses inherent in the convolutional model, deconvolution remains a cornerstone of seismic processing and results in improved higher resolution seismic data almost without exception.

Overviews of seismic processing theory and practise are widely available [11, 12, 22, 63, 64]. The literature pertinent to deconvolution is more fully referenced in Chapter 3.

2.5 Reflection Identification

For seismic to be useful as an exploration tool it is necessary to have some means of equating the appropriate reflections to specific geological interfaces of economic interest. Geologists ascertain rock units of supposed hydrocarbon potential from well information and geophysicists then attempt to identify the reflections which correspond to the selected rock units and correlate these reflections along the lines of survey in order to map the distribution of the units between points of well control. To effect accurate identification synthetic seismograms are generated from well data and matched to nearby seismic data. Synthetic seismograms are created by determining the reflection coefficient series from sonic and density logs and convolving the derived reflection coefficient series with a wavelet which approximates the seismic wavelet.

Sonic and density logs are records of the rock velocities and densities measured down the well bore with special tools. The tools are lowered to the bottom of the well bore and then slowly brought up to the surface taking continuous measurements of the adjacent rock properties during the ascent. The resultant "log" is the record of the measured rock properties as a function of depth. A sonic log, for example, records

the variation in the velocity of the adjacent rock with depth, yielding a graph of velocity versus depth (see Figure 2.4). Given a relationship between velocity and depth at the well it is straightforward to calculate a relationship between time and depth which can then be used to relate rock units at a given depth with seismic reflections at their corresponding times.

Unfortunately the interference of reflections spaced closer in time than the seismic wavelet breadth and the shape of the wavelet conspire to make simple time-depth identification extremely difficult. Furthermore for practical reasons the sonic logs cannot be recorded during the last 100 metres or so of the ascent to the surface and consequently a bulk time shift to account for the velocity of the near surface must be assumed making the time-depth correspondence from surface unreliable.

To overcome these problems in identification synthetic seismograms are generated. The sonic and density logs from a well are sampled and reflection coefficients are calculated with respect to depth as:

$$r_i = \frac{\rho_{i+1}v_{i+1} - \rho_i v_i}{\rho_{i+1}v_{i+1} + \rho_i v_i} \qquad i = 0,1,2, \ldots N-1 \qquad 2.20$$

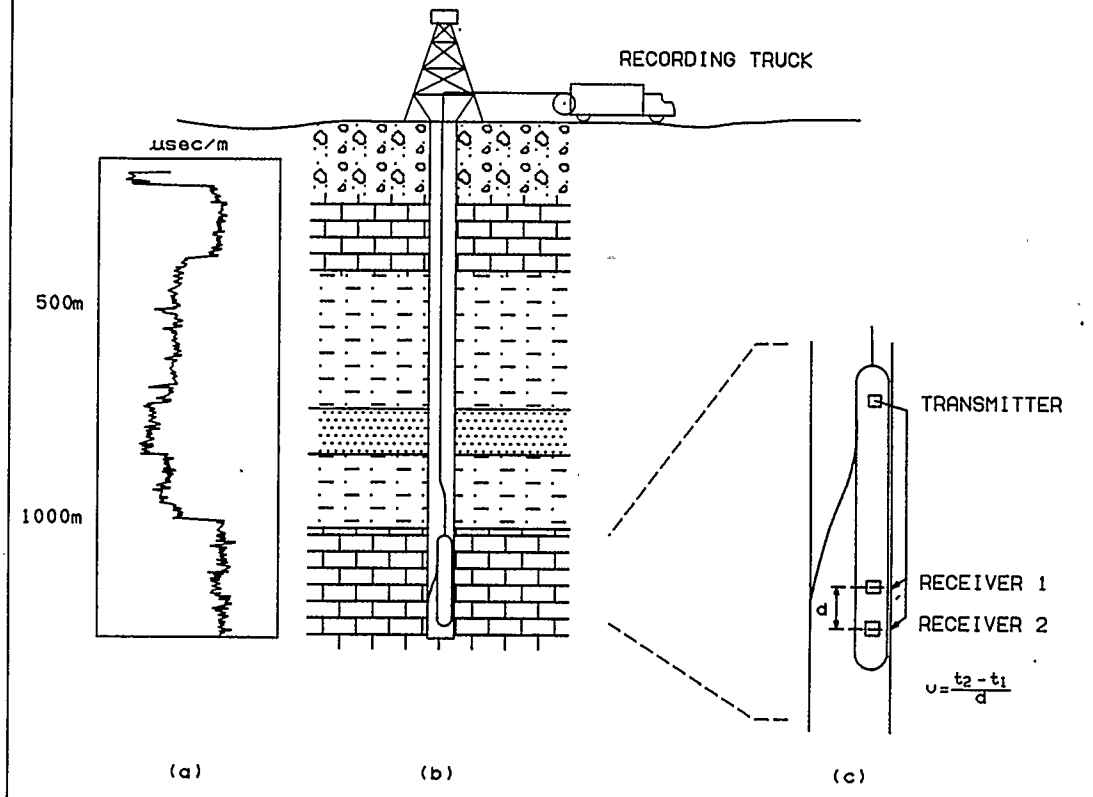

Figure 2.4 SONIC LOGGING: (a) SONIC LOG , (b) WELL LOGGING PROCEDURE , (c) SONIC LOGGING SONDE. SONIC LOGGING YIELDS A NEARLY CONTINUOUS VELOCITY SURVEY BY RECORDING THE DIFFERENCE IN TRAVELTIMES OF A TRANSMITTER PULSE MEASURED AT RECEIVERS 1 AND 2. (t_1 AND t_2).

where N depth samples are assumed. Then using the time-depth relationship derived from the velocity log velocity-depth plot, r_i is mapped into r(n) which is the discrete reflection coefficient series with respect to time.

Convolution of r(n) with an estimated wavelet w(n) yields an approximation to the seismic trace which is called a synthetic seismogram (illustrated in Figure 2.5). By matching similar patterns of reflections on the synthetic and true seismic traces, and relating these back to the well data, very accurate identification of reflections can be achieved.

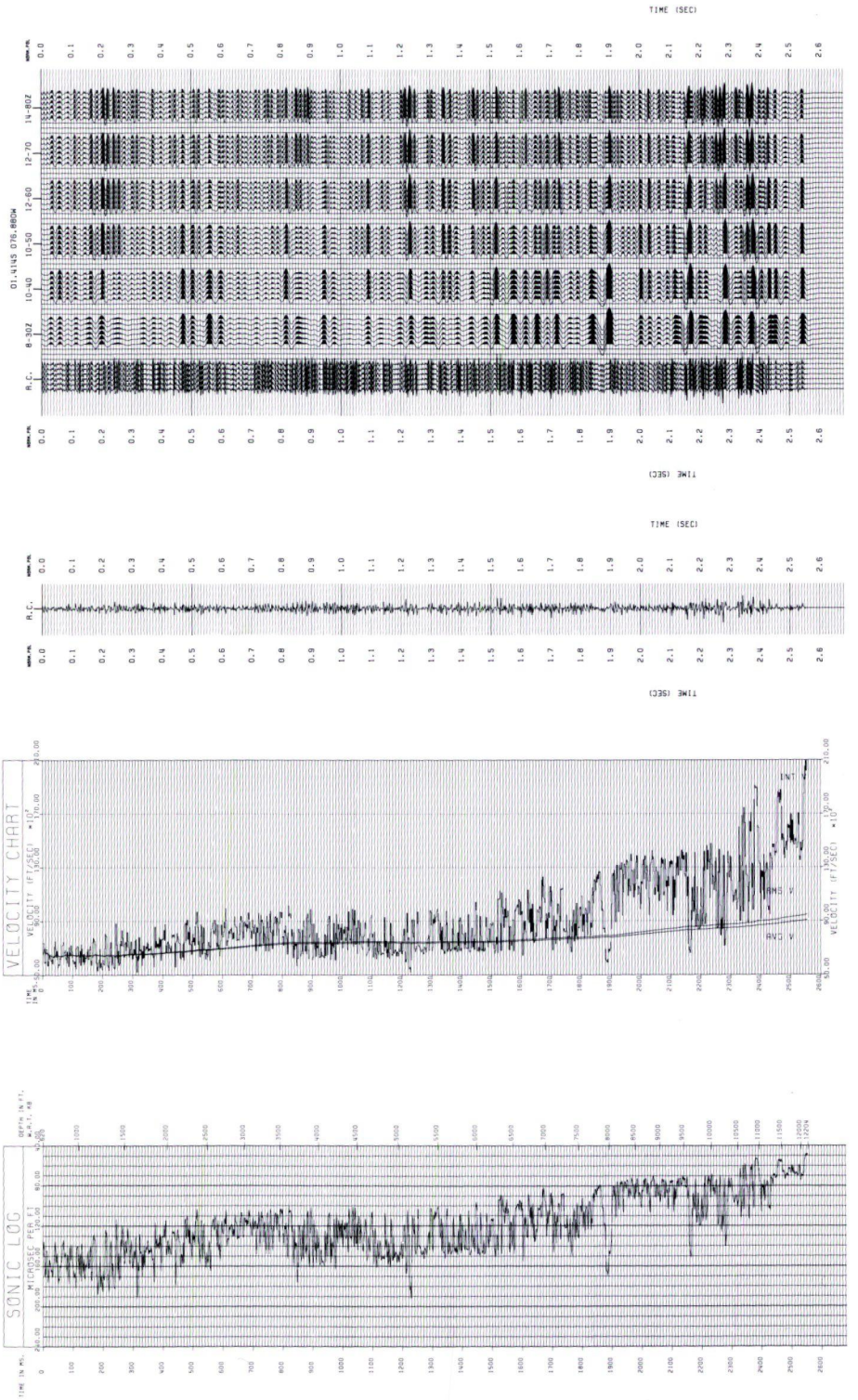

Figure 2.5 SYNTHETIC SEISMOGRAM

Chapter 3. Wavelet Estimation and Deconvolution

3.1 Introduction

The ultimate goal of the seismic reflection method is to provide unambiguous information on the relative strengths and positions of acoustic impedance contrasts in the subsurface. Deconvolution is an essential step toward the realization of this goal. The convolutional model representation of seismic data describes a process whereby the seismic wavelet smears the influence of the individual reflection coefficients over surrounding coefficients resulting in very ambiguous and generally undecipherable composite reflection response.

Deconvolution attempts to recover the unadulterated reflection coefficient series by undoing the smoothing filter effect of the wavelet. In the most general sense this is accomplished by 1) acquiring an estimate of the seismic wavelet, 2) designing an inverse filter which is the inverse wavelet, and 3) convolving the inverse filter with the seismic data to yield the reflection coefficients.

The relationship between wavelet estimation and deconvolution is obvious. Deconvolution requires an estimate of the inverse seismic wavelet. Given an estimate of the seismic

wavelet, the corresponding deconvolution operator can be determined by an inverse technique such as least squares, and vice versa.

A selection of wavelet estimation and deconvolution techniques are described in the following review. The choice of methods ranges from the deterministic to the purely statistical with a full spectrum of intermediate techniques, varying widely in the assumptions employed. The following review, therefore, is not intended to be exhaustive, but rather to illustrate the variety of approaches to wavelet estimation and deconvolution catalogued in the literature.

More detailed and complete reviews are available [1, 11, 20, 23, 27, 55, 63, 65].

3.2 Wavelet Estimation Techniques

The wavelet estimation problem is just a minor variant of the deconvolution problem. Given that

$$s(n) = w(n)*r(n)$$

and given $s(n)$, find $w(n)$.

The mathematics of the problems are identical; solving one equation with two unknowns, $w(n)$ and $r(n)$. Clearly any deconvolution estimation technique which solves for $r(n)$ can be applied in solving for $w(n)$. Rather than repeat description of generally applicable techniques, those described below are selected to illustrate approaches unique to the estimation of $w(n)$.

3.2.1 Signature Capture

The most obvious approach to estimating seismic wavelets is to record the wavelets directly from the first arrivals at geophones (or hydrophones) close to the source of seismic energy. Ideally the first arrivals will travel direct straight-line paths to the phones and be free from the interference of reflected and refracted energy superimposing. Also, if the phones are sufficiently close to the source absorptive losses and additive noise will be negligible such that the recorded signature is a good representation of the actual source pulse or wavelet. This technique is called signature capture and has been studied exhaustively by White and O'Brien for land seismic sources [24] and by the GeoQuest group and others [20, 25] for marine seismic. Applications of the technique in the design of inverse filters for deconvolution are presented by Carrol [26] for marine seismic, and Barry and Shugart [27] for land seismic.

The problems with the method are several. Routine signature capture from land sources other than Vibroseis is difficult because of the need to bury the geophone in proximity to the source. Furthermore, the near field response of a dynamite explosion in the earth differs significantly from the far field response which is really the desired estimated wavelet.

However, while the recorded far field response correctly includes absorptive losses, it suffers from interference and noise.

Signature capture from marine sources is less difficult and is now routine procedure. The direct arrivals can be measured without interference by the near hydrophones in average water depths or by an auxiliary hydrophone intermediate between the source and near hydrophone group in shallow waters or in a survey conducted with a particularly far offset distance between the source and near group. If the recorded signatures are noisy several can be averaged to improve signal to noise ratio [26]. Marine sources yield a fairly uniform signature and water is essentially isotropic so that absorptive losses are consistent from shot to shot.

A problem of the technique common to both land and marine data concerns the validity or utility of the estimated wavelet. The signature is captured close to the source to minimize absorptive losses and interference, but it could be argued that those very effects, particularly the absorptive losses, are essential characteristics of the wavelets which penetrate the earth, convolve with the reflection coefficient series and result in the seismic trace recorded at the surface. In other words, the wavelet in the convolutional

model of a seismic trace is not expected to be the source wavelet per se but a modified version thereof. Deterministic procedures could be developed to determine the necessary modifications to the captured source signature but would require empirical measurements at each source position. Instead techniques have been developed which estimate the seismic wavelet from the seismic trace itself thereby incorporating all the modifications inherent in far field measurement and more particularly, satisfying the definition of the wavelet in the convolutional mode.

Recent and ongoing research is focussed on far field measurement and estimation [67].

3.2.2 Response of a Known Layer

An alternative to shot signature capture is to record the wavelet response from a known reflector directly off the seismic data [28]. In many areas of Western Canada, for instance, the Wabamun is a thick uniform carbonate overlain by shales and provides a strong and consistent reflection. If the interference effects of overlying reflections and multiples on the reflection can be assumed to be negligible then the wavelet response of the Wabamun can be taken as a reasonable estimate of the seismic wavelet. This technique,

like signature capture, makes no assumptions about the phase of the wavelet. The convolutional model is assumed implicitly since the method is to pick one unchanging wavelet from one discrete reflection coefficient. The major assumption is that the wavelet is uniquely identifiable. A priori knowledge of the wavelet shape is required to choose the start and end points of a wavelet from typically ringing, narrowband data.

3.2.3 Wavelet Extraction by Sonic log correlation

In instances where seismic data are recorded in close proximity to a well location, correlation of reflection coefficients derived from the well sonic and density logs with the seismic trace provides an estimate of the seismic wavelet. The observational data are the seismic trace s(n) and the reflection coefficient series r(n); neglecting additive noise it is straightforward to determine the wavelet. Recall that

$$s(n) = w(n)*r(n)$$

where s(n) and r(n) are known and w(n) is to be determined. Cross-correlating r(n) with s(n) yields

$$s(n)*r(-n) = w(n)*r(n)*r(-n) \qquad 3.1$$

where the notation is such that x(n)*y(-n) denotes correlation of the series x(n) and y(n); that is

$$x(n)*y(-n) = \lim_{N\to\infty} \sum_{n=o}^{N-1} x(n)y(n+m) \qquad -\infty < m < \infty$$

Taking Fourier transforms of both sides of Equation 3.1

$$S(f)\cdot R^*(f) = W(f)\cdot R(f)\cdot R^*(f) = W(f)\cdot |R(f)|^2$$

where the superscript asterisk * denotes the complex conjugate.

On the right hand side of the equation

$$R(f)\cdot R^*(f) = |R(f)|^2$$

is recognized to be the Fourier transform of the autocorrelation of r(n). Obviously the phase of w(n) is preserved in the correlation and, better still, only the phase of w(n) persists. Furthermore, if the reflection coefficient series r(n) can be considered to be white over the correlation interval then $|R(f)|^2 = K$ where K is some constant, and

$$S(f)\cdot R^*(f) = W(f)\cdot K$$

or, taking inverse transforms

$$s(n)*r(-n) = w(n)*K\delta(n) = k\cdot w(n)$$

So, the correlation of the seismic trace with the reflection coefficient series yields a scaled version of the seismic wavelet preserving all phase information, provided the reflection coefficient series is white locally.

A related technique is the MLSE shaping filter approach [29]. That is

$$s(n) \approx w(n)*r(n)$$

where the "approximately equals" is properly introduced to account for additive noise and the possible deviation between the calculated r(n) from logs and true geological r(n).

Then

$$e(n) = s(n) - w(n)*r(n)$$

and w(t) can be determined such that $\overline{\Sigma e^2(n)}$ is minimized.

These methods have in common the assumptions that w(n) is stationary, that the additive noise is low amplitude, random, and uncorrelated with other components, and that r(n) as determined from the well logs is a good approximation to the "true" geological r(n).

It is this latter assumption that gives rise to most of the problems of the method. The correspondance between the r(n) derived from well logs and the "true" geological r(n) is

seriously affected by long period multiples (which, ironically, are present in the "true" r(n) and not the derived r(n)) and by the accuracy of the log data and the dependant depth to time conversion. As discussed more fully in Chapter 2 well logs are recorded in depth and so must be converted to time prior to correlating with the seismic data.

These sonic log correlation techniques of wavelet extraction are considered to be semi-deterministic because of their development from the log data as well as the recorded trace.

3.3 Deconvolution Techniques

The basic deconvolution problem is now familiar. Given that

$$s(n) = w(n)*r(n)$$

and given $s(n)$, determine $r(n)$.

The obvious approach is to design a wavelet inverse filter $g(n)$ such that

$$s(n)*g(n) = w(n)*g(n)*r(n)$$

$$= r(n)$$

or taking Fourier transforms

$$S(f) = W(f)R(f)$$

and solving for $R(f)$

$$R(f) = \frac{S(f)}{W(f)}$$

Unfortunately, these are one equation with two unknowns so

certain assumptions must be made in achieving a solution.

In the following, selected deconvolution techniques are described.

Inverting the wavelets output from the previously described estimation schemes would yield deterministic to semi-deterministic deconvolutions. The methods described below are clustered at the statistical end of the spectrum of techniques.

3.3.1 Least Squares Spiking Deconvolution

The deconvolution technique most widely used in the geophysical industry remains the original least squares inversion method proposed by Robinson in 1954 [16]. The approach is to design a least squares shaping filter g(n) which will convert a sequence w(n) into a desired output d(n). The discrepancy between the actual output of the filter c(n) and the desired output d(n) is called the error e(n). The filter g(n) is therefore designed so as to minimize the energy of the error.

Typically the input sequence w(n) is assumed to be the seismic wavelet and the desired output sequence d(n) is chosen to be a spike situated at the origin $d(n) = \delta(o)$, so the filter g(n) becomes the least squares inverse of the seismic wavelet. Since the seismic wavelet is generally not known a priori certain assumptions are made allowing the recorded seismic data s(n) to be used as the input sequence and modified in the least squares process so that in an indirect way the least squares spiking deconvolution process implicitly makes an estimate of the seismic wavelet by calculating its inverse.

The general least squares inversion procedure is straight forward. The problem is to design a least squares shaping filter g(n) of length M which will convert an input sequence w(n) of length N into a desired output sequence of length M + N - 1. Denoting c(n) as the actual output of g(n) the error is e(n) = d(n) - c(n), or

$$e(n) = d(n) - \sum_{k=o}^{M-1} g(k)w(n-k)$$

The energy of the error is then

$$E = \sum_{n=o}^{M+N-2} e^2(n) = \sum_{n=o}^{M+N-2} [d(n) - \sum_{k=o}^{M-1} g(n)w(n-k)]^2$$

To solve for g(n) so as to minimize the energy of the error partial derivatives are taken with respect to each coefficient of g(n) and set to zero, so for coefficient g(i) i = (0,1,2,...M-1)

$$\sum_{n=o}^{M+N-2} \{2[d(n)- \sum_{k=o}^{M-1} g(n)w(n-k)][-2(n-i)]\} = 0$$

or, collecting terms

$$\sum_{k=o}^{M-1} g(k) \sum_{n=o}^{M+N-2} w(n-k)w(n-i) = \sum_{n=o}^{M+N-2} d(n)w(n-i)$$

which can be written as

$$\sum_{k=o}^{M-1} g(k)R_w(i-k) = R_{dw}(-i) \qquad 3.2$$

where $R_w(k)$ is the autocorrelation of $w(n)$

$$R_w(k) = \sum_{n=o}^{M-1} w(n)w(n+k)$$

and $R_{dw}(k)$ is the cross-correlation of $d(n)$ and $w(n)$

$$R_{dw}(k) = \sum_{n=o}^{M+N-2} d(n)w(n+k)$$

Equations 3.2 are the familiar normal equations which are conveniently written in matrix form as

$$\begin{bmatrix} R_w(o) & R_w(1) & \cdots & R_w(M-1) \\ R_w(1) & R_w(o) & \cdots & R_w(M-2) \\ \vdots & \vdots & & \vdots \\ R_w(M-1) & R_w(M-2) & \cdots & R_w(o) \end{bmatrix} \begin{bmatrix} g(o) \\ g(1) \\ \vdots \\ g(M-1) \end{bmatrix} = \begin{bmatrix} R_{wd}(o) \\ R_{wd}(1) \\ \vdots \\ R_{wd}(M-1) \end{bmatrix}$$

Because of the Toeplitz form of the matrix, g(n) can be solved for very efficiently with the Weiner-Levinson algorithm [1, 11, 16].

It can be shown that the causal least squares inverse filter with finite duration of any causal energy bounded sequence is a minimum phase sequence [11]. Seismic wavelets are energy bounded sequences and are generally assumed to be causal and therefore if a causal output sequence is desired, for example the traditional spike at the origin $d(n) = \delta(o)$, then the filter is necessarily minimum phase. Therefore an important property of least squares deconvolution is that it harbours the tacit assumption of minimum phase.

As mentioned earlier the least squares process uses the seismic data s(n) as input and indirectly assumes the wavelet w(n) in the design of the inverse wavelet g(n). This follows from certain assumptions about the autocorrelation of the seismic trace and of the seismic wavelet.

Assume noise free seismic data s(n) resulting from the convolution of the reflection coefficient series r(n) and the seismic wavelet w(n), so $s(n) = w(n)*r(n)$.

In the least squares procedure the autocorrelation of the input sequence is used rather than the actual data so in terms of autocorrelations

$$R_s(k) = R_w(k)*R_r(k)$$

Now if the reflection coefficient sequence r(n) is totally random or "white" then $R_r(k) = K\delta(o)$, that is a spike at the origin, so that

$$R_s(k) = R_w(k)*K\delta(o) = KR_w(k)$$

K is a constant related to the energy of the seismic data so assuming unit wavelet energy $K = R_s(o)$ and therefore

$$\frac{R_s(k)}{R_s(o)} = R_w(k) .$$

Employing the normalized autocorrelation of the seismic signal in the spiking least squares procedure, therefore, implicitly assumes an estimate of the seismic wavelet and explicitly derives its inverse. The actual wavelet can be recovered by least squares inversion of the inverse wavelet, or by simply convolving the inverse wavelet with a spike. Figure 3.1 shows wavelets derived by the Levinson routine allowing inverse wavelets of varying length.

The assumptions of the technique are as follows.

1. The inverse filter is minimum phase.

2. The reflection coefficient series is white.

3. The noise in the seismic data is negligible.

4. The seismic wavelet (or the inverse filter) is time invariant.

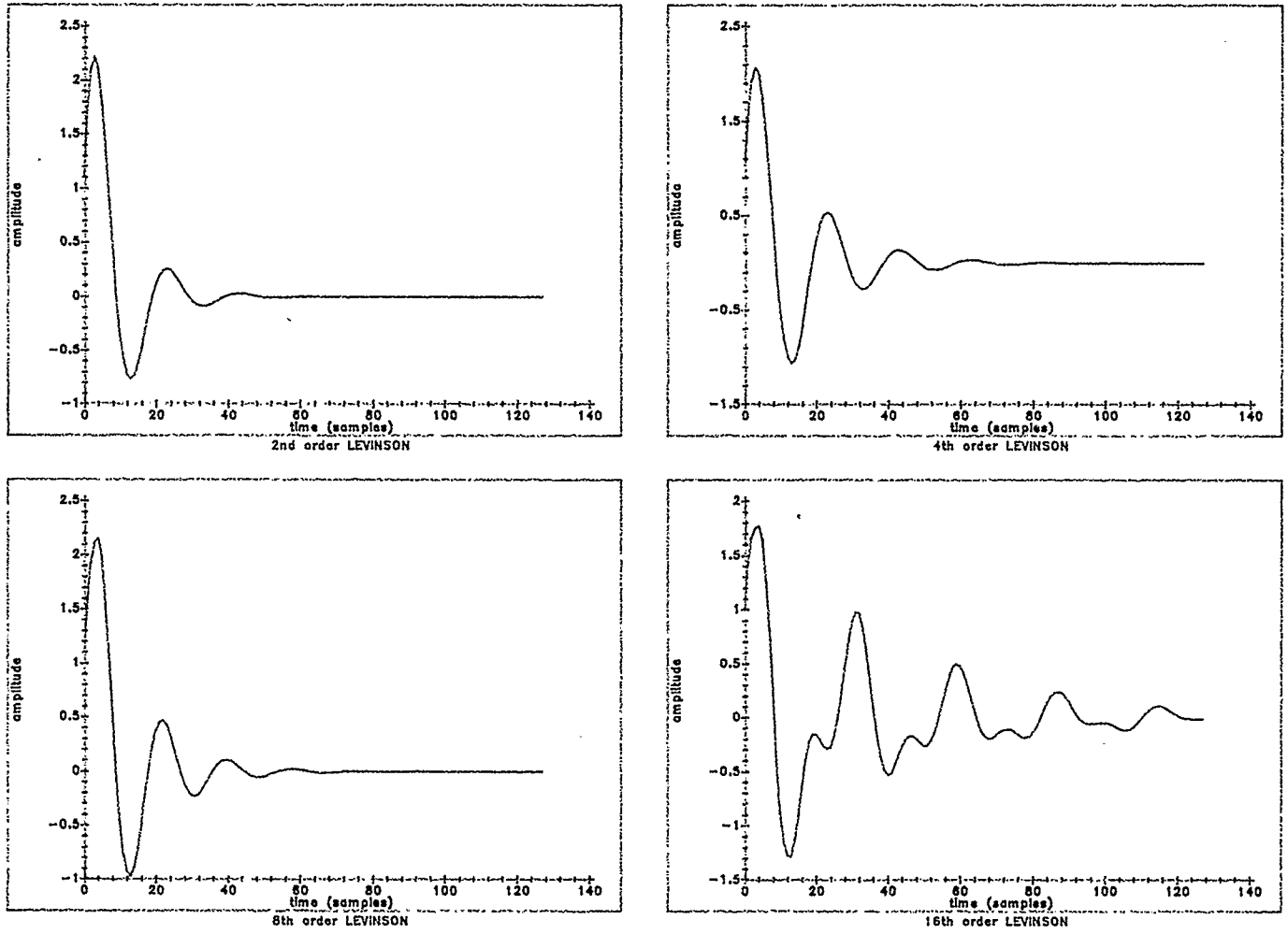

Figure 3.1 WAVELETS EXTRACTED BY LEVINSON DECONVOLUTION

The technique is considered to be purely statistical since no observational information is employed in the filter design. However empirical evidence for the assumption of white reflectivity is easily obtained by transforming reflectivity sequences r(n) derived from sonic and density logs at wells proximal to the seismic recording. Appendix A discusses the validity of the white r(n) assumption and illustrates with transforms of eighteen sonic derived reflectivity sequences that the assumption of whiteness is not unreasonable.

3.3.2 Frequency Domain Least Squares

Deconvolutions are not commonly designed in the frequency domain because of numerical problems. Nevertheless, inverse filter design is easily formulated in the frequency domain and consequently merits review.

As stated earlier, the convolutional model can be expressed as a simple multiplication in the frequency domain

$$S(f) = W(f) \cdot R(f)$$

Deconvolution is therefore accomplished by division and inverse transformation back into the time domain. Again there is the problem of one equation and two unknowns but assuming r(n) to be random, R(f) is white; that is, it has constant magnitude, K.

So deconvolution can be formulated as

$$R(f) = Ke^{j\emptyset(f)} = \frac{S(f)}{W(f)}$$

This does not yield the desired R(f) of course, but offers an approach to the design of an inverse wavelet, G(f)

$$G(f) = \frac{1}{W(f)} = \frac{Ke^{j\phi(f)}}{S(f)}$$

Since this equation still has two unknowns, (K is a constant, its value irrelevant), an extra explicit assumption has to be made regarding phase. The phase assumption was implicit in the least squares spiking inverse technique employing Levinson recursion.

If minimum phase is chosen, for example, $|G(f)|$ is easily determined as the quotient of K and $|S(f)|$ and the phase is calculated with the Hilbert transform.

If noise is present, G(f) can be selected so that the mean square error is a minimum. This is accomplished by windowing G(f) by a non-causal function of the power spectral density function of the seismic signal s(n) and the noise n(n). The noise is assumed to be additive and uncorrelated. The window restricts the gain of the inverse filter in regions where the signal to noise ratio is small.

3.3.7 Homomorphic Deconvolution

Homomorphic deconvolution is a non-linear technique which transforms signals combined by convolution into signals combined by addition, linearly separates the transformed signals, and then inverse transforms the separated signals back as deconvolved components of the original input data. The technique requires no knowledge or assumptions about the phase of the seismic wavelet or the distribution of reflection coefficients. In practice, however, these considerable advantages are outweighed by computational problems and at present homomorphic deconvolution is not widely utilized by the seismic geophysical community.

Homomorphic deconvolution is based on the work of Oppenheim on generalized superposition [30]. The application to seismic deconvolution was explored by Ulrych [31], Stoffa et al [32], Buttkus [68], and Tribolet [33], [34].

Generalized superposition requires that

$$H[c:x_1 \nabla d:x_2] = C_\iota[x_1] \Delta d_\iota H[x_2] \qquad 3.3$$

where

∇ is a rule for combining inputs

Δ is a rule for combining outputs

: is a rule for multiplying inputs with scalars

ι is a rule for multiplying outputs with scalars

H[ ] is a rule for system transformation, $y_i(n) = H[x_i(n)]$

Equation 3.3 defines a homomorphic system H[ ]. Oppenheim [30] has demonstrated that for such systems the operation H[ ] can be realized by a canonic representation where the output of a characteristic transform D[ ] is input to a linear time invariant system L[ ] and subsequently inverse transformed by D^{-1}[ ] as shown in Figure 3.2. The importance of this decomposition is that the output of generally non-linear D[ ] can be processed using standard linear filter techniques.

For seismic signals convolution is the rule for combining inputs, where the inputs are the seismic wavelet w(n) and the reflection coefficient series r(n). Homomorphic deconvolution invokes a characteristic transform D[ ] such that summation is the rule for combining outputs.

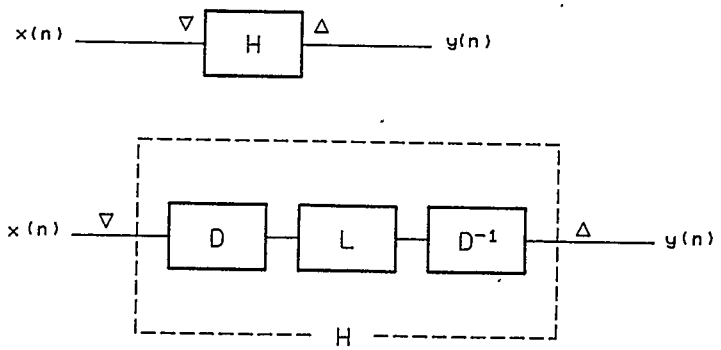

Figure 3.2 CANONIC REPRESENTATION OF A HOMOMORPHIC SYSTEM

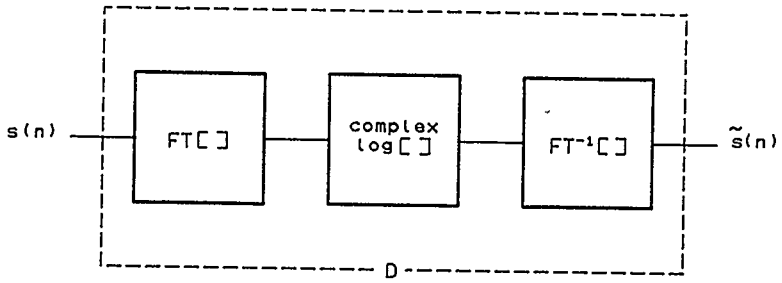

Figure 3.3 THE CHARACTERISTIC SYSTEM D[ ]

$D[s(n)] = \tilde{s}(n)$

$D[w(n) * r(n)] = \tilde{w}(n) + \tilde{r}(n)$

$$D[w(n) * r(n)] = D[w(n)] + D[r(n)]$$

This is achieved by Fourier transforming the convolution of w(n) and r(n) and taking the complex logarithm of the result. The inverse Fourier transform is then taken yielding the complex cepstrum in the pseudo-time domain, $\tilde{s}(n)$.

That is

$$s(n) = w(n) * r(n)$$

taking Fourier transforms

$$S(f) = W(f)R(f)$$

then taking complex logarithms

$$\log[S(f)] = \log[W(f)] + \log[R(f)]$$

which can be denoted

$$\tilde{S}(f) = \tilde{W}(f) + \tilde{R}(f)$$

finally, taking inverse Fourier transforms

$$\tilde{s}(n) = \tilde{w}(n) + \tilde{r}(n)$$

The above sequence of operations realize the characteristic transform D[ ] as depicted in Figure 3.3.

An important characteristic of the cepstral domain is that the cepstra of sequences with smooth amplitude spectra tend to concentrate around the origin. Since seismic wavelets are expected to have smooth spectra compared to the reflection coefficient series, low pass filtering of the cepstrum preserves wavelet information while attenuating reflection coefficient components. High pass filtering does the opposite. Homomorphic deconvolution, therefore, achieves isolation of the seismic wavelet or the reflection coefficient series by simple linear filtering in the cepstral domain. The isolated cepstra are then transformed back into the time domain by $D^{-1}[\ ]$. $D^{-1}[\ ]$ involves Fourier transforming, exponentiating, and then inverse Fourier transforming to get cepstral components from the pseudo-time domain to the time domain. The whole canonic system realizing Homomorphic deconvolution is shown in Figure 3.4.

Homomorphic deconvolution is conceptually appealing. It requires few explicit assumptions and separately yields both the seismic wavelet and the reflection coefficient series. Unfortunately the technique is plagued by computational problems arising from a variety of implicit assumptions.

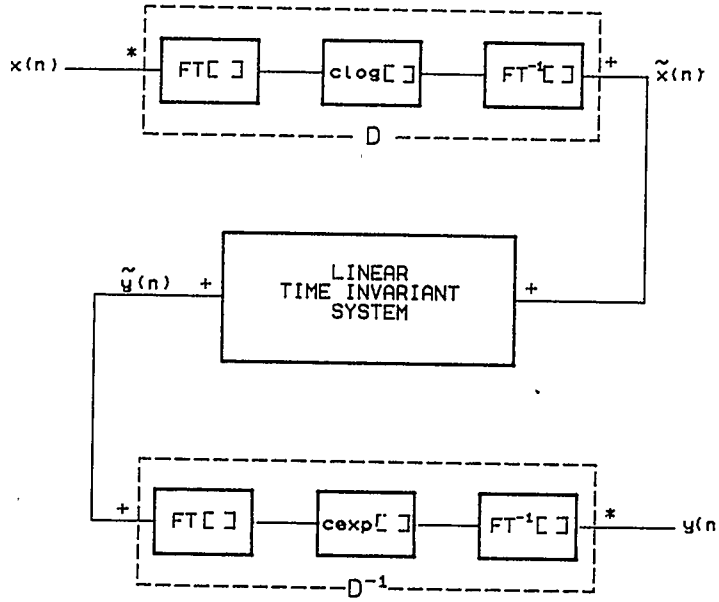

$x(n) = w(n) * r(n)$ $\quad \tilde{y}(n) = \tilde{r}(n)$ (OR $\tilde{w}(n)$)

$\tilde{x}(n) = \tilde{w}(n) + \tilde{r}(n)$ $\quad y(n) = r(n)$ (OR $w(n)$)

Figure 3.4 CANONICAL SYSTEM REALIZATION OF HOMOMORPHIC DECONVOLUTION

Aside from numeric problems of computing the true complex logarithm of the transformed data there are three major concerns.

Firstly, separation of the wavelet components and the reflection coefficient components in the cepstral domain is not entirely straightforward. Reflection coefficient components generally persist near the origin in the cepstral domain where the wavelet components cluster, so that low-pass cepstral filtering intended to preserve wavelet components necessarily includes some reflection components. Ironically it is necessary that the reflection coefficient series be minimum phase to realize adequate separation in the cepstral domain. Stoffa et al [32] recommend exponential weighting to insure a minimum phase reflection coefficient series.

Secondly, aliasing of the phase spectrum creates uniqueness problems in specifying the complex logarithm of Fourier transformed data. That is

$$\hat{S}(f) = \log[S(f)] = \log|S(f)| + i\Phi_S(f)$$

where

$$\Phi_S(f) = \tan^{-1}\frac{\text{Im } S(f)}{\text{Re } S(f)}$$

Since the inverse tangent function is multivalued the phase is necessarily ambiguous.

Several techniques have been prescribed for phase determination but none are completely effective [33], [34].

Thirdly, oversampling in the time domain creates severe problems. Inherent in the characteristic system is the requirement of full band data; zeroes in the frequency domain become unrealizable infinities in the log-frequency domain. Tribolet has detailed a time resampling procedure to guarantee against zeroes the frequency domain in consideration of the severely band-limited nature of seismic signals [33]. The procedure is shown in Figure 3.5.

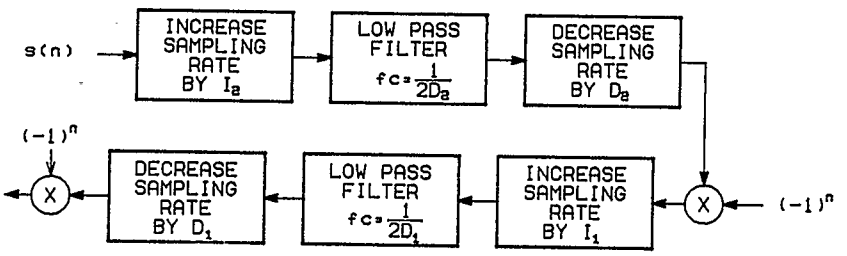

f_1 IS THE DATA FREQUENCY CUTOFF ON THE LOW SIDE

f_2 IS THE DATA FREQUENCY CUTOFF ON THE HIGH SIDE

$f_2 = \frac{I_2}{D_2} \cdot \frac{1}{2}$ I_2, D_2 INTEGERS ; $f_1 = (1-\frac{I_2}{D_2}) f_2$ I_1, D_1 INTEGERS

Figure 3.5 RESAMPLING TECHNIQUE OF TRIBOLET TO ENSURE DATA NOT OVERSAMPLED SINCE THE HOMOMORPHIC SYSTEM REQUIRES FULL BAND DATA.

3.3.4 "Optimal Deconvolution" Using State Variables

A very involved deconvolution scheme has been developed by Mendel and his students at U.S.C. over the past five years [35]. Described as optimal deconvolution because of its affinity to optimal Kalman filtering the technique represents the seismic process by a state variable model and yields a maximum likelihood estimate of the reflection coefficient series via a complicated iterative scheme which requires the separate but dependant estimation of the statistics of the reflection coefficients, the position of the reflection coefficients, the seismic wavelet, and ultimately the magnitude and polarity of the respective reflection coefficients. The method provides a model which can accommodate fewer constraints than previously described techniques. The principal advantage is that time-varying signals can be handled. The state variable model can also be modified to incorporate effects such as instrument response and spherical divergence. The technique assumes a white Bernoulli-Gaussian sparse spike reflection coefficient series and an ARMA (p,q) representation of the seismic wavelet. Other minor assumptions will be discussed as they occur in the following summary description of the method.

The convolutional model of seismic data can be expressed in terms of a state variable model. That is, the convolutional model

$$s(k) = w(k) * r(k) + n(k)$$

can be equivalently described by the state equation

$$\underline{x}(k + 1) = \Phi\underline{x}(k) + \underline{\sigma}\, r(k)$$

and the corresponding measurement equation

$$s(k) = \underline{h}^T\underline{x}(k) + n(k)$$

Φ is an n x n transition matrix, $\underline{\sigma}$ is an n x 1 input distribution vector, and $\underline{h}$ is an n x 1 observation matrix. Underlined variables denote vectors. The equivalence of the convolutional and state variable descriptions requires that

$$\underline{x}(o) = \underline{o},\ r(o) = o,\ w(o) = o, \text{ and}$$

$$w(\ell) = \underline{h}^T\Phi\ell^{-1}\,\underline{\sigma}\ ,\ \ell = 1,\ 2,\ \ldots.$$

These conditions specify that the initial state is zero, that there is no direct reflection, and that the wavelet is not only causal but zero valued at zero time.

The appropriate choice of transition matrix Φ, input distribution vector $\underline{\sigma}$ and observation matrix $\underline{h}$ results in an ARMA (p,q) model representation of the seismic wavelet w(k), that is:

$$\begin{vmatrix} x_1(k+1) \\ x_2(k+1) \\ \cdot \\ \cdot \\ \cdot \\ x_n(k+1) \end{vmatrix} = \underbrace{\begin{vmatrix} 0 & 1 & 0 & \cdots & 0 \\ 0 & 0 & 1 & \cdots & 0 \\ \cdot & \cdot & \cdot & & \cdot \\ \cdot & \cdot & \cdot & & \cdot \\ \cdot & & & & \cdot \\ -a_n & -a_{n-1} & -a_{n-2} & & -a_1 \end{vmatrix}}_{\Phi} \begin{vmatrix} x_1(k) \\ x_2(k) \\ \cdot \\ \cdot \\ \cdot \\ x_n(k) \end{vmatrix} + \underbrace{\begin{vmatrix} 0 \\ 0 \\ \cdot \\ \cdot \\ \cdot \\ 1 \end{vmatrix}}_{\underline{\sigma}} r(k)$$

and

$$s_T(k) = \underbrace{(b_n, b_{n-1}, \cdots b_1)}_{\underline{h}^T} \underline{x}(k)$$

where $s_T(k)$ denotes the "true" seismic signal, uncontaminated by noise, so that $s(k) = s_T(k) + n(k)$.

w(k) can then be expressed in z-transform notation as an ARMA (p,q) process.

$$w(z) = \frac{b_1 z^{n-1} + b_2 z^{n-2} + \ldots b_{n-1} z + b_n}{z^n + a_1 z^{n-1} + \ldots a_{n-1} z + a_n}$$

Note that this description implicitly requires at least one less zero than poles.

To accomplish deconvolution using this state variable model of the seismic process, the variance of the state vector $\underline{x}(k)$ is minimized with a Kalman optimal smoother. The variance of the state vector $\underline{x}(k)$ is equivalent to an estimate of the reflection coefficient series r(k) under a "sparse spike" assumption. That is, for any combination of wavelets and reflection coefficients which convolve to produce the observational data the reflection coefficient series with the fewest reflections (but more than one) is considered to be the best estimate, and its corresponding wavelet is the best wavelet estimate. The reflection coefficient series is further assumed to be Bernoulli-Gaussian. That is

$$r(k) = \Sigma \mu_i \delta_{k,m_i}$$

Where the m_i are randomly occurring integer values of discrete time and $\delta_{k,m_i} = 1$ for $k = m_i$ and $\delta_{k,m_i} = 0$ for $k \neq m_i$. μ_i denote a set of identically distributed uncorrelated Gaussian random variables, statistically independent of the m_i. Under this model $E\{r^2(k)\} = \delta_\mu^2 \lambda$ where λ is the

average number of spikes occurring within the subject length of data. The sparse spike assumption constrains λ to the minimum value compatible with the data.

Optimal deconvolution attempts to simultaneously determine r(k) and w(k) in an involved updating procedure which interrelates the parameters of r(k) and w(k) to effect a jointly optimal solution. To determine r(k) the number of reflection coefficients, λ, must be determined, so must the position of the spikes $\underline{q}$ (related to m_i) and their amplitudes $\mu(k)$. To determine w(k) the ARMA coefficients $\underline{a}$ and $\underline{b}$ must be determined. In order to accommodate noise in the system, the variance of the noise ρ must also be determined. The parameters $\underline{a}$, $\underline{b}$, and ρ are treated together as a vector of statistical parameters $\underline{\theta}$. Parameter $\underline{q}$ is solved for in loose conjunction with λ in a separate iterative loop. The block diagram of Figure 3.6 illustrates the overall computational scheme and some of the components. The hat symbol "^" denotes an estimate. An initial guess at the parameters $\hat{\underline{\theta}}$ initializes the event detector which solves for $\hat{\underline{q}}$, the value $\hat{\lambda}$ is then updated and fed back into the event detector. When a converging estimate $\hat{\underline{q}}$ is found the algorithm drops to an outer loop in which the parameters $\hat{\underline{\theta}}$ are updated in a maximum likelihood scheme. These updated $\hat{\underline{\theta}}$

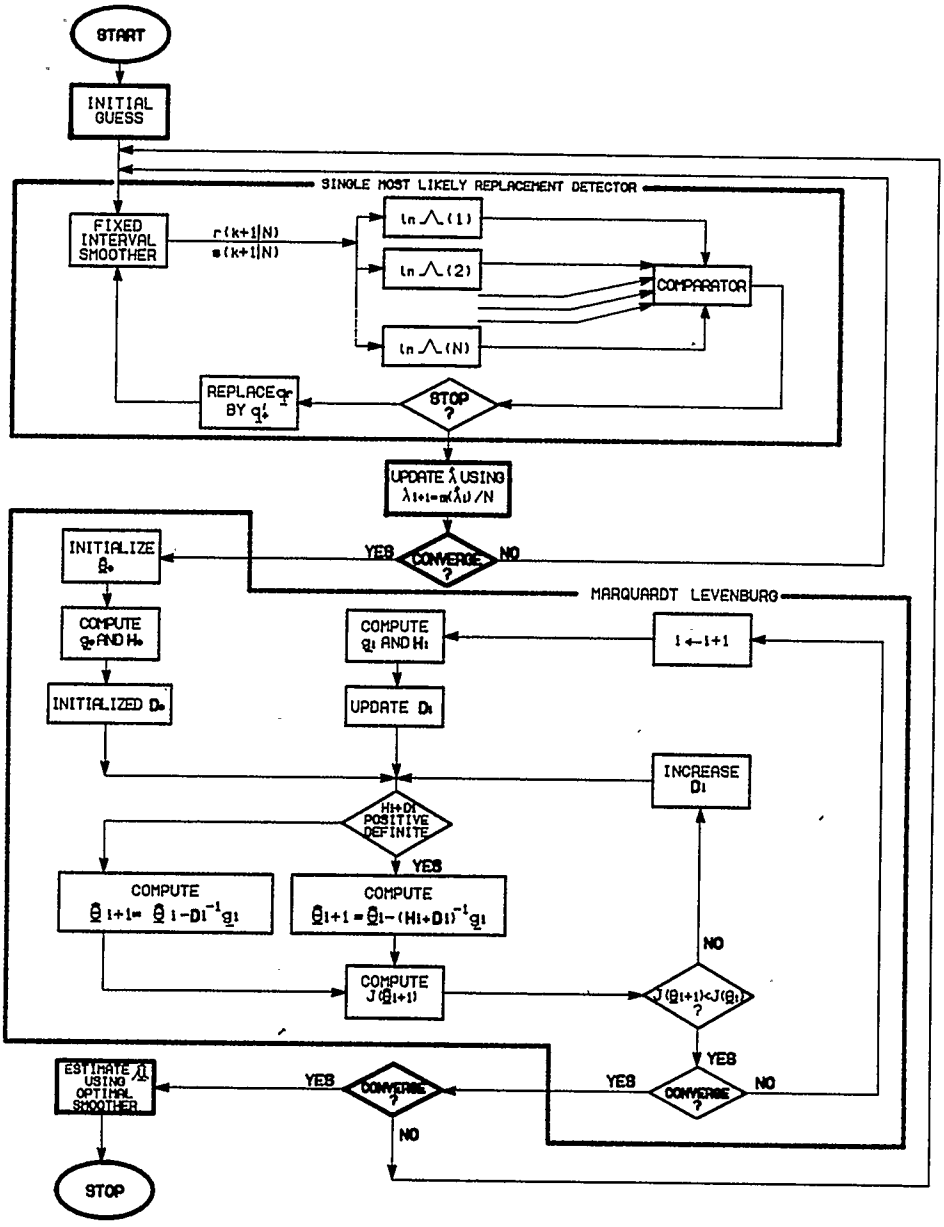

Figure 3.6 BLOCK COMPONENT DIAGRAM OF THE OPTIMAL DECONVOLUTION ALGORITHM OF MENDEL (AFTER MENDEL [35]).

estimates are then fed back into the event detector and a new $\underline{q}$ and λ are obtained. This procedure ensures that overall likelihood increases. When convergence in both loops is achieved $\mu(k)$ can be estimated in one pass with the estimated parameters through a Kalman optimal smoother which provides the minimum variance estimate of the state equation for which all the parameters are now provided. This result, $\mu(k)$, finally allows for the determination of $r(k)$ by $r(k) = \mu(k)q(k)$. The seismic wavelet is provided by the optimal estimates of $\underline{a}$ and $\underline{b}$.

The state variable representation of the seismic process promises fewer constraining assumptions than conventional least squares techniques and the facility for incorporating deterministic processes such as spherical divergence directly into the seismic model. The iterative "block component" method of Mendel et al [35] described above has the additional advantages of providing maximum likelihood estimates of the wavelet parameters and the placement of the reflection coefficients, and an optimal estimate of the reflection coefficient series.

The principle disadvantage of the method is the required computational intensity; the maximum-likelihood solution requires non-linear gradient search optimization.

The state variable model turns out to be less flexible than expected in practice. The restrictive assumptions of the least-squares technique require the data to be time invariant and the reflection coefficient series to be Gaussian. The state variable model allows time variance but only in the reflection coefficients; it is the wavelet that is expected to be time variant in seismic data. The state variable model also allows relaxation from the requirement of Gaussian reflection coefficients but only so far as to permit Bernoulli-Gaussian statistics, which still require the reflection coefficient series to be white.

One final weakness in the state variable approach is that rather than minimizing a physically meaningful criterion, such as mean squared error, the minimization is performed on the variance of the state variable equation which has no physically interpretable meaning.

Chapter 4. Estimation Techniques Employing Linear ARMA (p,q) Models

4.1 Introduction

Much of the recent literature in signal processing and time series analysis concerns the estimation of spectra using linear models. Linear models represent signals as linear combinations of their past values and the past and present values of a hypothetical input signal which is generally assumed to be white noise with variance σ^2. The corresponding models in the frequency domain are rational functions of polynomials whose coefficients specify the poles and zeroes of their spectra.

It is particularly convenient to consider linear models in terms of filter theory. The linear model of an observed time series (e.g. seismic trace) corresponds to the transfer function of the filter required to generate the observed trace from a white noise input. That is, the linear model is the filter, white noise is the filter input, and the observed trace is the resultant filter output. This relationship is illustrated in Figure 4.1.

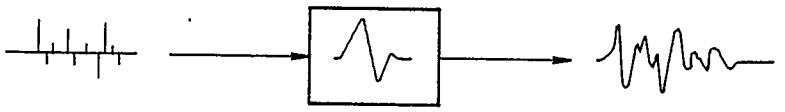

INPUT
x(n)

FILTER
h(n)

OUTPUT
y(n)

$x(n) * h(n) = y(n)$

$X(z) \cdot H(z) = Y(z)$

$x(n) \equiv$ WHITE NOISE "INNOVATION" OR "SHOCK" SEQUENCE

$h(n) \equiv$ LINEAR TIME INVARIANT FILTER IMPULSE RESPONSE

Figure 4.1 LINEAR WHITE NOISE MODEL

Linear models are especially suited to the representation of seismic data. As described in Chapter 2 seismic data is considered to be the result of seismic wavelet convolved with a random reflection coefficient spike series.

An equivalent description of the process is that the reflection coefficient spike series is filtered by the seismic wavelet. The seismic wavelet is consequently the impulse response of the earth filter which comprises all of the effects which modify the assumed spike input, resulting in the seismic wavelet. Therefore, although geophysicists tend to consider the seismic process strictly in terms of the seismic wavelet travelling into the earth and encountering and responding to the reflection coefficients in a directed convolution, it is equivalent to consider the spike series as passing through a filter whose impulse response is the seismic wavelet and yielding to the seismic trace. As such the seismic process is ideally represented by linear modelling. The reflection coefficient spike series corresponds to the white noise input, the seismic trace corresponds to the output, and the seismic wavelet corresponds to the linear model filter whose parameters must be determined.

Linear models have a number of advantages. Since the parameters of the model specify the transfer function of the equivalent filter, calculation of a power spectrum and an inverse filter are straightforward once the model parameters have been determined. Furthermore, given the correct choice of model, it is usually sufficient to estimate a relatively small number of parameters and therefore very accurate results can often be obtained with short data lengths.

The disadvantages of linear models are that the model type must be known a priori and parameter determination is often difficult. Most troublesome is the specification of a model order [5, 6].

The most general of the linear model formulations is the pole-zero or auto-regressive-moving-average model with a p^{th} order demoninator polynomial ($p>o$) and a q^{th} order numerator polynomial ($q>o$).

$$H(z) = \frac{B(z)}{A(z)}$$

$$B(z) = b_o + b_1 z^{-1} + b_2 z^{-2} + ... + b_q z^{-q}$$

$$A(z) = 1 + a_1 z^{-1} + a_2 z^{-2} + ... + a_p z^{-p}$$

This model is conveniently denoted as ARMA (p,q). The ARMA (p,q) model is of particular interest in the representation of seismic signals because the seismic process is considered to be expressible in this way. Unfortunately, because of the difficulty in estimating the coefficients or parameters of ARMA (p,q) models there has been little interest demonstrated in the geophysical literature in pursuing the advantages of ARMA (p,q) models in either spectral analysis or seismic deconvolution.

By far the most popular of the linear models is the all-pole or auto-regressive model. The auto-regressive model has a p^{th} order denominator coefficient (p>o) and $zero^{th}$ order numerator of unit value.

$$H(z) = \frac{1}{A(z)}$$

$$A(z) = 1 + a_1 z^{-1} + a_2 z^{-2} + \ldots a_p z^{-p}$$

The model is denoted AR (p). Although use of the AR (p) model in spectral estimation is relatively recent and remains the subject of the bulk of the literature in the field of modern spectral estimation, its use in geophysics dates back to the early days of deconvolution where its application was implied in the recursive scheme of Wiener-Levinson advocated

by Robinson [16]. Most of the recent contributions to the methodology of deconvolution are variations on AR (p) models [27, 55, 69].

The last of the linear model formulations is the all-zero or moving-average model which has a q^{th} order numerator polynomial (q>o) and a unit denominator.

$$H(z) = B(z)$$

$$B(z) = b_o + b_1 z^{-1} + b_2 z^{-2} + ... + b_q z^{-q}$$

The moving-average model is denoted MA (q). Classical lag window spectral estimation techniques are expressible as MA (q) models as are Ricker seismic wavelets [11].

Table 4.1 provides a summary description of the three linear model types. In this study the concern is with ARMA (p,q) models and their application to seismic deconvolution and wavelet estimation.

AR (p) (all-pole)	$H(z) = \frac{1}{A(z)} = \frac{1}{1+a_1z^{-1}+a_2z^{-2}+\ldots a_pz^{-p}}$	$y(n) = 1 - \sum_{i=o}^{p} a_i h(n-i)$
MA (q) (all-zero)	$H(z) = B(z) = b_o+b_1z^{-1}+b_2z^{-2}+\ldots b_qz^{-q}$	$y(n) = \sum_{i=o}^{q} b_i x(n-i)$
ARMA (p,q) (pole-zero)	$H(z) = \frac{B(z)}{A(z)} = \frac{b_o+b_1z^{-1}+b_2z^{-2}+\ldots b_qz^{-q}}{1+a_1z^{-1}+a_2z^{-2}+\ldots a_pz^{-p}}$	$y(n) = \sum_{i=o}^{q} b_i x(n-i) - \sum_{i=1}^{p} a_i h(n-i)$

Table 4.1 Linear White Noise Models

$y(n) = h(n)*w(n)$

$x(n)$ is a white noise innovation sequence

AUTOREGRESSIVE (AR) MODEL

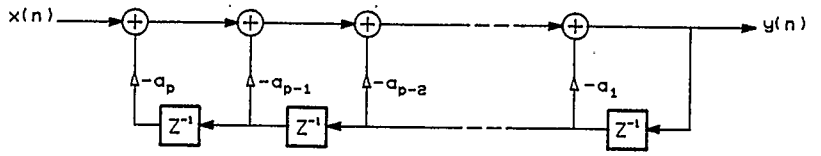

$$Y(z) = \frac{1}{1 + a_1 z^{-1} + a_2 z^{-2} + \ldots a_p z^{-p}} \cdot X(z)$$

MOVING AVERAGE (MA) MODEL

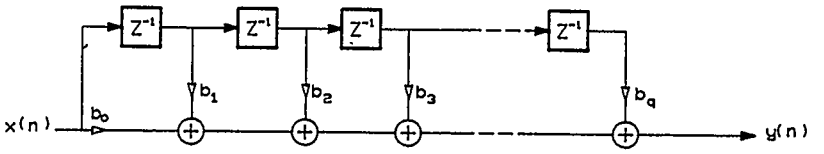

$$Y(z) = b_o + b_1 z^{-1} + b_2 z^{-2} + \ldots . b_q z^{-q} \cdot X(z)$$

AUTOREGRESSIVE - MOVING AVERAGE (ARMA) MODEL

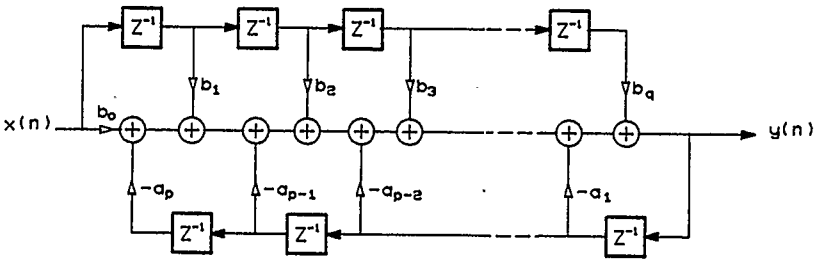

$$Y(z) = \frac{b_o + b_1 z^{-1} + b_2 z^{-2} + \ldots . + b_q z^{-q}}{1 + a_1 z^{-1} + a_2 z^{-2} + \ldots . + a_p z^{-p}} \cdot X(z)$$

Figure 4.2 DIRECT FORM REALIZATIONS AND Z-TRANSFORM DESCRIPTIONS OF THE THREE LINEAR MODEL TYPES

4.2 ARMA (p,q) Representation of Seismic Signals

The motivation for applying ARMA (p,q) models to the analysis of seismic data is that seismic data is considered to be expressible as ARMA (p,q) and hence such a model will provide the most parsimonious parameterization. The only formal development of the ARMA (p,q) characterization of seismic data in the literature is by Robinson [36, 37] and is described below. The Robinson model is considered to be too restrictive and of little value in modelling because of its assumption of lossless transmission and its development from a unit spike rather than white noise input. A preferred ARMA (p,q) seismic signal characterization is offered and is developed descriptively drawing from the work of Ricker on the properties of seismic wavelets and the work of Robinson and others on the feedback characteristics of horizontally stratified media. This Ricker/Feedback model assumes the reflection coefficient series as a white noise input and consequently models only the seismic wavelet whereas the Robinson model models the entire seismic trace. Gutowski and Frisillo [38] developed a model similar to the Ricker/ Feedback model for analysing the absorptive properties of rocks under ultrasonic excitation.

4.2.1 Robinson ARMA (p,q) Seismic Model

Assuming a lossless horizontally stratified earth model Robinson [36] demonstrated that a seismic trace can be expressed as an ARMA (p,q) model (p = q) with a z-transform given by

$$R(z) = \frac{C(z)}{D(z)}$$

where C(z) the moving-average component represents the desired primary events on the seismic trace, corresponding to reflections from geologically meaningful interfaces between rock types, and D(z) the auto-regressive component represents the reverberation characteristic waveform shape.

Using the seismic model of a horizontally layered elastic medium with homogeneous and isotropic layers subject to plane compressional motion at normal incidence (see Chapter 2) Robinson's development invokes energy considerations; since the system is lossless the energy input to the system must equal the output from the system. Given a unit spike input and characteristic impedances of Z_o and Z_{N+1} respectively for the air and the basement rock

$$Z_o = Z_o\, R(z)R(z^{-1}) + Z_{N+1}T(z)T(z^{-1})$$

where R(z) is the z-transform of the reflected (upgoing) wavetrain and T(z) is the z-transform of the transmitted (downgoing) wavetrain. The reflected wavetrain R(z) is the seismic trace which is recorded at the surface. Isolating R(z), therefore,

$$1 - R(z)R(z^{-1}) = \frac{Z_{N+1}}{Z_o} T(z)T(z^{-1}) \qquad 4.1$$

The characteristic impedances are related to the transmission coefficients as demonstrated in Chapter 2

$$t_n = \frac{2Z_n}{Z_n + Z_{n+1}} \quad , \quad t'_n = \frac{2Z_{n+1}}{Z_n + Z_{n+1}}$$

and consequently

$$\frac{t'_n}{t_n} = \frac{Z_{n+1}}{Z_N} \text{ and } \frac{t'_o t'_1 \cdots t'_N}{t_o t_1 \cdots t_N} = \frac{Z_1 Z_2 \cdots Z_N}{Z_o Z_1 \cdots Z_N} = \frac{Z_{N+1}}{Z_o} \qquad 4.2$$

Using an earlier argument that the sedimentary system acts as a pure feedback system in producing the transmitted wave, T(z) must be proportional to the reciprocal of a polynomial

D(z). Choosing D(z) so that its leading coefficient is unity, the proportionality factor is equal to the downward transmission factor. Therefore the transmitted wave can be expressed as

$$T(z) = \frac{t_o t_1 \cdots T_N}{D(z)} \qquad 4.3$$

Substituting the results of 4.2 and 4.3 in 4.1

$$1 - R(z)R(z^{-1}) = \frac{t'_o t'_1 \cdots t'_N}{t_o t_1 \cdots t_N} \quad \frac{(t_o t_1 \cdots t_N)^2}{D(z)D(z^{-1})} \qquad 4.4$$

$$= \frac{\sigma_N^2}{D(z)D(z^{-1})}$$

where

$$\sigma_N^2 = t'_o t_o t'_1 t_1 \cdots t'_N t_N = (1-r^2_o)(1-r^2_1)\cdots(1-r^2_N)$$

Since R(z) is the reflected wave recorded at the surface and σ_N^2 is a constant, D(z) and the value of σ_N^2 can be determined as follows.

The autocorrelation of the seismic trace is computed

$$R_s(k) = \sum_{k=o}^{M} s(n+k)\, s(n)$$

then since the source is assumed to be a unit spike input its autocorrelation is a unit spike at zero lag and the difference between the source and trace autocorrelations, which is also an autocorrelation, is given by

$$R_x(o) = 1 - R_s(o)$$

$$R_x(k) = -R_s(k) \quad , \quad k \neq o$$

Note that the z-transform of this autocorrelation function is formed by the left hand side of equation 4.4. That is, taking z-transforms

$$Z\{R_x(k);\ k = o, \pm 1, \ldots \pm M\} = 1 - R(z)R(z^{-1}) = \frac{\sigma_N^2}{D(z)D(z^{-1})}$$

where $Z\{\ \}$ denotes the z-transform operation:

$$Z\{x(n)\} = \sum_{n=-\infty}^{\infty} x_n z^{-n}$$

The coefficients of D(z) are calculated by solving the normal equations

$$\sum_{i=o}^{N} d_i \; R_{dx}(-k) \qquad \text{for } k = 1,2,....N$$

The constant σ_N^2 can then be determined by

$$\sigma_N^2 = \sum_{i=o}^{N} d_i \; R_s(i)$$

An important feature of D(z) is that because from 4.3

$$D(z)T(z) = t_o t_1 ... t_N = \text{constant}$$

D(z) must be the z-transform of the prediction error filter which compresses the transmitted wave T(z) to a spike.

The feedforward or moving-average component of the reflected seismic trace is invoked by similar means. The reflected seismic trace comprises direct reflections and delayed reverberated reflections increasing in abundance and variety with each successive layer. For the n^{th} layer the contributions can be described by

$$R(z)^n = r'_n + t_n R_{n-1} t'_n z + t_n R_{n-1} r'_n R_{n-1} t_n z^2 + ...$$

which can be factored to yield

$$R(z)^n = r'_n + t_n R_{n-1} t'_n z \, [1 + r'_n R_{n-1} z + (r'_{n-1} z)^2 + \ldots]$$

Using the geometric series the expression for R(z) becomes the more manageable

$$R(z)^n = \frac{r'_n + t_n R_{n-1} t'_n z}{1 - r'_n R_{n-1} z}$$

The reflected seismic trace R(z) which comprises all of the $R(z)^n$ for n = 0,1,2,...N is therefore composed of a melange of purely reverberatory transmitted waves, characterized by the reciprocal of the polynomial D(z), and the purely feed-forward reflected energy which can be characterized by the polynomial C(z) resulting in the total reflected seismic trace R(z) characterized by

$$R(z) = \frac{C(z)}{D(z)}$$

Hubral et al subsequently demonstrated that this result is equivalent to a sum auto-regressive characterization of the seismic process with higher order auto-regressive terms [39].

It is recognized that this discussion does not constitute a proof of the ARMA (p,q) model characterization of the seismic reflection trace. It is intended only to provide motivation for the preferred application of ARMA (p,q) models in the representation and analysis of seismic data. Ironically the ARMA (p,q) characterization developed by Robinson argues against the use of ARMA (p,q) models in the analysis of seismic data. The model intimates a correspondence between the coefficients of the numerator feedforward polynomial and the reflection coefficient series,

$$(c_0, c_1, \ldots . c_N) \cong (r_0, r_1, \ldots . r_N)$$

Consequently the ARMA (p,q) representation of the data includes the entire trace and not just the wavelet. Deconvolution with the ARMA (p,q) model would yield not the desired reflection coefficient series but the source spike alone. This, however, is consistent with the assumptions on which Robinson's development is based. Generally in linear modelling a white noise input is assumed and in applications to seismic data the reflection coefficient series is typically considered to constitute the white noise excitation so that the model parameterizes the source wavelet and subsequent modifying influences such as earth filtering. But Robinson's model was developed with a unit spike excitation

representing the source wavelet. The model, therefore, had to include all modifying influences between that spike source wavelet and the resultant reflected seismic trace and predominant amongst those modifiers are the reflection coefficients.

It would seem then that an AR (p) model with an assumed white noise excitation corresponding to the reflection coefficient series should provide as useful an analytical tool as an ARMA (p,q) model with a unit spike input for handling seismic data. The ARMA (p,q) model of Robinson, however, makes no assumptions about the statistical properties of the reflection coefficient series. The AR (p) models will overfit to compensate for a non-white reflection coefficient series and may thereby incorporate geological information in the model. AR (p) deconvolution, therefore, has an undesirable potential for deconvolving geology. The AR (p) component of the Robinson ARMA (p,q) model would not suffer the same overfitting problems and if isolated should provide a superior model for the design of deconvolution operators.

4.2.2 Ricker/Feedback ARMA (p,q) Seismic Model

The Ricker/Feedback model depicts the absorptive earth filtering effect as a moving-average process, the reverberatory feedback characteristics of multiple reflectors as an auto-regressive process, the reflection coefficient series as white noise input to the model and the recorded seismic data as the model output. The result is a more general and useful model representation of seismic data than offered by Robinson.

The moving-average description of the absorptive earth filtering process is derived from the work of Ricker on wavelet theory. The auto-regressive description of the feedback process is familiar from Chapter 2 and was employed in the Robinson model.

In the early 1940's Norman Ricker developed the "Wavelet Theory of Seismogram Structure [40 - 43]. His work was motivated by the failure of classical wave theory to describe observed seismic data, and was revolutionary in its description of the seismogram as a superposition of transient waveforms varying in amplitude but deterministic in shape, or character. Ricker's work implied but fell just short of stating the convolutional model of the seismogram as a

wavelet convolved with a reflection coefficient series. Robinson and others at MIT in the early 1950's formally recognized the convolutional model implied in the work of Ricker and brought the then recently developed field of signal processing to bear on the enhancement of seismic data - the most important result of which was development of the process of seismic deconvolution.

Although in retrospect providing the foundation for the development of the convolutional model is the most important result of Ricker's work, what Ricker developed was a theory describing transient waves in visco-elastic media. Classical wave theory does not allow for the absorptive effects of internal friction as wave passes through the earth so Ricker used Stoke's wave equation which incorporates a dissipation term.

Assuming, without loss of generality, plane waves travelling along the positive x-axis the classical wave equation is

$$\frac{\partial^2 \chi(x,t)}{\partial x^2} = \frac{2}{v^2} \frac{\partial^2 \chi(x,t)}{\partial t^2} \qquad 4.5$$

where $\chi(x,t)$ is the elastic displacement, and v is longitudinal wave velocity. The general solution of 4.5 is

$$\chi(x,t) = f_1(x-vt) + f_2(x+vt)$$

where f_1 and f_2 are arbitrary functions, or wavelets, f_1 travelling in the direction of the positive x-axis and f_2 travelling in the direction of the negative x-axis. Both f_1 nd f_2 travel at velocity v and remain unchanged in shape with respect to time and distance. Observational data, however, suggest that wavelets change dramatically with time and distance.

Asuming absorption to be the major inflouence on the modification of wavelet shape Ricker used Stoke's wave equation, namely:

$$\frac{\partial^2}{\partial x^2}\left(\chi(x,t) + \frac{4\eta}{3\rho v^2}\frac{\partial \chi(x,t)}{\partial t}\right) = \frac{1}{v^2}\frac{\partial^2 \chi(x,t)}{\partial t^2}$$

where $(4\eta/3\rho v^2)(\partial/\partial t)$ is a dissipation term which takes into account losses due to viscosity. η denotes viscosity and ρ denotes density.

The solution of wave equation proposed by Ricker is

$$\chi(x,t) = \frac{A\partial}{\partial t}\Phi(x,t) \cdot \equiv A\dot{\Phi}(x,t)$$

where A is a constant and

$$\Phi(x,t) = \Phi(u) = \sum_{n=o}^{\infty} \left(\frac{2}{x}\right)^{(n+1)/2} \Psi_n(u)$$

and where

$$u = \frac{t - x}{(x/2)^{1/2}} \quad .$$

The $\Phi(u)$ are termed generating functions. The $\Psi_n(u)$ Ricker described as wavelet functions, and are defined in terms of Hermite functions.

$$\Psi_o^o(u) \equiv \frac{\pi}{2} \exp\left(\frac{-u^2}{4}\right)$$

$$\Psi_o^m(u) \equiv \frac{d^m}{du^m} \Psi_o^o(u)$$

Ricker's solution in spherical coordinates is written as

$$\Phi(u) = \sum_{n=o}^{\infty} \left(\frac{2}{R}\right)^{(n+3)/2} \Psi_n(u)$$

where R is a dimensionless radial distance number.

Since geophones typically record the velocity of the earth's motion, however, it is necessary to determine $\dot{\chi}(R,t) = \Phi(u)$, the velocity function

$$\Phi(u) = \sum_{n=o}^{\infty} \left(\frac{2}{R}\right)^{(n+5)/2} \Psi_n^2(u)\ \eta\ \left(\frac{2}{R}\right)^{5/2} \gamma(u/R)$$

where notation used is such that

$$\frac{d^m}{du^m} \Psi_n(u) = \Psi_n^m(u)$$

and a dot denotes a derivative with respect to time.

$\gamma(u/R)$ is called the velocity wavelet form function which specifies the shape of the wavelet. At $R \to \infty$ $\gamma(u/R) \simeq \Psi_o^2(u)$, that is the wavelet assumes a constant shape with distance travelled and further absorptive effects have negligible influence.

The steady state velocity wavelet form function is therefore

$$\gamma(u/\infty) \simeq \underset{o}{\Psi 2}(u) = \kappa(u^2-2)\ \frac{\pi}{2}\ \exp\left(\frac{-u^2}{4}\right)$$

where κ is a gain constant.

Since R is fixed u becomes a function of time alone and so for discrete time samples a moving average process can be defined in terms of z-transforms as

$$Z\{\gamma(n/\infty)\} = \kappa\frac{\pi}{2} \sum_{n=o}^{\infty} (n^2-2)\ \exp\left(\frac{-n^2}{4}\right)\ z^{-n}$$

But the term $\exp(\frac{-n^2}{4})$ rapidly becomes negligible with increasing n such that, to good approximation, the summation can be considered to range over M, where M is finite. Furthermore the exponential is an analytic function so that the z-transform is analytic.

The seismic wavelet shape due to travel through an absorptive media is therefore expressible as a moving-average process with z-transform N(z). The wavelet shape due to the superposition of reverberated impulse reflections has already been demonstrated to be expressible as an auto-regressive process

with z-transform 1/D(z). An ARMA description of seismic data consequently models both the earth filtering and multiple feedback facets of impulse wavelet modification. Figure 4.3 illustrates this result.

As mentioned earlier these descriptions are only intended to provide motivation for the use of ARMA (p,q) models in the analysis of seismic data. However, whereas the Robinson model suggested that only the auto-regressive component, the undesirable reverberation characteristics should be deconvolved out of the data, the Ricker/Feedback model indicates that a full ARMA (p,q) deconvolution operator should be used to get rid of the undesirable effects of both feedback and absorbtion.

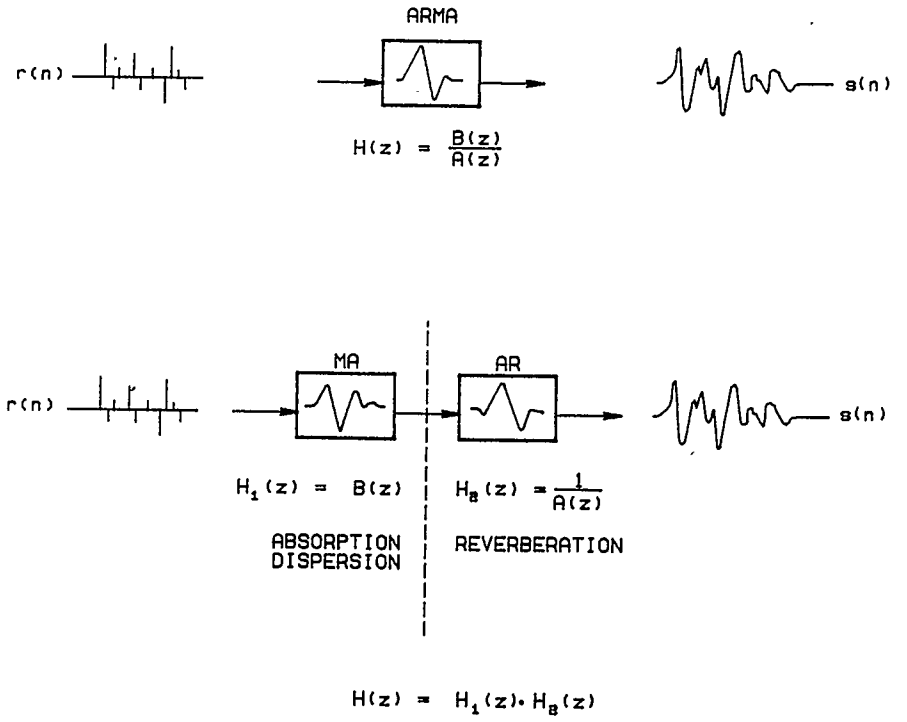

Figure 4.3 EQUIVALENT SYSTEMS DEMONSTRATING THE ARMA DESCRIPTION OF THE SEISMIC PROCESS $r(n) * h(n) = s(n)$ WHERE $h(n)$ COMPRISES SOURCE SIGNATURE AND EARTH FILTERING EFFECTS - GENERALLY CONSIDERED TOGETHER AS THE "SEISMIC WAVELET" $w(n)$.

4.3 ARMA (p,q) Parameter Determination

4.3.1 Box-Jenkins Method [7]

The characteristic difference equation for an ARMA model excited by a white noise sequence $\{\varepsilon(n)\}$ with variance σ_ε^2 is:

$$x(n) = -\sum_{i=1}^{p} a_i\, x(n-i) + \sum_{i=0}^{q} b_i\, \varepsilon(n-i)$$

multiplying both sides of the characteristic equation by $x^*(n-m)$ and taking expectations

$$E\{x(n)x^*(n-m)\} = E\{-\sum_{i=1}^{p} a_i\, x(n-i)x^*(n-m)\} + E\{\sum_{i=0}^{q} b_i\, \varepsilon(n-i)x^*(n-m)\}$$

or

$$R_x(m) = -\sum_{i=1}^{p} a_i\, R_x(m-i) + \sum_{i=0}^{q} b_i R_{x\varepsilon}(m-i)$$

where $R_x(k)$ denotes the autocovariance of the sequence $\{x(n)\}$ and $R_{x\varepsilon}(k)$ denotes the cross covariance between $\{x(n)\}$ and $\{\varepsilon(n)\}$. Since $R_{x\varepsilon}(k) = E\{x(n-k)\varepsilon(n)\}$, and $x(n-k)$ depends

only on inputs which have occurred up to time n-k it follows that

$$R_{X\varepsilon}(k) = 0 \quad k>0$$

$$R_{X\varepsilon}(k) \neq 0 \quad k \leq 0$$

Consequently $\sum_{i=o}^{q} b_k R_{X\varepsilon}(m-i) = 0$ for $m-i>0$ or $m \leq q+1$

and so the previous expression for $R_X(m)$ can be rewritten as

$$R_X(m) = -\sum_{i=1}^{p} a_i R_X(m-i) \quad \text{for } m \leq q+1$$

which can conveniently be written in matrix form as

$$\begin{bmatrix} R_X(q) & \cdots & R_X(q-p+1) \\ \vdots & & \vdots \\ R_X(q+p-1) & \cdots & R_X(q) \end{bmatrix} \begin{bmatrix} a_1 \\ \vdots \\ a_p \end{bmatrix} = \begin{bmatrix} R_X(q+1) \\ \vdots \\ R_X(q+p) \end{bmatrix}$$

The auto-regressive parameters a_i i=1,2,...p are then determined using the recursive formulae of Durbin.

The moving-average parameters are calculated using the auto-regressive coefficients and the first q+1 auto-covariances. As described earlier the first q+1 lags of the autocovariance function contain information about both the auto-regressive and moving-average parameters whereas the far lags beyond q+1 contain only auto-regressive components, consequently it is standard practice in ARMA parameter estimation to determine the auto-regressive parameters at the far lags of the autocovariance function and then use those information in conjuction with the near lags to determine the moving-average parameters.

Using the auto-regressive parameters a new sequence $\{x'(n)\}$ is derived, namely $x'(n) = x(n)-a_i x(n-1)-\ldots-a_p x(n-p)$. The autocovariances $R_x'(k)$ (k=0,1,...q) of this derived sequence are then calculated and the moving-average components are determined using the iteration

$$\sigma_x = \frac{R_x'(0)}{1+b_1^2+\ldots b_q^2}$$

$$b_k = \frac{-(R_x'(k) - b_1 b_{k+1} - b_2 b_{k+2} - \ldots - b_{q-k} b_1)}{\sigma_x^2}$$

where $b_o=0$ and b_k $k=1,2,\ldots q$ are set to zero to start the iteration and the values b_k and σ_x^2 to be used in any subsequent calculation are the most up to date values available.

4.3.2 The Cadzow Method

Fundamental to Cadzow's approach to determining ARMA model coefficients is the development of a recursive relationship between the autocorrelation function of the model time series and the coefficients of the model (8, 44-46).

To facilitate this development Cadzow splits the autocorrelation function into its causal and non-causal images such that $r_x(n) = r_x^+ + r_x^+(-n)^*$ where

$$r_x^+(n) = \begin{cases} 0.5\, r_x(o), & n = o \\ r_x(n), & n > o \\ o, & n < o \end{cases}$$

The postscripted asterisk denotes the complex conjugate.

Then, since by definition $S_x(w) = F\{r_x(n)\}$

$$S_x(w) = F\{r_x(n)\} = F\{r_x^+(n) + r_x^+(-n)^*\} = F\{r_x^+(n)\} + F\{r_x^+(-n)^*\}$$

$$= \sum_{n=-\infty}^{\infty} r_x^+(n) e^{-jwn} + \sum_{n=-\infty}^{\infty} r_x^+(-n)^* e^{-jwn}$$

$$= \sum_{n=-\infty}^{\infty} r_x^+(n) e^{-jwn} + \left[\sum_{n=-\infty}^{\infty} r_x^+(-n) e^{jwn}\right]^*$$

$$= \sum_{n=-\infty}^{\infty} r_x^+(n)e^{-jwn} + [\sum_{n=-\infty}^{\infty} r_x^+(n)e^{-jwn}]^* = S_x^+(w) + S_x^+(w)^*$$

$$= 2\mathrm{Re}[S_x^+(w)]$$

Now since an ARMA spectral model is assumed, the power spectral density function is defined as

$$S_x(w) = \frac{|\, b_o + b_1e^{-jw} + \ldots + b_qe^{-jqw} \,|^2}{|\, 1 + a_1e^{-jw} + \ldots + a_pe^{-jpw} \,|} = 2\mathrm{Re}[S_x^+(w)]$$

$S_x^+(w)$ is chosen to be a rational function $S_x^+(w) = \frac{C(w)}{D(w)}$

so if

$$S_x(w) = \left|\frac{B(w)}{A(w)}\right|^2 \text{ then } \left|\frac{B(w)}{A(w)}\right|^2 = 2\mathrm{Re}\ \frac{[C(w)]}{[D(w)]}$$

and $$\frac{C(w)}{D(w)} = \frac{C(w)}{D(w)} \cdot \frac{D(w)^*}{D(w)^*} = \frac{C(w)D(w)^*}{|\, D(w) \,|^2}$$

Since

$$\left|\frac{B(w)}{A(w)}\right|^2 = \left|\frac{B(w)}{A(w)}\right|^2_2 = 2\mathrm{Re}[\frac{C(w)D(w)^*}{|\, D(w) \,|^2}] \text{ then } |\, A(w) \,|^2 = |\, D(w) \,|^2$$

so that the autoregressive coefficients (i.e. denominator coefficients) of the ARMA spectral model are identical to the denominator coefficients of the rational model for $S_x^+(w)$.

Looking at the numerators again $|B(w)|^2 = 2Re[C(w)D(w)^*]$ B(w) is order q and D(w) is order p so C(w) must be of order 2q-p.

Cadzow then restricts $p \leq q$ for further development.

Under the restriction that $p \leq q$ and assuming $p = q$, or equivalently $c_{q+1} = c_{q+2} = \ldots = c_p = o$, then

$$S_x^+(w) = \frac{C(w)}{D(w)}$$

$$= \frac{c_o + c_1 e^{-jw} + \ldots + c_p e^{-jpw}}{1 + a_1 e^{-jw} + \ldots + a_p e^{-jpw}} = \frac{\sum_{i=o}^{p} c_i e^{-jiw}}{1 + \sum_{i=1}^{p} a_i e^{-jiw}}$$

multiplying both sides by $1 + \sum_{i=1}^{p} a_i e^{-jiw}$

$$S_x^+(w)\left[1 + \sum_{i=1}^{p} a_i e^{-jiw}\right] = \sum_{i=o}^{p} c_i e^{-jiw}$$

$$\text{so } S_X^+(w) = \sum_{i=o}^{p} c_i e^{-jiw} - \left[\sum_{i=1}^{p} a_i e^{-jiw}\right] S_X^+(w)$$

taking inverse z-transforms and re-arranging summations gives

$$r_X^+(n) = \sum_{i=o}^{p} c_i \delta(n-i) - \sum_{i=1}^{p} a_i r_X^+(n-i)$$

This recursive relationship is the basis for Cadzow's method of estimating the coefficients of the ARMA model.

The recursive determination of $r_X^+(n)$ is in general not the same as

$$\hat{r}_X^+(n) = \frac{1}{N-p} \sum_{k=1}^{N-p} x(n)\, x(n+p)$$

since the recursive determination of $r_X^+(n)$ does not suffer end effect or truncation problems. Consequently, if $\hat{r}_X^+(n)$ is substituted into the relation for $r_X^+(n)$ as

$$\hat{r}_X^+(n) = \sum_{i=o}^{p} c_i\, \delta(n-i) - \sum_{i=1}^{p} a_i \hat{r}_X^+(n-i)$$

equality is not to be expected given the same c_i and a_i $(i=1,2,\ldots.p)$ as in the derived equation. The discrepancy

$$e(n) = r_x^{\pm}(n) + \sum_{i=1}^{p} a_i r_x^{\pm}(n-i) - \sum_{i=o}^{p} c_i \delta(n-i)$$

$o \leq n \leq N - 1$ is termed the error and is squared and minimized with respect to the a_i coefficients at lags $q \leq m \leq N$ at which the c_i coefficients are zero, such that

$$e(n) = \hat{r}_x^m(n) + \sum_{i=1}^{p} a_i \hat{r}_x^m(n-i)$$

where $\hat{r}_x^m(n)$ denotes the autocorrelation of $x(n)$ at lags exceeding m.

Phrasing the same result in a slightly different way, the coefficients a_i are chosen so as to force a best fit in a least squares sense of the model autocorrelation to the estimated autocorrelation.

Cadzow's development arrives at the same end (i.e. the same error to be minimized) but without specific recourse to the recursive relation, as follows:

The characteristic difference equation for an ARMA model excited by a white noise sequence $\{\varepsilon(n)\}$ is

$$x(n) = \sum_{i=o}^{q} b_i \varepsilon(n-i) - \sum_{i=1}^{p} a_i x(n-i)$$

multiplying both sides by $x^*(n-m)$ gives

$$x(n)x^*(n-m) = \left[\sum_{i=o}^{q} b_i\varepsilon(n-m) - \sum_{i=1}^{p} a_i x(n-i)\right]x^*(n-m) \qquad 4.6$$

Now $\varepsilon(m)$ and $x(n)$ are uncorrelated for $m > n$ so

$$\sum_{i=o}^{q} b_i\varepsilon(n-i)x^*(n-m) \to 0$$

for $n-i > n-m$ or $i < m$, but since $o \leq i \leq q$ we require $q < m$.

The arrow is used instead of equality because although $\varepsilon(n-i)$ and $x^*(n-m)$ are uncorrelated for $i < m$ and have zero mean over the summation for $o \leq i \leq q$; $q < m$, the product $\varepsilon(n-i)x^*(n-m)$ for any particular value of i in the summation need not be exactly zero, it is only required that the products average to zero over the summation. This opportunity for non-zero products, denoted here by the arrow, forms the basis for Cadzow's error term and subsequent estimation of the a_i coefficients.

Summing equation 4.6 over $m < n \leq N$ and dividing by N-m yields

$$\frac{1}{N-m}\sum_{n=m+1}^{N} x(n)x^*(n-m)$$

$$= \frac{1}{N-m} \sum_{n=m+1}^{N} \sum_{i=o}^{q} b_i \varepsilon(n-i)x^*(n-m) - \frac{1}{N-m} \sum_{n=m+1}^{N} \sum_{i=1}^{p} a_i x(n-i)x^*(n-m)$$

recognizing that the estimate of the autocorrelation is defined as

$$\hat{r}_x^m(m) = \frac{1}{N-m} \sum_{n=m+1}^{N} x(n)x^*(n-m)$$

where $\hat{r}_x^m(m)$ denotes the estimate of the autocorrelation of input x(n) for lags exceeding m, and rearranging summations provides the following relation

$$\hat{r}_x^m(m) = \sum_{i=o}^{q} b_i \left[\frac{1}{N-m} \sum_{n=m+1}^{N} \varepsilon(n-i)x^*(n-m)\right] - \sum_{i=1}^{p} a_i \left[\frac{1}{N-m} \sum_{n=m+1}^{N} x(n-i)x^*(n-m)\right]$$

$$= \sum_{i=o}^{q} b_i \left[\frac{1}{N-m} \sum_{n=m+1}^{N} \varepsilon(n-i)x^*(n-m)\right] - \sum_{i=1}^{p} a_i \hat{r}_x^m(m-i)$$

$$\text{or } \hat{r}_x^m(m) + \sum_{i=1}^{p} a_i \hat{r}_x^m(m-i) = \sum_{i=o}^{q} b_i \left[\frac{1}{N-m} \sum_{n=m+1}^{N} \varepsilon(n-i)x^*(n-m)\right] \text{ where } q < m.$$

As mentioned earlier the right hand side should tend to zero but may not be identically zero for particular values of i. Cadzow defines this term as the error e(m) such that

$$e(m) = \hat{r}_x^m(m) + \sum_{i=1}^{p} a_i \hat{r}_x^m(m-i)$$

and proposes minimization of this error squared and weighted as an appropriate method for determining the a_i coefficients (minimization is with respect to the a_i coefficients).

Note that this expression for the error is the same as that which was derived independently directly from the recursive relation.

By either development then the error relation is

$$e(m) = \hat{r}_x^m(m) + \sum_{i=1}^{p} a_i \hat{r}_x^m(m-i)$$

This error relation can be rewritten in terms of matrix notation to give

$$\underline{e} = \underline{r} + R\underline{a} \qquad 4.7$$

where $\underline{e}$ is the (N-p-1) x 1 vector of error terms, $\underline{r}$ is the (N-p-1) x 1 vector of autocorrelation terms, $\underline{a}$ is the p x 1 vector and autoregressive coefficients and R is the (N-p-1) x p correlation matrix.

Cadzow proposes minimization of a quadratic functional f(a) of e(m) with respect to the coefficients a_i defined as

$$f(a) = \sum_{m=p+1}^{N} W(m)e^2(m)$$

which can be expressed in matrix notation as the Hermitian form

$$f(a) = \underline{e}^{\neq}W\underline{e} \qquad 4.8$$

where $^{\neq}$ denotes the complex conjugate transpose operation and W is a (N-p-1) x (N-p-1) positive semi-definite Hermitian weighting matrix. Substituting equation 4.7 into 4.8 and minimizing with respect to the coefficients $\underline{a}$ yields a set of p linear equations described by

$$[R^{\neq}WR]\underline{a} = -R^{\neq}Wr$$

The selection of appropriate elements in the weighting matrix W can be accomplished by the iterative technique developed by Moses [45, 47].

Finally, the numerator coefficients c_i are computed by substituting the estimated a_i coefficients and an estimate of $r_x^+(n)$ into the recursive relationship

$$r_x^+(n) = \sum_{i=o}^{p} c_i \delta(n-i) - \sum_{i=1}^{p} a_i r_x^+(n-i)$$

such that

$$\sum_{i=o}^{p} c_i \delta(n-i) = \hat{r}_x^o(m) + \sum_{i=1}^{p} a_i \hat{r}_x^o(n-i)$$

where

$$\hat{r}_x^o(n) = \frac{1}{N-p} \sum_{i=1}^{N-p} x(i)x^*(n-i)$$

or

$$c_k = \hat{r}_x^o(k) + \sum_{i=1}^{k} \hat{r}_x^o(k-i) \qquad o \leqslant k \leqslant p.$$

Note that at lags $k \leqslant (p = q)$ both c_k and a_k terms contribute.

Cadzow's method is computationally efficient and has been shown to yield high resolution spectral estimates [48]. Ogino [49, 50] has demonstrated that further computational improvement can be realized by appropriate modification of the vector and matrix entries in an equivalent but more general formulation of the error relation when q = p.

The method has two serious shortcomings, however. Firstly, the MA coefficients are not explicitly determined. The modified coefficients are suitable for spectral estimation but cannot be related to the MA parameters of the ARMA model. Secondly, the spectral estimates generated by the method can be negative. Kay [51] recognized this problem and proposed a solution which ensures that the autocorrelation function of the residual "MA" time series obtained from the a_i estimates and the input data yields a positive semi-definite sequence. Moses [47] proposed two similar solutions also based on the residual "MA" time series. Recently Salami [10] proposed an extension of Cadzow's method which yields the direct MA coefficients and ensures non-negative spectral estimates. Salami's method is described in section 4.3.3.

Two further problems with Cadzow's method are the requirement that $q \leq p$ and the need for a priori knowledge of the model order (p,q).

4.3.3 The Method of Salami

Salami has proposed a modified Cadzow algorithm which ensures positive real power spectral estimates and provides direct estimates of the MA coefficients [10, 66]. The method involves obtaining estimates of the AR and modified MA coefficients via the Cadzow method, defining the MA power spectral density function in terms of the estimated coefficients, modifying the coefficients in a purposeful manner so as to make the MA spectral estimates positive real, and computing the direct MA coefficients from the MA power spectral density function using Kolmogorov spectral factorization. Salami has also proposed a modified singular valued decomposition (SVD) technique to determine the order of the AR polynomial [10]. The SVD technique employs iterative spectral matching and monitoring of the effective rank of the covariance matrix to determine the AR sub-model order.

Salami initially uses Cadzow's approach (Section 4.3.2) to split the autocorrelation function into its causal and non-causal images and define causal and non-causal power spectral density functions by Fourier transform operations on the autocorrelations.

That is

$$r_x(n) = r_x^+(n) + r_x^-(n)^*; \text{ where } r_x^-(n)^* = r_x^+(-n)^*$$

and

$$S_x(w) = S_x^+(w) + S_x^-(w) \; ; \text{ where } S_x^-(w) = S_x^+(w)^*, \text{ and}$$

where

$$S_x^+ = \sum_{n=-\infty}^{\infty} r_x^+(n)e^{-jwn}; \; S_x^-(w) = \sum_{n=\infty}^{-\infty} r_x^-(n)^*e^{-jwn}$$

Defining the causal power spectral density function as the ratio of two polynomials C(w) and D(w) and recognizing complex symmetry it follows that

$$S_x(w) = 2\text{Re}[S_x^+(w)] = 2\text{Re}\left[\frac{C(w)}{D(w)}\right] \qquad 4.9$$

Employing the ARMA spectral model and rewriting equation 4.9

$$S_x(w) = \frac{|B(w)|^2}{|A(w)|^2} = \frac{2\text{Re}[C(w)D(w)^*]}{|D(w)|^2} \qquad 4.10$$

Therefore, assuming D(w) = A(w) such that coefficents $d_i = a_i$, i = 1,2,....p for AR order p, equation 4.10 becomes

$$S_x(w) = \frac{|B(w)|^2}{|A(w)|^2} = \frac{2Re[C(w)A(w)]}{|A(w)|^2} \quad . \qquad 4.11$$

Cadzow's method then develops a recursive relationship for the causal image of the autocorrelation function in terms of the AR and modified MA parameters [8] as follows.

$$r_x^+(n) = \sum_{i=o}^{p} c_i \delta(n-i) - \sum_{i=1}^{p} a_i r_x^+(n-i) \qquad 4.12$$

Restricting n>m to lags beyond which the c_i coefficients are zero and defining e(n) as the error or non-zero residual which is present when the causal autocorrelation calculated from the data, $\hat{r}_x^m(n)$ is substituted into the recursive relationship of equation 4.12 to give

$$e(n) = \hat{r}_x^m(n) + \sum_{i=1}^{p} a_i \hat{r}_x^m(n-i) \quad .$$

Minimization of the squared error yields the AR coefficients. The modified MA coefficients are then calculated via

substitution into the recursive definition of the causal autocorrelation function in equation 4.12 at lags where the c_i coefficients are non-zero.

$$c_k = \sum_{i=1}^{k} a_i \hat{r}_x^+(k-i) \; ; \; o \leq k \leq p \qquad 4.13$$

The method of Salami extends the Cadzow method so as to evaluate the actual MA coefficients, b_i, rather than the modified coefficients, c_i; $i = 1,2,....q$ $(q<p)$. Salami's method also ensures against undesirable negative spectral estimates. Salami's method recognizes that rearrangement of equation 4.11 isolates the actual MA spectral estimate in terms of the AR and modified MA parameters.

$$| B(w) |^2 = A(w)*C(w) + A(w)C(w)*$$

Letting G(w) denote the right-hand side of the equation and substituting the Fourier transform of equation 4.13 for C(w) yields

$$G(w) = A(w)*A(w)\hat{R}_x^+(w) + A(w)A(w)*\hat{R}_x^+(w)* \; .$$

where $\hat{R}_x^+(w)$ denotes the Fourier transform of the causal autocorrelation $\hat{r}_x^+(n)$.

Taking inverse transforms and utilizing complex symmetry

$$g(k) = \sum_{i=1}^{p} \sum_{j=1}^{p} a_i^* a_j \hat{r}_x(k+i-j)$$

where g(k) is the inverse Fourier transform of G(w).

To ensure non-negative MA spectral estimates it is necessary that g(k) be positive definite; Salami proposes two methods to accomplish this. The first method is to increase the g(o) term such that

$$g'(k) = g(k) + \sigma^2$$

The second method is to apply an exponential weighting function ζ^i to the modified MA coefficients c_i and/or the AR coefficients a_i.

With g'(k) positive real it follows that $|B'(w)|^2$ is positive real and spectral factorization can be applied to determine the direct MA coefficients b'_i. Unfortunately, factorization does not yield a unique set of coefficients b'_i, since G(w) can be generated by many different series.

Only one series b'_i can be minimum phase, however, and Salami determines the unique minimum phase sequence via Kolmogorov factorization following Silvia and Robinson [1].

The z-transform of B'(w), denoted by B'(z), can be expressed in terms of its coefficients b'_i as follows:

$$B'(z) = \sum_{i=o}^{\infty} b'_i z^{-i} \qquad 4.14$$

As discussed above the b'_i are not unique. Imposing a minimum phase requirement on B'(z), however, dictates that all the zeroes of the system response lie within the unit circle in the z-plane: furthermore, MA systems, such as B'(z), have no poles where values approach infinity and so outside the unit circle the natural logarithm of B'(z) can be defined and expressed as a Taylor series expansion. That is,

$$\log B'(z) = \sum_{i=o}^{\infty} \beta_i z^{-i} \quad ; \quad |z| > 1 \ . \qquad 4.15$$

Rewriting 4.15 letting $z = e^{-jw}$, then taking only the real part and expanding using the complex conjungate yields

$$\log|B'(w)| = \beta_o + \sum_{i=-\infty}^{-1} \frac{\beta_{-i}^*}{z} e^{-jwi} + \sum_{i=1}^{\infty} \frac{\beta_i e^{-jwi}}{z} \qquad 4.16$$

Noting that $\log|B'(w)|$ is a periodic function its discrete Fourier transform can be expressed as

$$\log|B'(w)| = \sum_{i=-\infty}^{\infty} \partial_i e^{-jwi}; \qquad 4.17$$

$$\partial_i = \frac{1}{2\pi} \int_{-\pi}^{\pi} \log|B'(w)| e^{jwi} dw \qquad i = 0, \pm 1, \pm 2, \ldots.$$

$$= \frac{1}{4\pi} \int_{-\pi}^{\pi} \log G'(w) e^{jwi} dw \qquad i = 0,1,2,\ldots.$$

Equating the expressions for $\log|B'(w)|$ in equation 4.15 and 4.17 yields the coefficients β_i of the Taylor series for $\log B'(z)$ in terms of the b'_i so that finally the desired coefficients of the minimum phase MA system $B'(z)$ can be uniquely determined by comparing equivalent descriptions of descriptions of $B(z)$ in equations 4.14 and 4.15 and solving for b'_i. That is

$$\sum_{i=o}^{\infty} b'_i z^{-i} = \exp\{\sum_{i=o}^{\infty} \beta_i z^{-i}\} \qquad 4.18$$

By dividing equation 4.18 into its derivative with respect to z and rearranging terms, a recursive relation can be developed to compute the direct minimum phase MA coefficients b'_i [30]

$$(i+1)b'_{i+1} = \sum_{n=o}^{i} b'_n(i+1-n)\beta_{i+1-n}; \quad i = 0,1,2,\ldots., n-1$$

where n is the number of points in the discrete Fourier transform and $b'_o = \exp\{\beta_o\}$.

4.3.4 GRT Method

Gutowski, Robinson and Treitel (9, 52, 53) have suggested an iterative least squares method of determining the parameters of an ARMA model. The method is conceptually simple and easy to implement but has several shortcomings, chief of which is the requirement of a good initial estimate of the moving-average parameters of the model to initialize the iteration. Starting with an estimate of the moving- average parameters and the known output series response to a unit spike excitation, the auto-regressive parameters are estimated by a least squares shaping filter (Wiener Filter) and the shaping filter estimate is then used to refine the initial estimate as illustrated in Figure 4.4.

The method develops as follows: Consider a sequence x(n) which is the output response to an ARMA model with input u(n) where u(n) is a unit spike situated at the origin. Then

$$x(n) = -\sum_{i=1}^{p} a_i x(n-i) + \sum_{i=0}^{q} b_i u(n-i)$$

taking z-transforms of both sides

$$\Omega(z) = \frac{B(z)}{A(z)} U(z) = \frac{B(z)}{A(z)} \text{ since } U(z) = 1$$

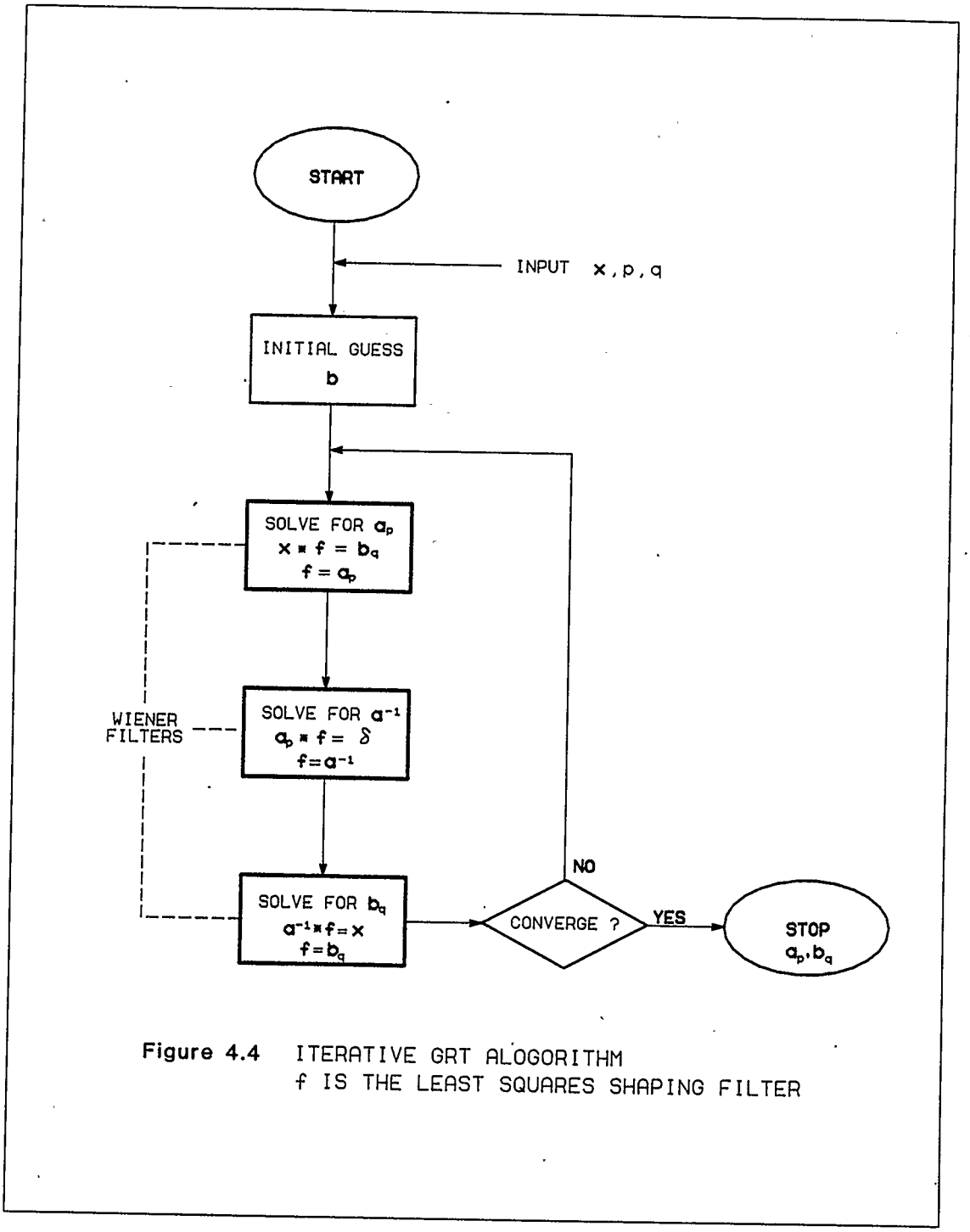

Figure 4.4 ITERATIVE GRT ALOGORITHM
f IS THE LEAST SQUARES SHAPING FILTER

then $A(z)\ \Omega(z) = B(z)$ or $\underline{a} * \underline{x} = \underline{b}$ where

$$\underline{a} = a(i),\ i = 0,1,2,....q;\ \underline{b} = b(j),\ j = 0,1,2,...p;$$

$$\underline{x} = x(k),\ k = 0,1,2,....s$$

Knowing $\underline{x}$ and making an initial guess at $\underline{b}$, $\underline{a}$ is calculated as the shaping filter $\underline{f}$ in the equation $\underline{x} * \underline{f} = \underline{b}$

Then, using the previously determined $\underline{a}$, $\underline{a}^{-1}$ is determined as $\underline{f}$ by $\underline{a} * \underline{f} = \delta$ where δ is the kronecker delta. Similarly the estimate $\underline{b}$ can be refined as $\underline{f}$ by $\underline{a}^{-1} * \underline{f} = \underline{x}$. The procedure is repeated until convergence occurs. The method guarantees a minimum phase $A(z)$ because of the Toeplitz recursion employed in the shaping filter determinations.

The method varies significantly from the previously described procedures in that it does not work off the autocovariance function calculating the auto-regressive parameters first at the far lags and then iteratively solving for the moving-average parameters. However, the requirement of a good initial estimate of the moving-average parameters severely limits the value of the method since unlike the auto-regressive parameters the moving-average parameters cannot be conveniently estimated from the data.

4.4 Deconvolution Using ARMA (p,q) Models

An ARMA (p,q) model of seismic data is expected to yield an analytic estimate of the seismic wavelet provided the reflection coefficient series of the earth is white. This seismic wavelet can therefore be used to design an inverse wavelet for deconvolution. Recall that the wavelet is really the impulse response of the filter whose transfer function is described by the ARMA (p,q) model estimate. Given an ARMA (p,q) model estimate

$$\hat{H}(z) = \frac{b_o+b_1z^{-1} + \ldots + b_qz^{-q}}{1+a_1z^{-1} + \ldots + a_pz^{-p}} \qquad 4.19$$

the wavelet estimate $\hat{w}(n)$ can be calculated using the direct method assuming a unit impulse input,

$$\hat{w}(n) = \sum_{i=o}^{q} b_i \delta(n-i) - \sum_{i=1}^{p} a_i w(n-i)$$

The inverse wavelet estimate required for deconvolution must have a model estimate $\hat{G}(z)$ such that $\hat{G}(z)\hat{H}(z) = 1$ or equivalently $\hat{G}(z) = [\hat{H}(z)]^{-1}$ so, obviously

$$\hat{G}(z) = \frac{1 + a_1 z^{-1} + \ldots + a_p z^{-p}}{b_o + b_1 z^{-1} + \ldots + b_q z^{-q}}$$

Taking the inverse z-transform yields

$$\hat{g}(n) = \frac{1}{b_o} \left[\delta(n) + \sum_{i=1}^{p} a_i \delta(n-i) - \sum_{i=o}^{q} b_i g(n-i)\right]$$

where g(n) is the inverse wavelet estimate, more often termed the deconvolution operator. Convolving $\hat{g}(n)$ with the seismic trace, s(n), under all of the invoked assumptions of stationarity of the wavelet, w(n), whiteness of the reflection coefficient spectra, guassian distribution of reflection coefficient amplitudes, r(n), no noise, and the appropriateness of the convolutional model yields the desired estimate of the reflection coefficient series $\hat{r}(n)$. That is

$$s(n) = w(n) * r(n)$$

$$\hat{r}(n) = s(n) * \hat{g}(n) \quad ; \quad \hat{g}(n) * w(n) \simeq \delta(o)$$

4.4.1 Stability Considerations

Since deconvolution requires the realizability of both the ARMA (p,q) model, $\hat{H}(z)$, and its inverse, $\hat{G}(z)$, it is necessary that both coefficient series a_i; i = 1,2,...p and b_i; i = 1,2,...q be minimum phase sequences. This important constraint ensures stability of the wavelet estimate and of the inverse wavelet estimate [30, 54].

Constraining the coefficient sequences a_i and b_i to be minimum phase is equivalent to ensuring that the poles and zeroes of $\hat{H}(z)$ lie within the unit circle in the z-plane. The expression for $\hat{H}(z)$ in equation 4.19 can be factored in terms of the roots of the numerator and denominator polynomials as follows [54]

$$\hat{H}(z) = K \frac{(1-z_1z^{-1})(1-z_2z^{-1})\ldots(1-z_qz^{-1})}{(1-p_1z^{-1})(1-p_2z^{-1})\ldots(1-p_pz^{-1})}$$

where K is an arbitrary constant and the z_i; i = 1,2,...q and the p_i; i = 1,2,...p are called the zeroes and poles respectively. Note that it is necessary that $|p_i| < 1$; i = 1,2,...p to ensure the stability of $\hat{H}(z)$.

Recall that $\hat{G}(z) = [\hat{H}(z)]^{-1}$, it follows that

$$\hat{G}(z) = \frac{1}{K} \frac{(1-p_1z^{-1})(1-p_2z^{-1})\ldots(1-p_pz^{-1})}{(1-z_1z^{-1})(1-z_2z^{-1})\ldots(1-z_qz^{-1})}$$

The poles of $\hat{H}(z)$ are therefore the zeroes of $\hat{G}(z)$ and the zeroes are the poles. To ensure the realizability of $\hat{G}(z)$, then, it is also necessary that $|z_i| < 1$; $i = 1,2,\ldots q$.

4.4.2 Phase Modification

The poles and zeroes of $\hat{H}(z)$ must lie within the unit circle to ensure stability and invertibility during deconvolution operator design. Once G(z) has been established, however, only the poles of $\hat{G}(z)$, z_i; $i = 1,2,\ldots q$, must remain within the unit circle; there is no need to similarly constrain the zeroes, p_i; $i = 1,2,\ldots p$. The zeroes of $\hat{G}(z)$ can be reflected outside the unit circle singly or in combination by filtering with the appropriate all pass networks. This has the effect of leaving the power spectrum of $\hat{G}(z)$ unchanged while changing the phase spectrum in a systematic way. The procedures yields a finite number of possible phase spectra for a given estimate.

Chapter 5. Results

5.1 Introduction

Various parametric modelling techniques, both AR (p) and ARMA (p,q), were applied to real and synthetic seismic data. The quality of the resultant models was assessed qualitatively by visual comparison with periodogram spectral estimates of the source data. The closer the fit of the model to the spectral shape of the periodogram, the better the model was judged to be.

Deconvolutions were performed by convolving the model inverses with the source data. The results with the most spiked output and flattest spectra were judged to be best. These performance assessment criteria did not discriminate against undesirable boosting of noise from the low S/N portions of the data spectrum, so that ultimately conclusions were inferred principally from study of spectral fits.

Decimation and demodulation were applied to the seismic data to alleviate oversampling. The models were re-run, and again the results were assessed on the basis of closest spectral match.

Modelling techniques illustrated are Least Squares, Levinson, and Burg AR (p) parameter estimators and Kay, Cadzow, Salami,

and Transient Error Method ARMA (p,q) parameter estimators. The ARMA (p,q) techniques of Box-Jenkins and Gutowski, Robinson and Treitel (GRT) were tested but did not yield usable results. The GRT method was particularly sensitive to the accuracy of an initial guess at the MA (q) parameters.

5.2 Model Input Data

Three data types were utilized as input to the modelling procedures: 1) seismic data; 2) synthetic seismic data; and 3) decimated seismic data. The seismic data were treated as the principle data set and the corresponding models are the focus of the results.

5.2.1 Seismic Data

Two seismic traces from a single shot file were considered. One a near offset trace, the other a middle offset trace. The two traces and their corresponding periodograms are illustrated in Figure 5.1 The near offset trace was studied extensively as it was considered more problematic and had already been briefly investigated in the work of Salami [66]. The data were acquired using a 3 hole pattern of shallow shots recorded through Mark 14 H_Z geophones into a DFSV recording system. The sampling rate was 2 milliseconds. The

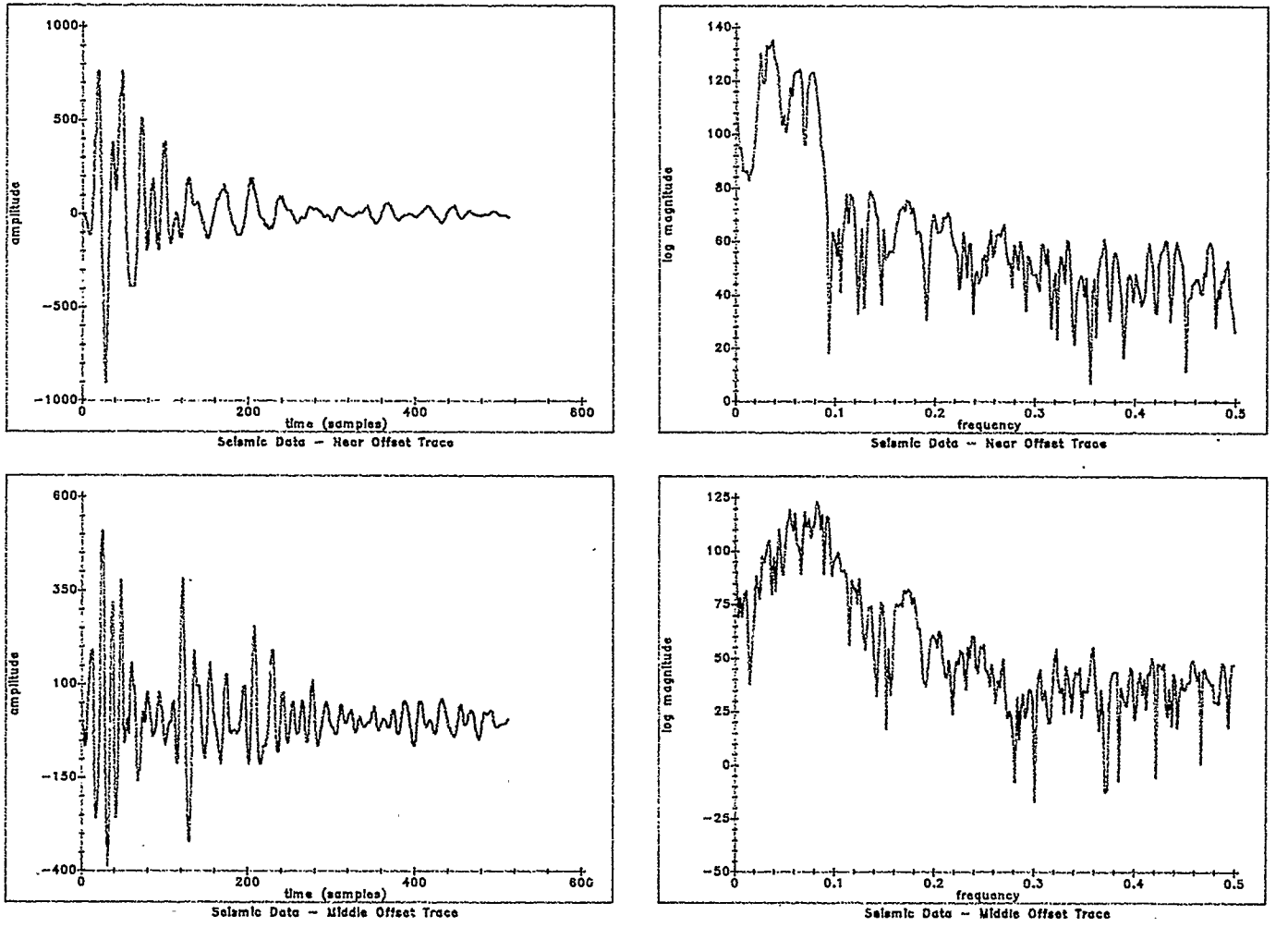

Figure 5.1 SEISMIC DATA – NEAR AND MIDDLE OFFSETS

data are considered to be of good quality although the near trace data were dominated by ground roll (low frequency surface waves).

5.2.2 Synthetic Data

Synthetic data were produced by creating a random sequence of primary events and generating the corresponding multiple (reverberation) sequence using a Weunchel algorithm [17]. Figure 5.2 depicts the primary events, the reverberations, and the resultant spike trace. Theory developed in Chapters 2 and 4 described the primary events as the innovation input to the white noise model and the multiple sequence as an autoregressive model response. Comparing the periodograms of the primary and multiple sequences in Figure 5.3 it is evident that the AR (p) filter generating the multiples is of extremely high order such that its parameterization is indistinguishable from overfitting the variance of the input. This result has serious implications for the utility of ARMA (p,q) models in seismic deconvolution. The sad fact is that although seismic data can be characterized as comprising MA (q) and AR (p) components which are theoretically distinct, these same components are not observationally distinct; consequently ARMA (p,q) models can provide little advantage over AR (p) or MA (q) models.

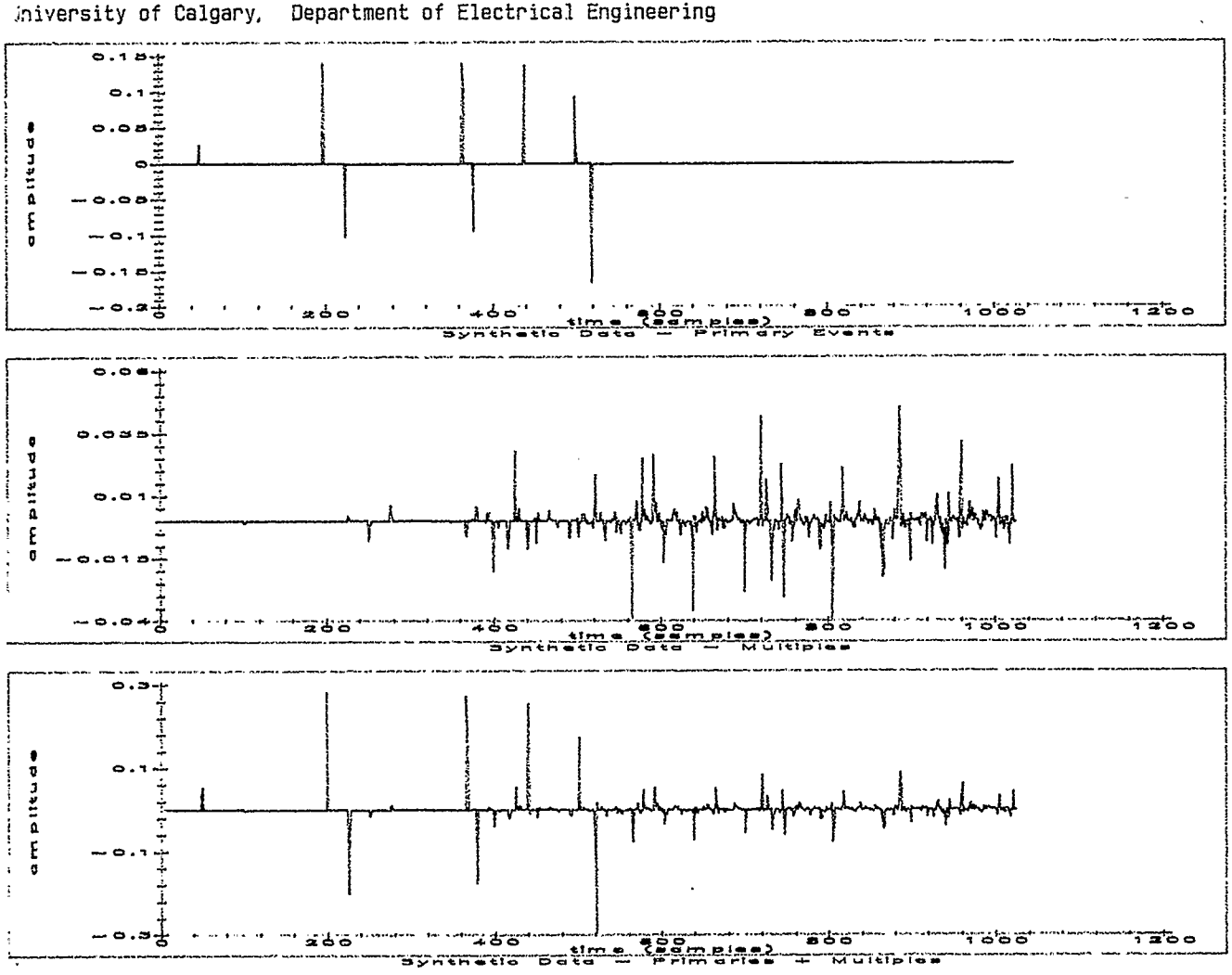

Figure 5.2 SYNTHETIC DATA – SPIKE SEQUENCES

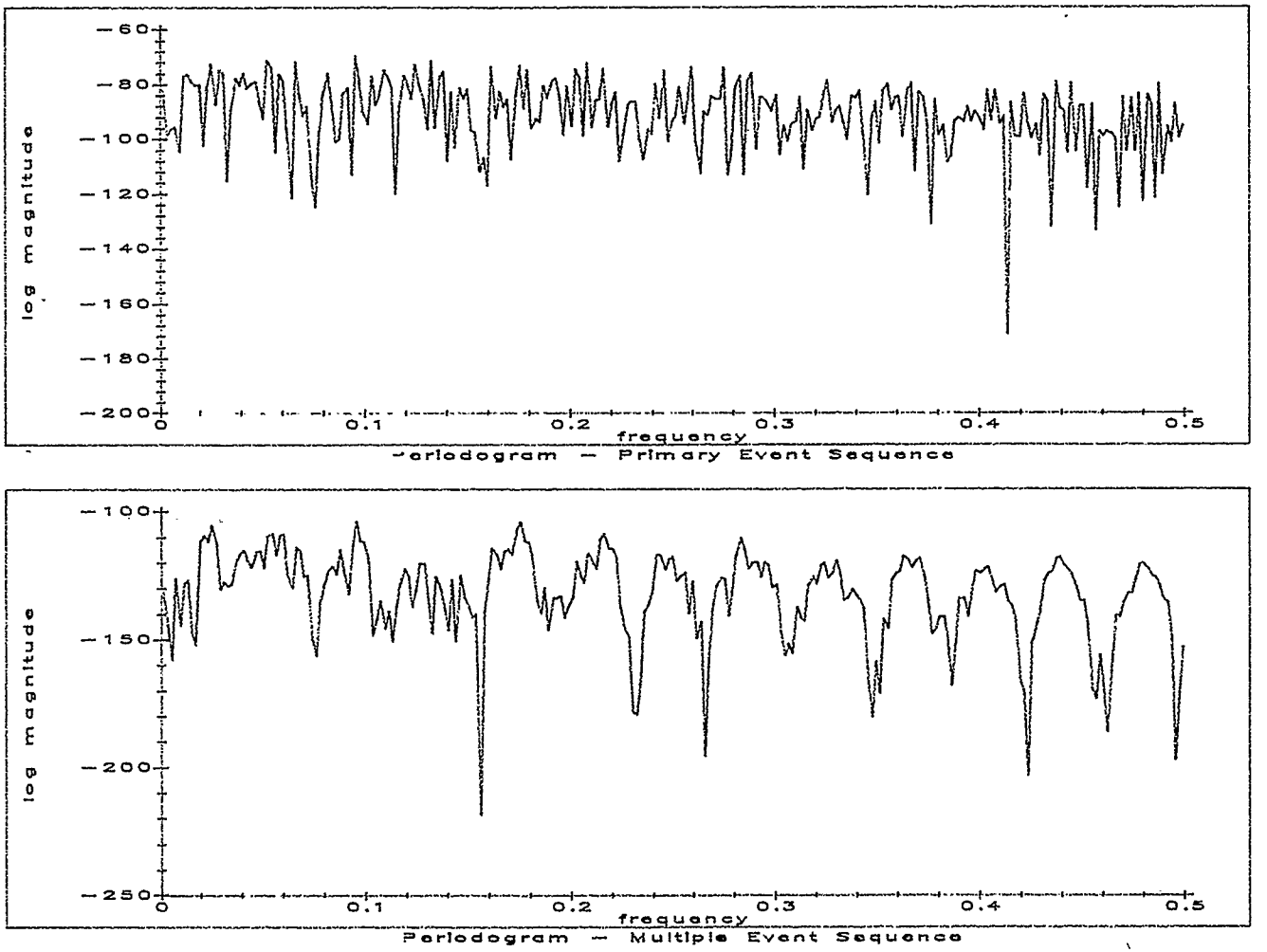

Figure 5.3 PERIODOGRAMS OF PRIMARY AND MULTIPLE SEQUENCES

5.2.3 Decimation and Demodulation

Seismic data is typically oversampled during acquisition to accommodate useful information which may persist to higher than anticipated frequencies. The logic is good considering the high cost of seismic acquisition (up to $20,000/km in the Alberta foothills) relative to the negligible incremental cost of oversampling. The same rationale is carried over to the processing of seismic data. In processing, however, oversampling can be detrimental. The abrupt decay of signal in the near trace spectrum of Figure 5.1 occurs at 0.1 demonstrating five times oversampling of the data. Recognizing that higher order models on the seismic data tended to work at fitting the variance outside of the signal portion of the oversampled spectrum, a decimated data set was generated by sampling every fourth value of the seismic data. The decimated seismic data set and its periodogram are contrasted with the seismic data in Figure 5.4.

In the expectation that low-pass data requires less fitting than band pass data, such as seismic, the data were also demodulated. Demodulation effects a shift of the centre frequency to the origin. This was accomplished by windowing out the frequency band of interest with a hamming filter and multiplying by complex exponentials.

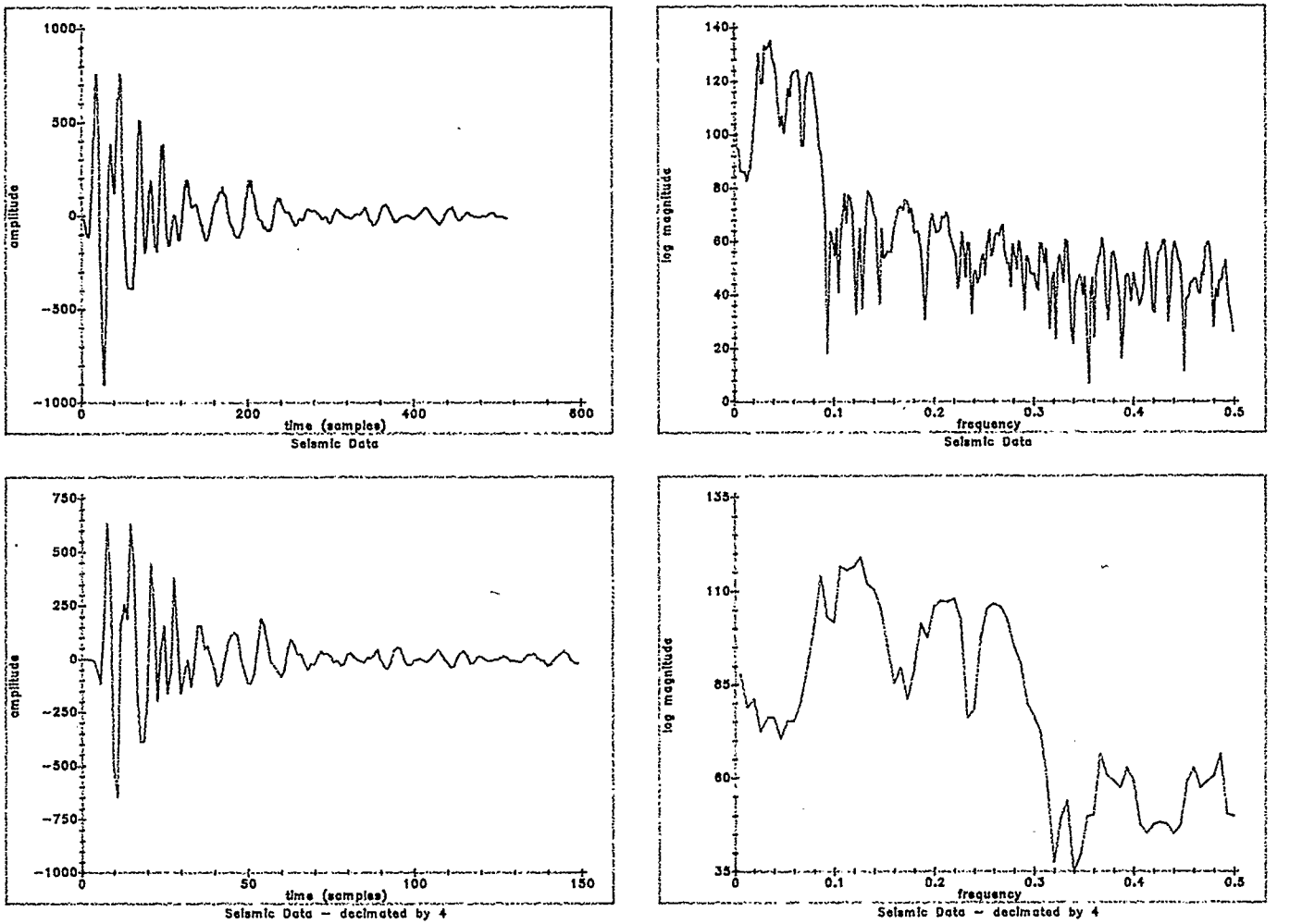

Figure 5.4 DECIMATED SEISMIC DATA

5.3 Spectral Fitting

Although deconvolution is the focus of this report, spectral fitting is the focus of the results. There are two reasons for this. First, the conformity with which model spectra match the shape of the data periodogram is considered to be diagnostic of the quality of the model. This inference makes intuitive sense and has much precedent in the literature [5, 6, 66]. Second, without the coherancy recognition engendered by multichannel seismic data, differentiating between spiked up signal and spiked up noise is questionable. The performance of deconvolution on single channel data sets can therefore be evaluated more meaningfully with reference to the spectral fits.

5.3.1 AR (p) Techniques

Burg, Least Squares, and Levinson AR (p) modelling techniques were run on the various data sets. Figures 5.5 through 5.7 illustrate model fits to the periodogram for the seismic data at orders 2, 4, 8, and 16. The different techniques yield almost identical model spectra at these orders. In all cases the models indiscriminately fit the large magnitude contrast caused by oversampling where signal drops off to noise. The additional fitting allowed in going from 4th order to 8th

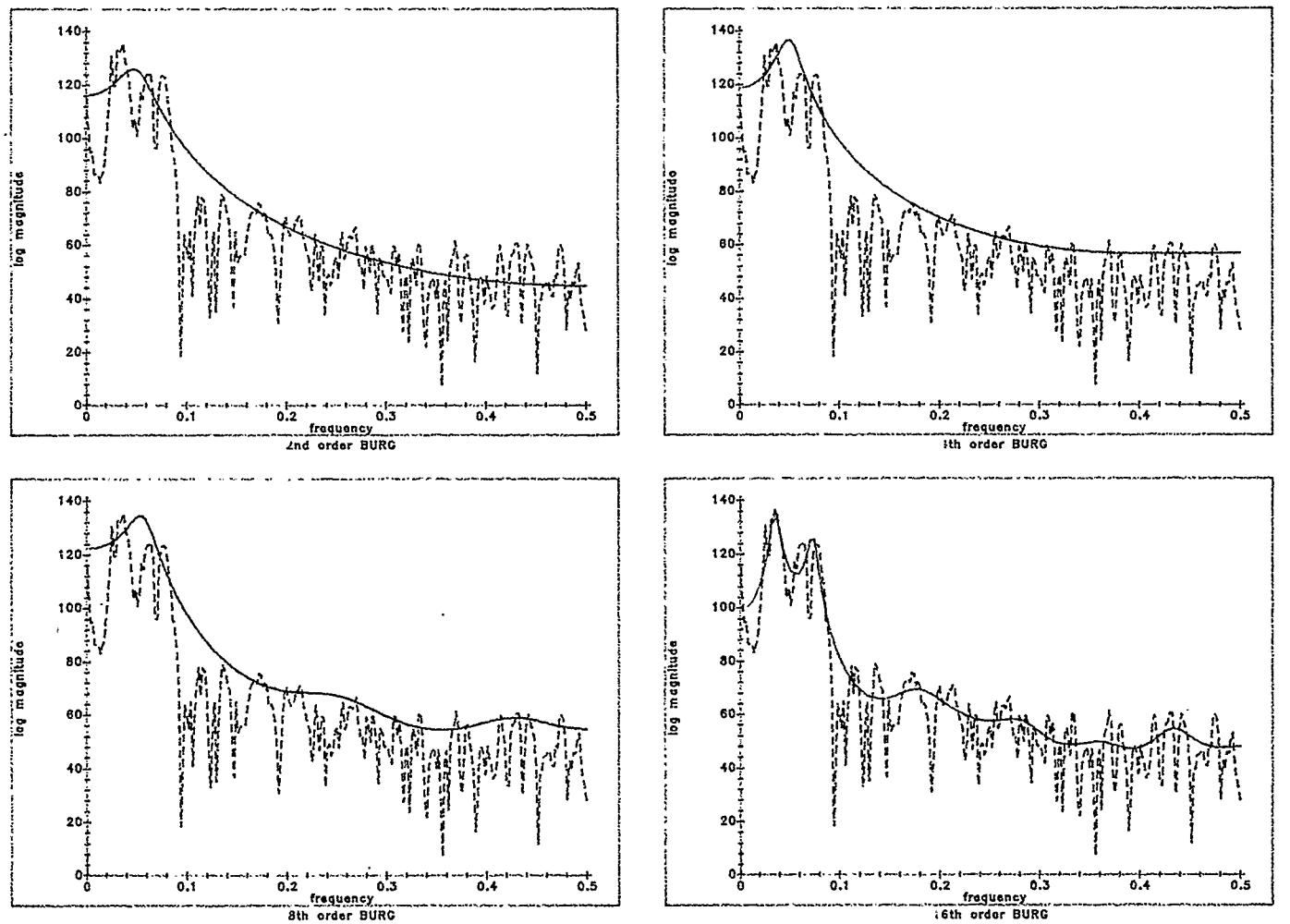

Figure 5.5 BURG MODEL FITS TO SEISMIC DATA

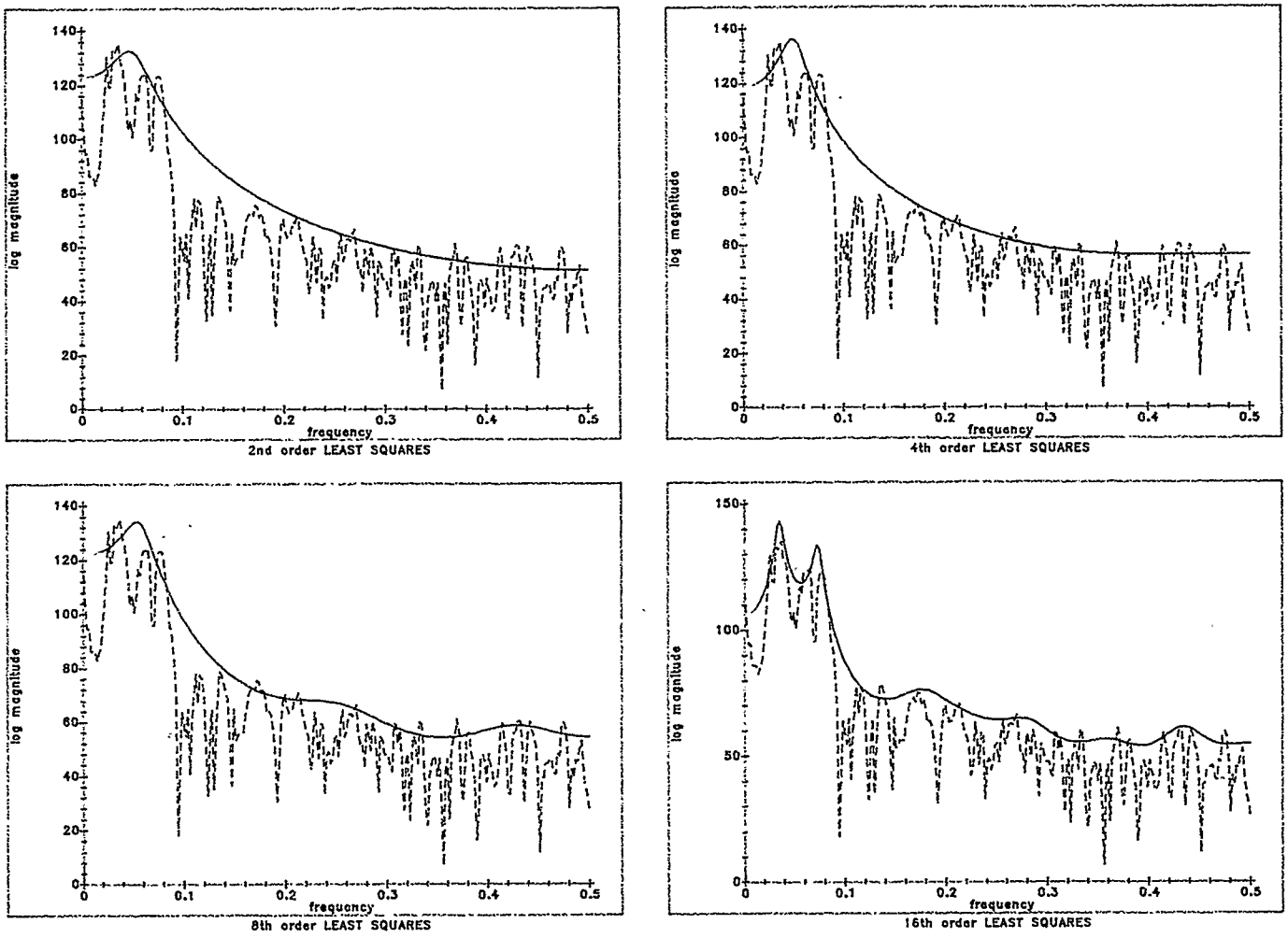

Figure 5.6 LEAST SQUARES MODEL FITS TO SEISMIC DATA

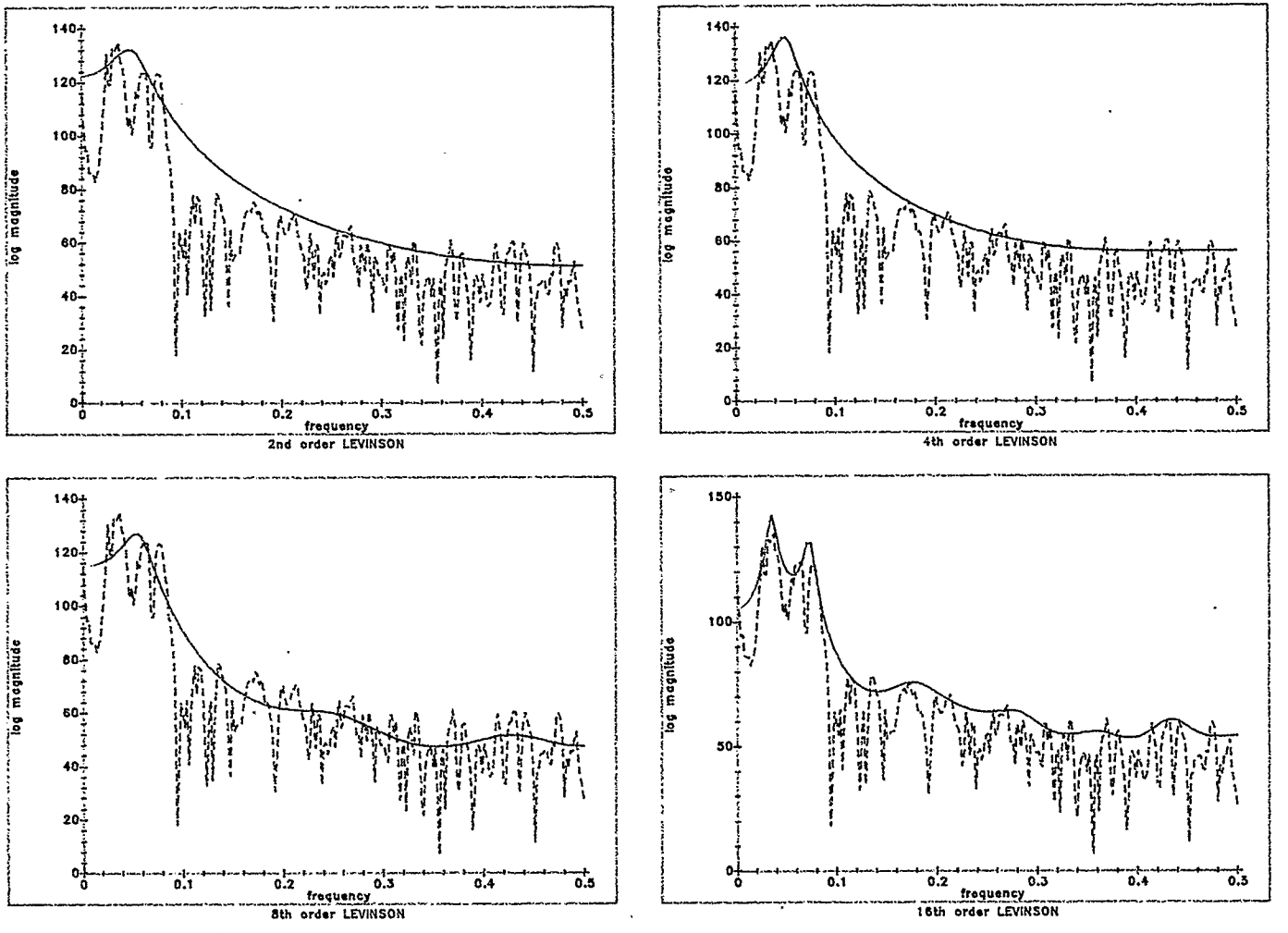

Figure 5.7 LEVINSON MODEL FITS TO SEISMIC DATA

order is squandered in fitting some arbitrary apparent trend in the variance of the noise. Only at 16th order does the model begin to distinguish in the high signal portion of the spectrum but even then more shape is found (and model order wasted) in the noise. The trend persists with increasing order. Models to 64th order were examined.

It is obvious from the model spectra that there can be little difference in the deconvolutions and wavelet estimates output from these models. This is confirmed with illustrations in Section 5.4

Figure 5.8 through 5.10 illustrate model fits on the decimated seismic data at the same orders: 2, 4, 8, and 16. Without noise constituting 80% of the spectrum the models work much more effectively on the signal; shape in the signal portion begins to be recognized at 4th order. The results for the different techniques are very similar up to 8th order. At 16th order the known tendency of the Least Squares and Burg algorithms to overspike certain frequencies at increasing orders becomes evident. The cause and effect relationship between model order and spiking is demonstrated in Figure 5.11 where Burg model spectra are presented for 8th, 16th, and 32nd order. The 32nd order spectrum offers little additional frequency differentiation compared with

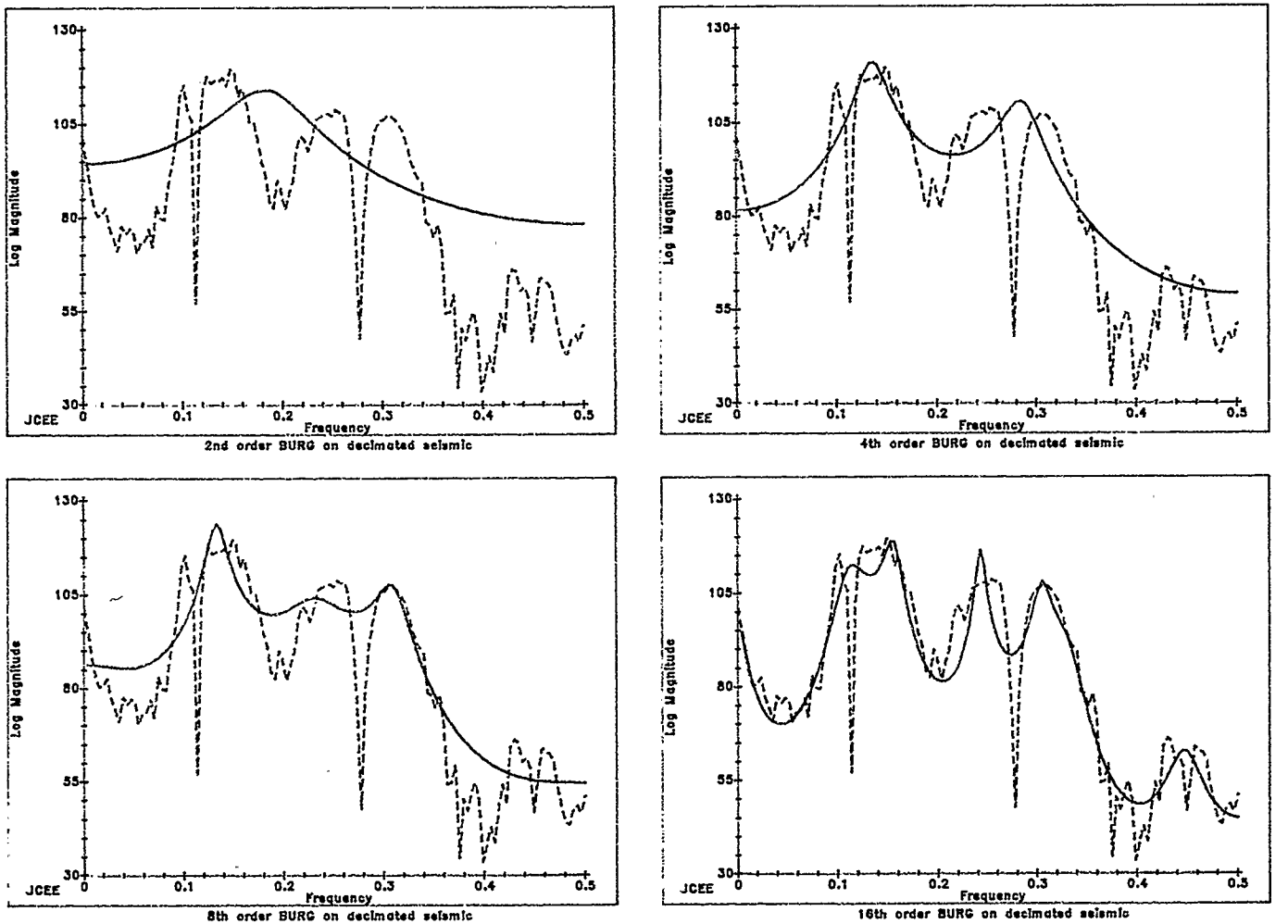

Figure 5.8 BURG MODEL FITS TO DECIMATED SEISMIC DATA

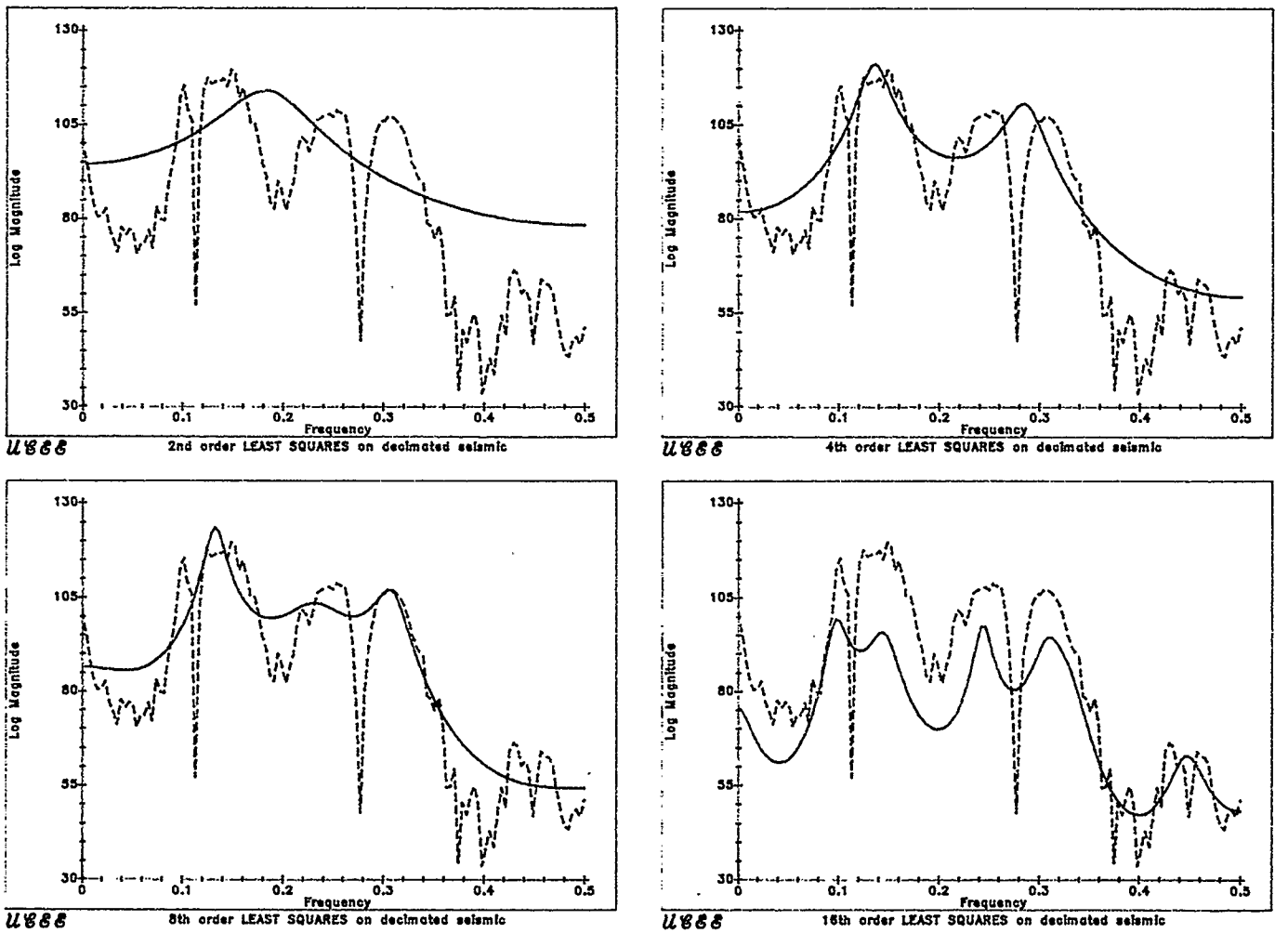

Figure 5.9 LEAST SQUARES MODEL FITS TO DECIMATED SEISMIC DATA

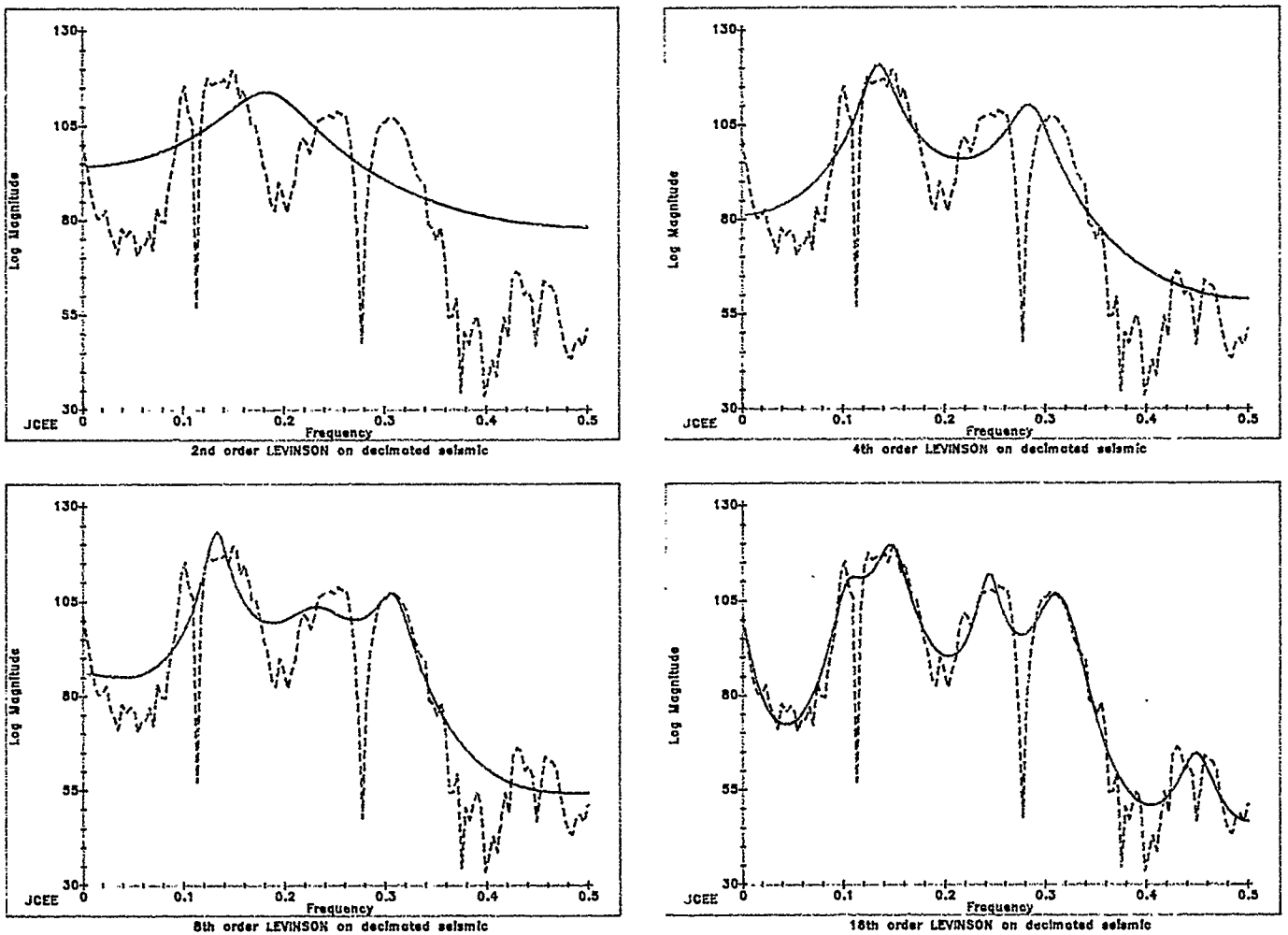

Figure 5.10 LEVINSON MODEL FITS TO DECIMATED SEISMIC DATA

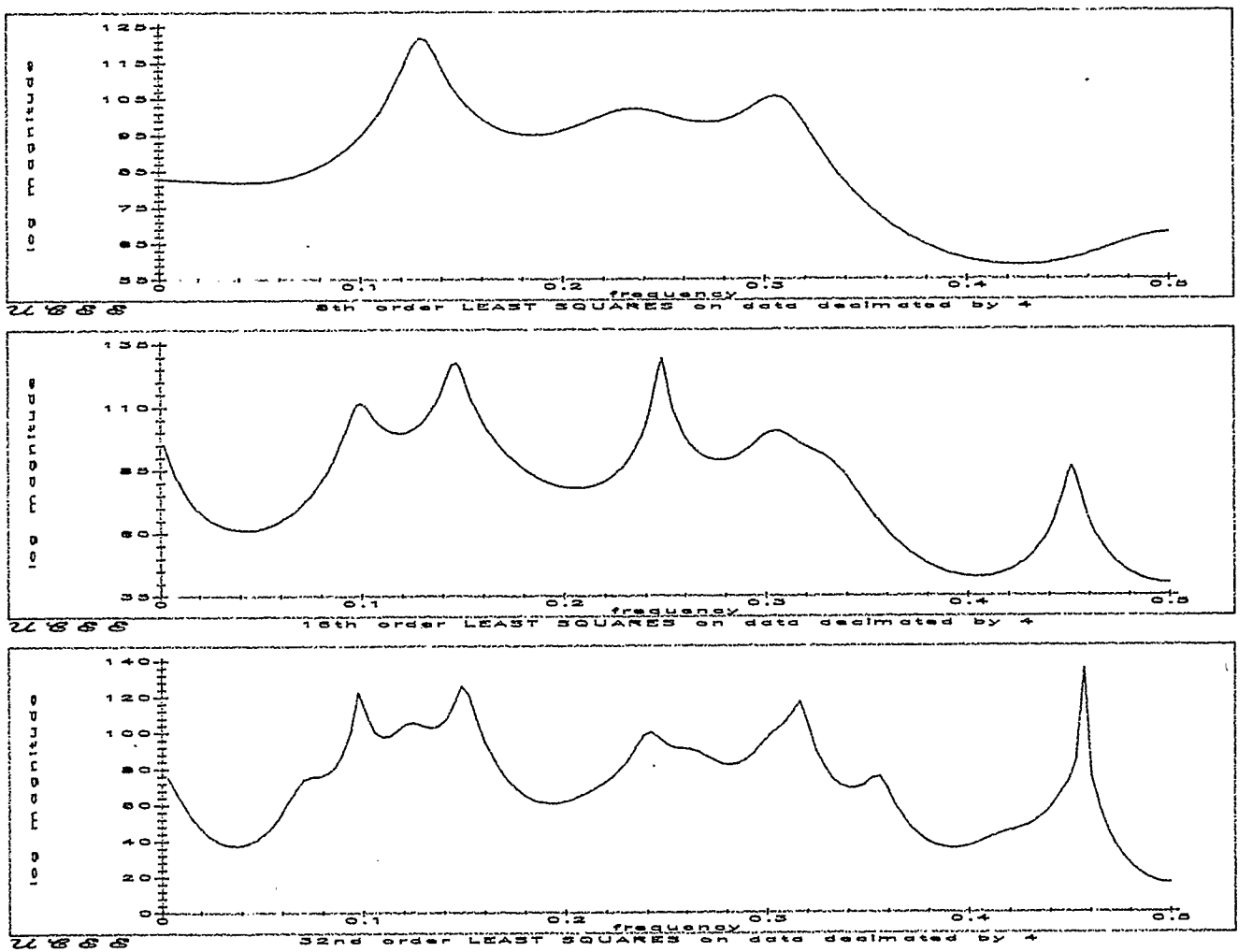

Figure 5.11 BURG MODELS ON DECIMATION DATA TO 32nd ORDER

16th order but severely overspikes those frequencies previously distinguished by the 16th order fit.

5.3.2 ARMA (p,q) Techniques

Salami, Kay, Cadzow, and Transient Error Method techniques were used for ARMA (p,q) modelling. Box-Jenkins and GRT procedures were attempted but both techniques were found to be extremely unstable on seismic data and sensitive to choice of model order. The GRT method was also very sensitive to an initial guess at the MA (q) coefficients. The GRT method could be used in conjunction with the method of Salami, since Salami outputs a minimum phase MA (q) sequence suitable for input to GRT, but the additional benefit of "tweaking" the ARMA (p,q) coefficients at that stage is expected to be minimal.

Figures 5.12 and 5.13 illustrate the model outputs of the methods of Salami and Kay respectively, as applied to the seismic data with orders (2,2), (4,4), (8,8), and (16,16). The models are recognized to distinguish frequencies in the signal zone at (4,4) yielding results comparable to those of

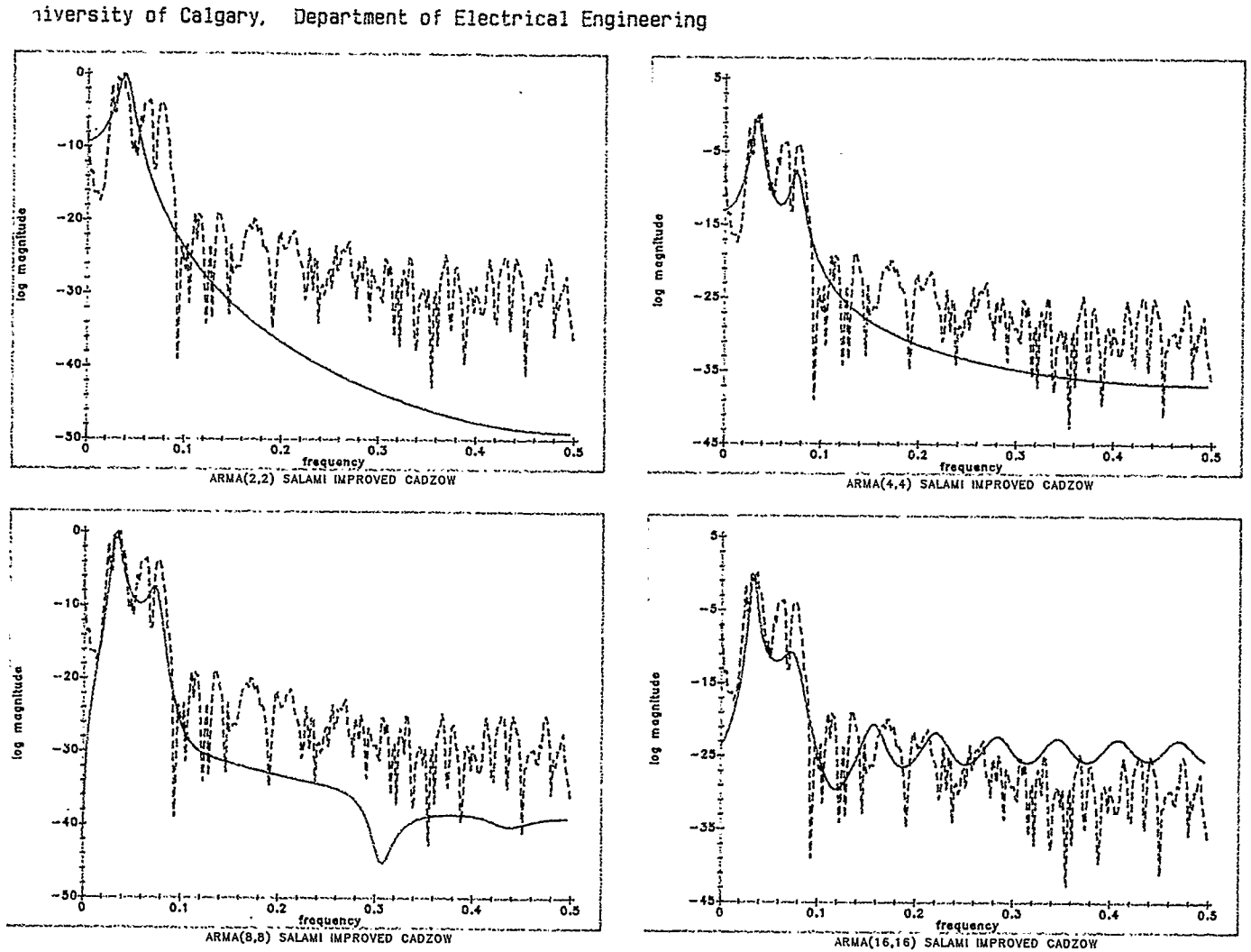

Figure 5.12 SALAMI MODEL FITS TO SEISMIC DATA

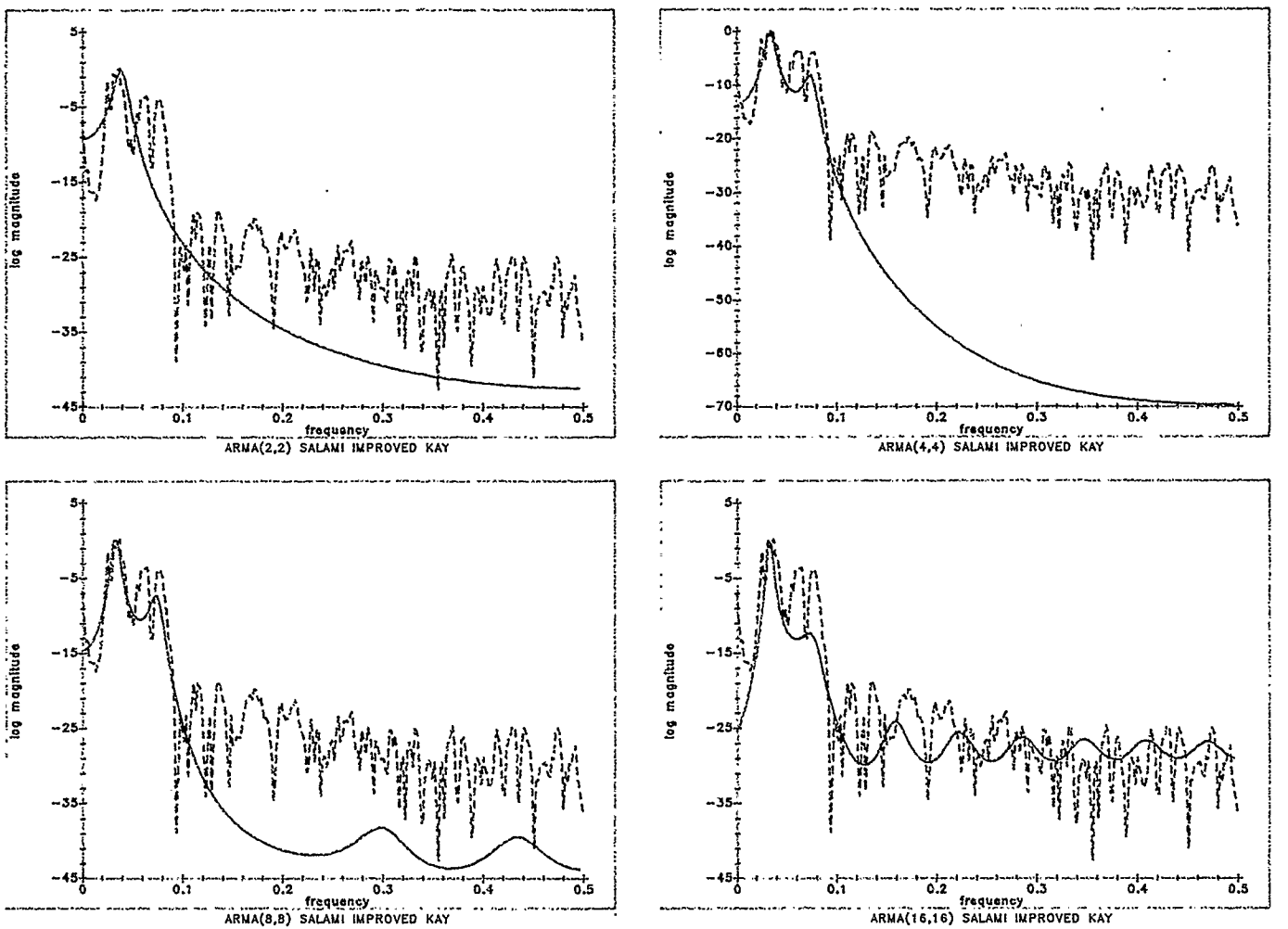

Figure 5.13 KAY MODEL FITS TO SEISMIC DATA

the AR (p) techniques at 16th order. At increasing orders, however, both ARMA (p,q) techniques begin to overfit the noise and weaken the fit to the periodogram in the signal portion of the spectrum. By order (16,16) both Salami and Kay models show marked deterioration in spectral matching the signal, and meaningless oscillating fits in the noise.

A concern with the ARMA (p,q) models is their tendency to fit the shape of the roll off from signal to noise. The steep slope is fit with the initial consequence, at lower orders, of undermodelling the noise, particularly in Kay (4,4) and Salami (2,2). A problem arises, therefore, with deconvolution. Particularly at Kay (4,4) and Salami (2,2) the noise is strongly overgained in the deconvolutions. These consequences are illustrated in Section 5.4.

Cadzow fits are not discussed because they fail without fail on seismic data. Figure 5.14 illustrates a comparison of Salami, Kay, and Cadzow methods on the seismic data at order (4,4). Salami modified Kay is included. It differs little from Kay except for slight modification of the MA (q) coefficients. Cadzow is recognized to fail with negative spectral values.

The model fits of Salami and Kay on decimated seismic data

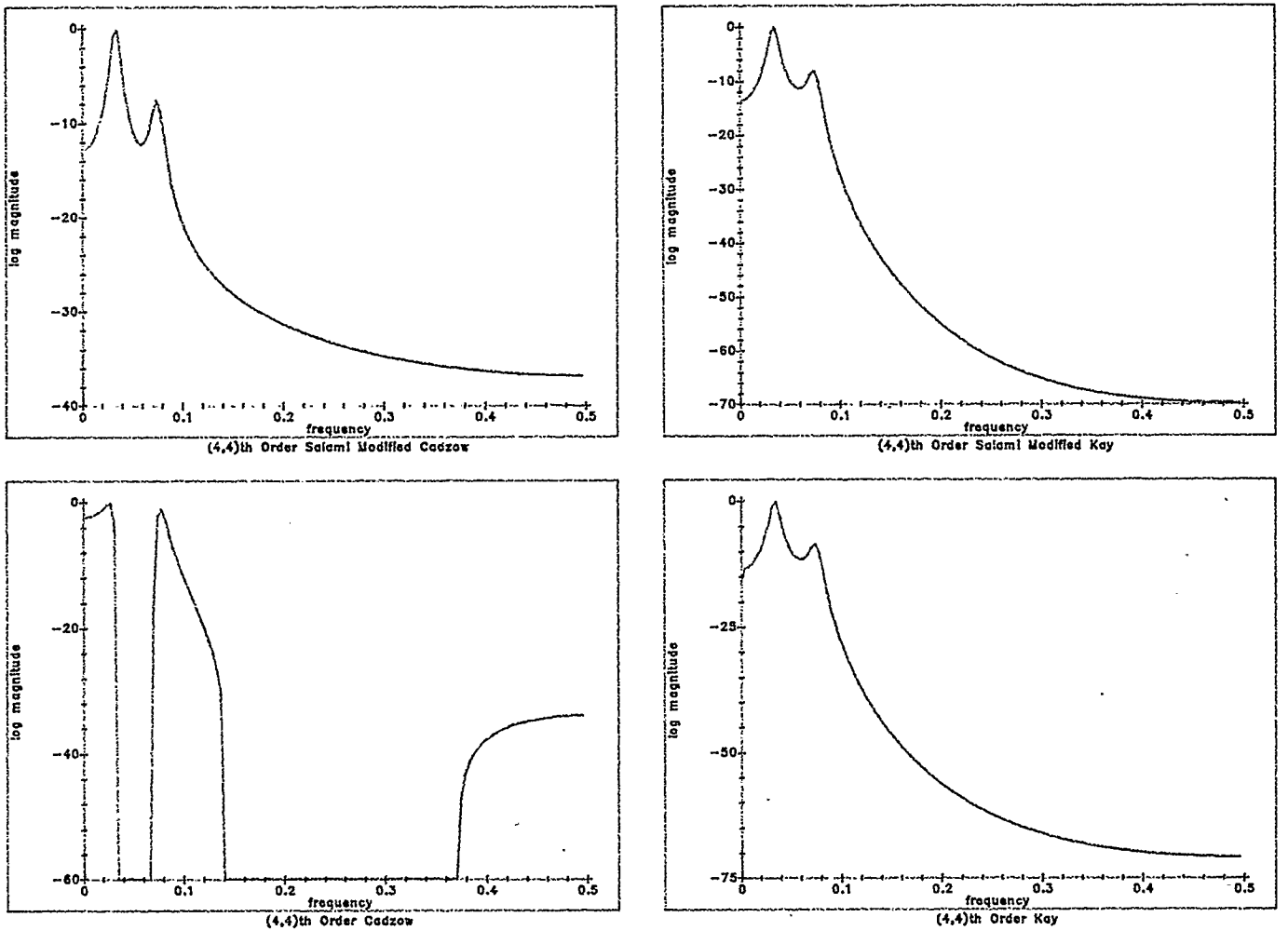

Figure 5.14 SALAMI, KAY, AND CADZOW (4,4) FITS TO SEISMIC DATA

are presented in Figures 5.15 and 5.16. Both techniques severely overspike the data with increasing model order. Salami fits are seen to best honour the shape of the periodogram. At orders in excess of (8,8) the additional parameters seem to do more harm than good. In contrast, Figure 5.17 shows excellent fits, improving with order, with the Transient Error Method on demodulated data.

Demodulation proves to be a powerful technique for pre-processing the input to modelling programs. The Transient Error Method is the best behaved of the techniques tested; it does not spike with increasing order, but otherwise on seismic data it provides fits comparable to those of Salami. Demodulated data, however, greatly enhances the fitting ability of all techniques. Figure 5.18 is a comparison of spectral fits modelled with the Transient Error Method and Levinson routines. With increasing order Levinson closely rivals the fit of the Transient Error Method and both yield superb spectral matches to the periodogram.

ARMA (p,q) and AR (p) techniques provided comparable spectral fits in each data type. ARMA (p,q) fits are better at lower orders but fit the slope of roll off in the seismic data at the expense of providing a correct fit to the magnitude of the noise. With increasing order all techniques excepting

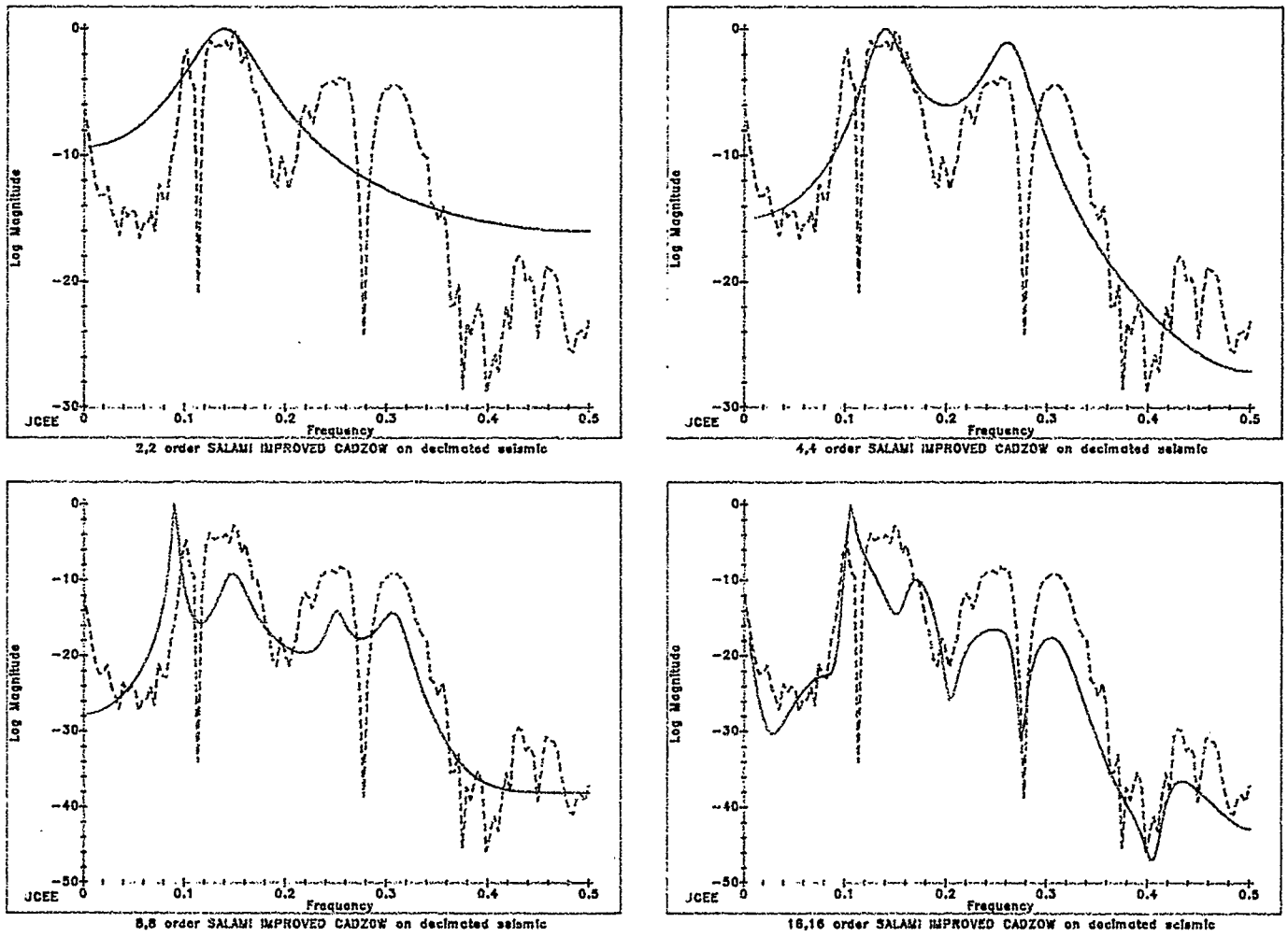

Figure 5.15 SALAMI MODEL FITS TO DECIMATED SEISMIC DATA

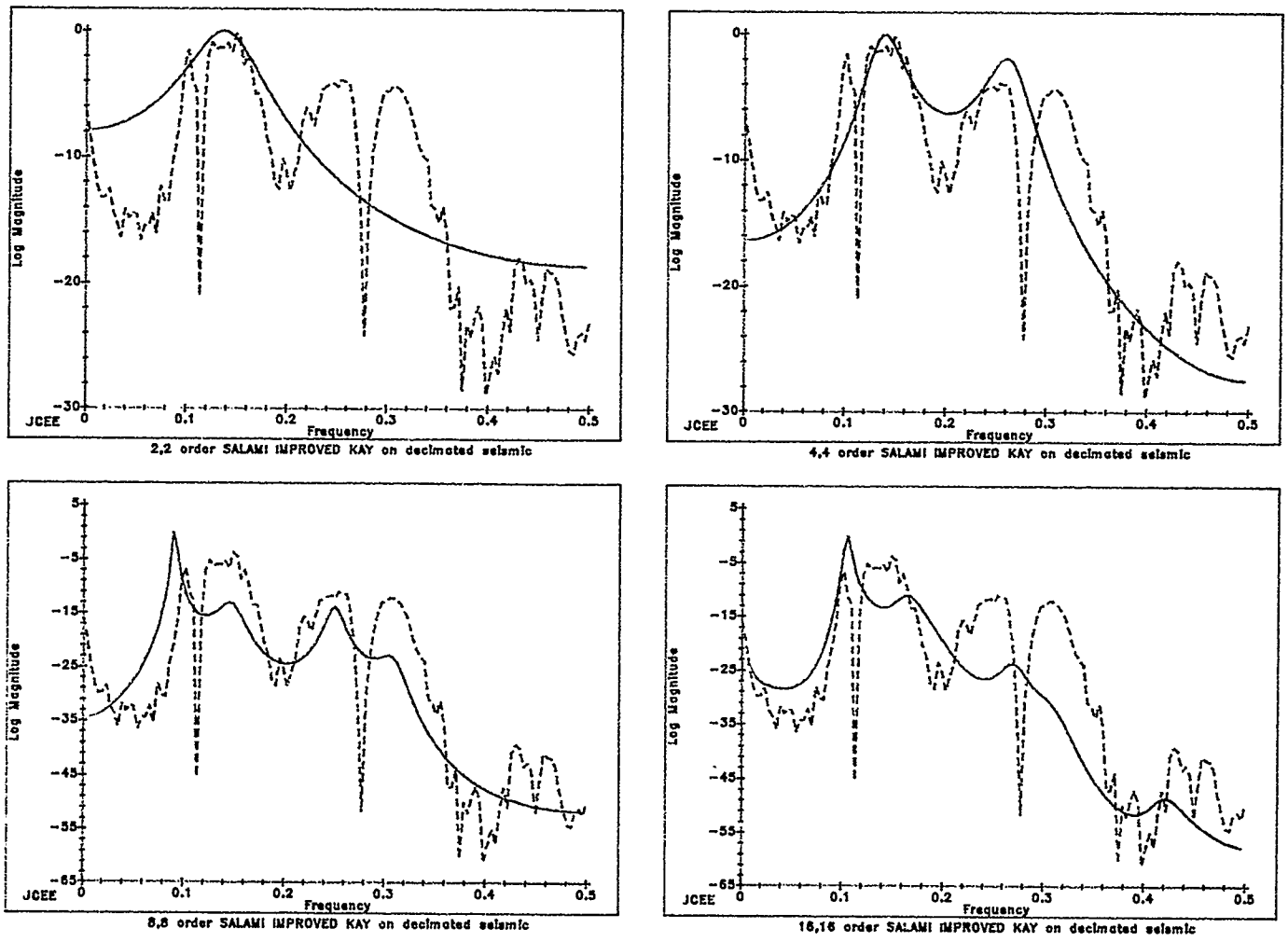

Figure 5.16 KAY MODEL FITS TO DECIMATED SEISMIC DATA

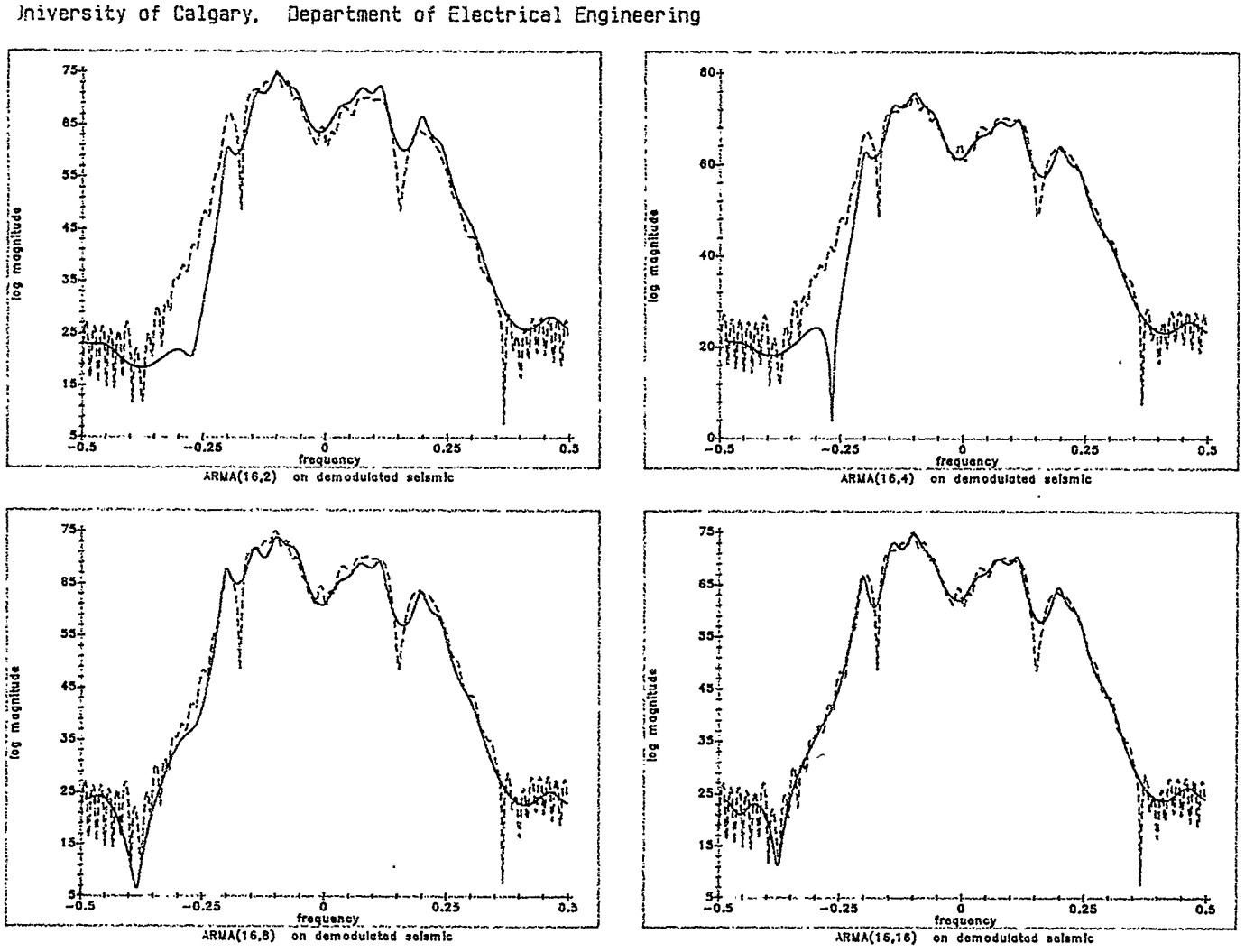

Figure 5.17 TRANSIENT ERROR METHOD FITS TO DEMODULATED SEISMIC DATA

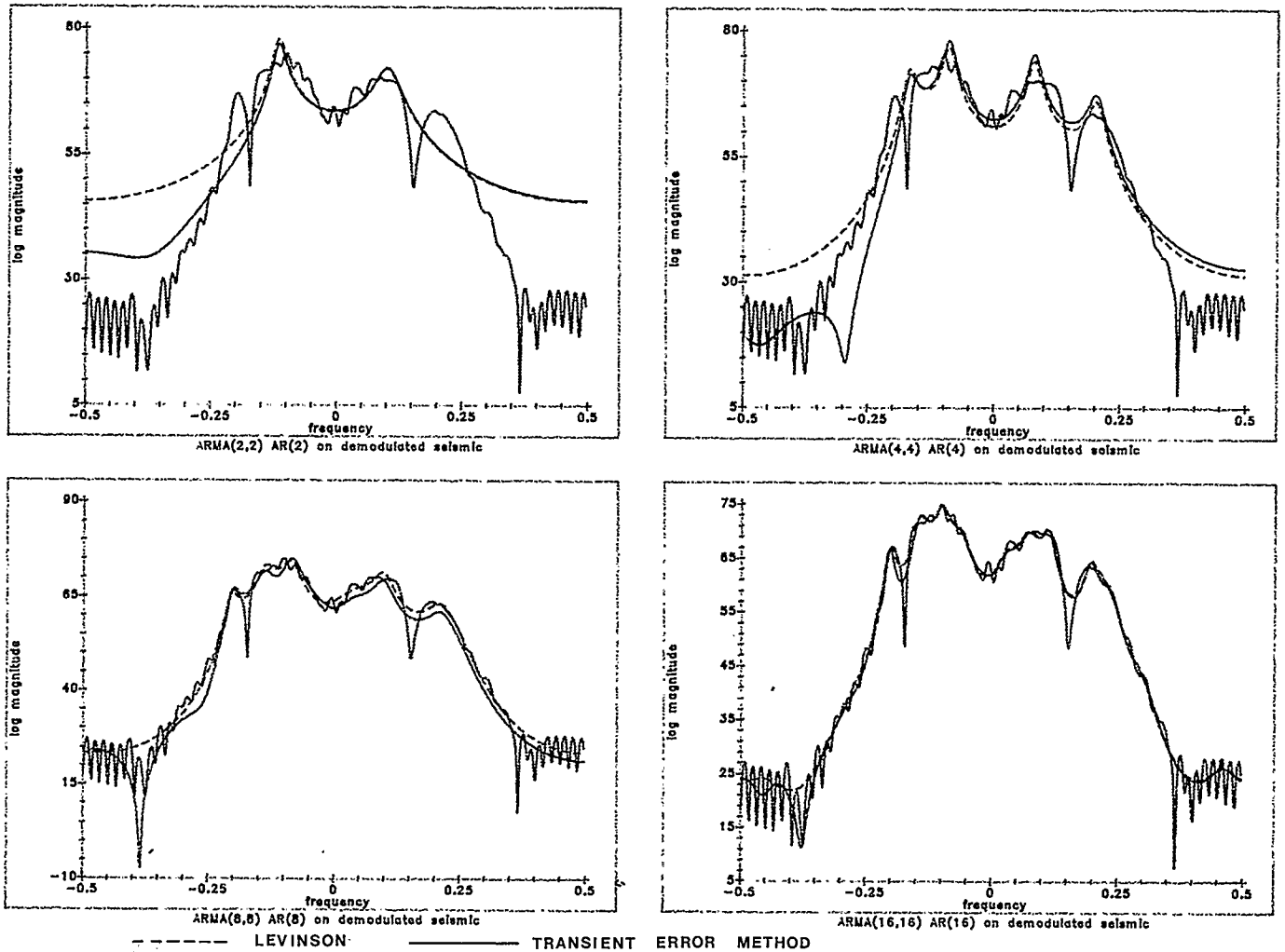

Figure 5.18 TRANSIENT ERROR METHOD AND LEVINSON FITS TO DEMODULATED SEISMIC DATA

Levinson and the Transient Error Method spike the data.

Model coefficients of order (4,4) are presented in Table 5.1. At the significant values chosen all AR (p) coefficients are the same, as are the autoregressive coefficients of the ARMA (p,q) models; the moving average coefficients, however, vary considerably.

5.4 Deconvolution

As mentioned earlier, it is difficult to quantitatively assess model quality based on deconvolved output. However, a sense of the effectiveness of the deconvolution can be achieved by comparison with the original data.

5.4.1 AR (p) Techniques

Figures 5.19 through 5.21 illustrate deconvolution of the seismic data with Burg, Least Squares, and Levinson respectively, at model orders of 2, 4, 8, and 16. As expected from study of the spectral fits there is little difference in results between model orders and less between techniques.

	a_1	a_2	a_3	a_4	b_o	b_1	b_2	b_3	b_4
Burg	-1.53	0.40	0.27	-0.03					
Least Squares	-1.53	0.40	0.27	-0.03					
Levinson	-1.53	0.40	0.27	-0.03					
Salami	-3.62	5.14	-3.39	0.88	28.23	-62.79	49.97	-13.78	-0.68
Kay	-3.62	5.14	-3.39	0.88	123.22	-48.04	13.69	-6.19	-3.50

Table 5.1 Comparison of 4th Order Model Coefficients

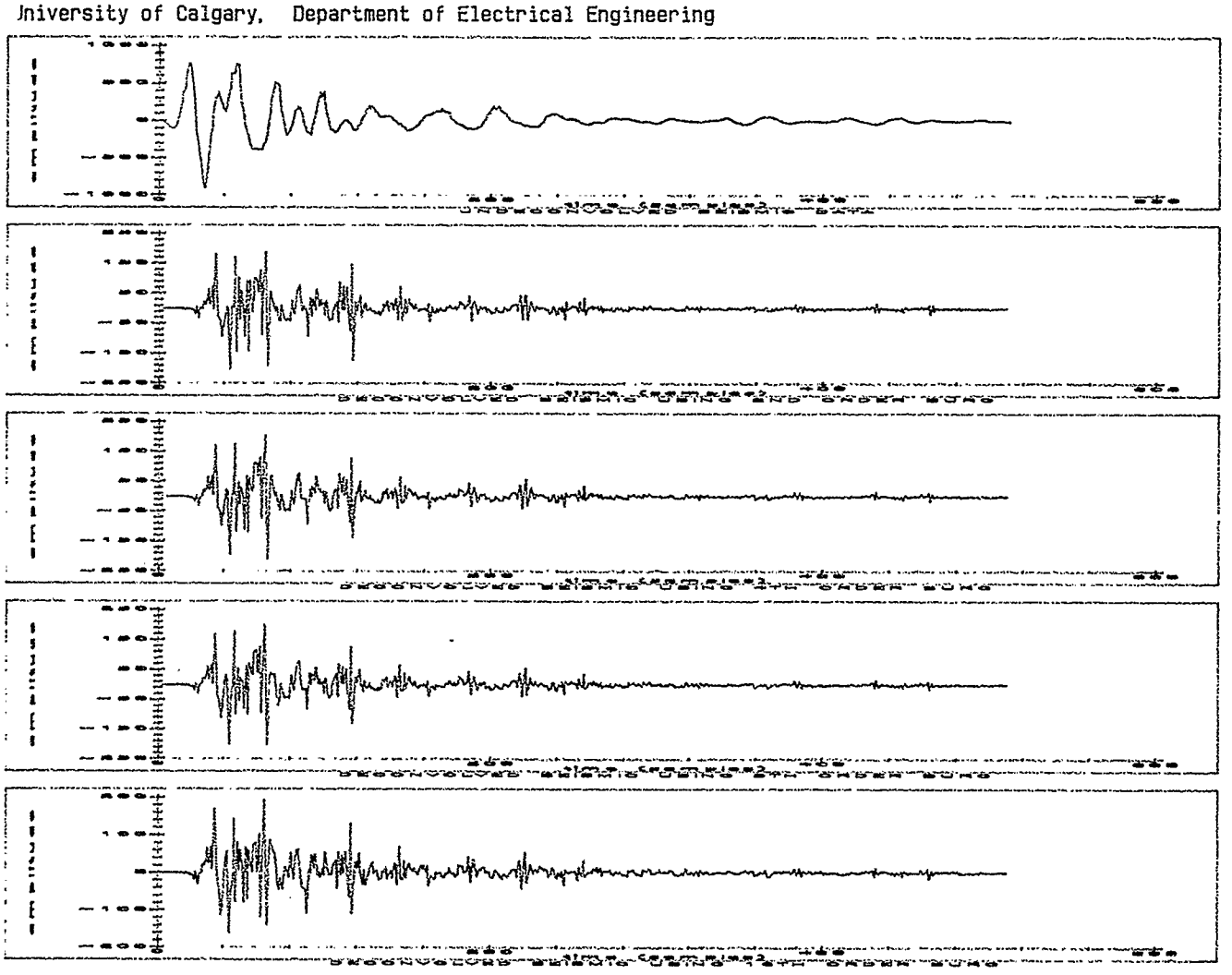

Figure 5.19 BURG DECONVOLUTION OF SEISMIC DATA

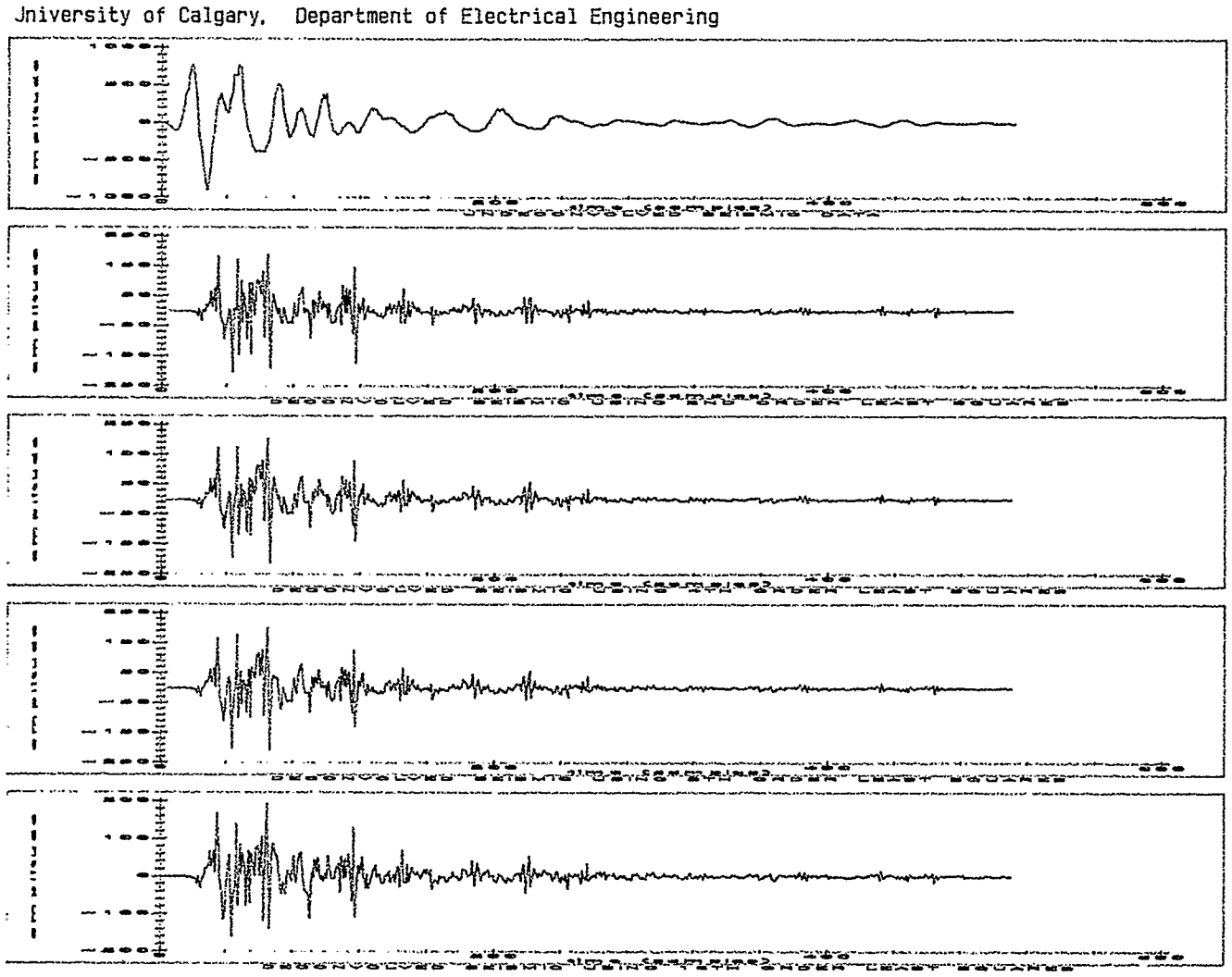

Figure 5.20 LEAST SQUARES DECONVOLUTION OF SEISMIC DATA

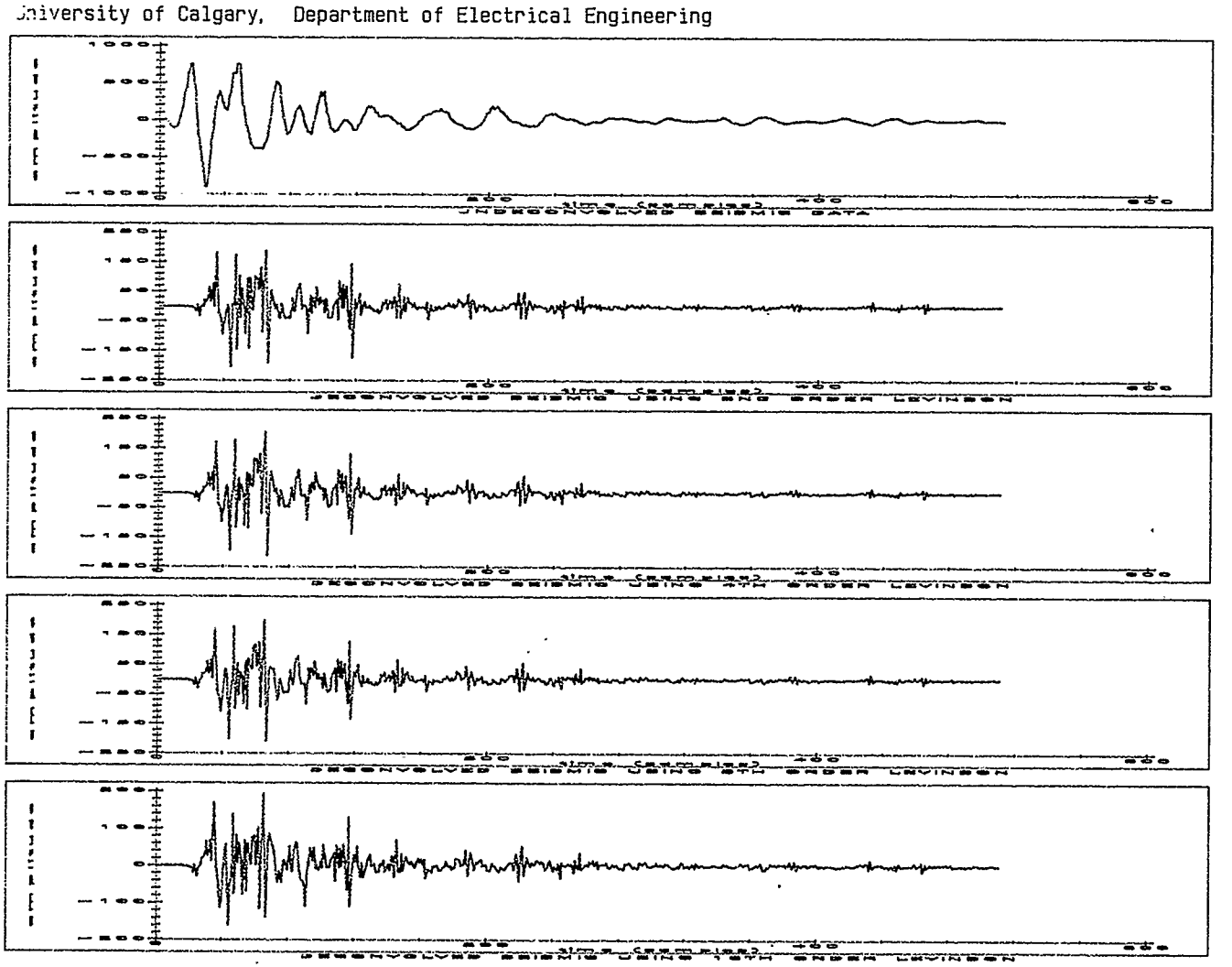

Figure 5.21 LEVINSON DECONVOLUTION OF SEISMIC DATA

5.4.2 ARMA (p,q) Techniques

Figures 5.22 through 5.24 illustrate Salami deconvolution at (2,2), (4,4), and (16,16) respectively in comparison with the AR (p) techniques, and Figures 5.25 and 5.26 compare Salami and Kay at (4,4) and Salami at (2,2) and (4,4) respectively.

The ARMA (p,q) deconvolutions are seen to produce noisy results at low orders as anticipated from review of the spectral plots. The noise is particularly evident on Salami (2,2) and Kay (4,4).

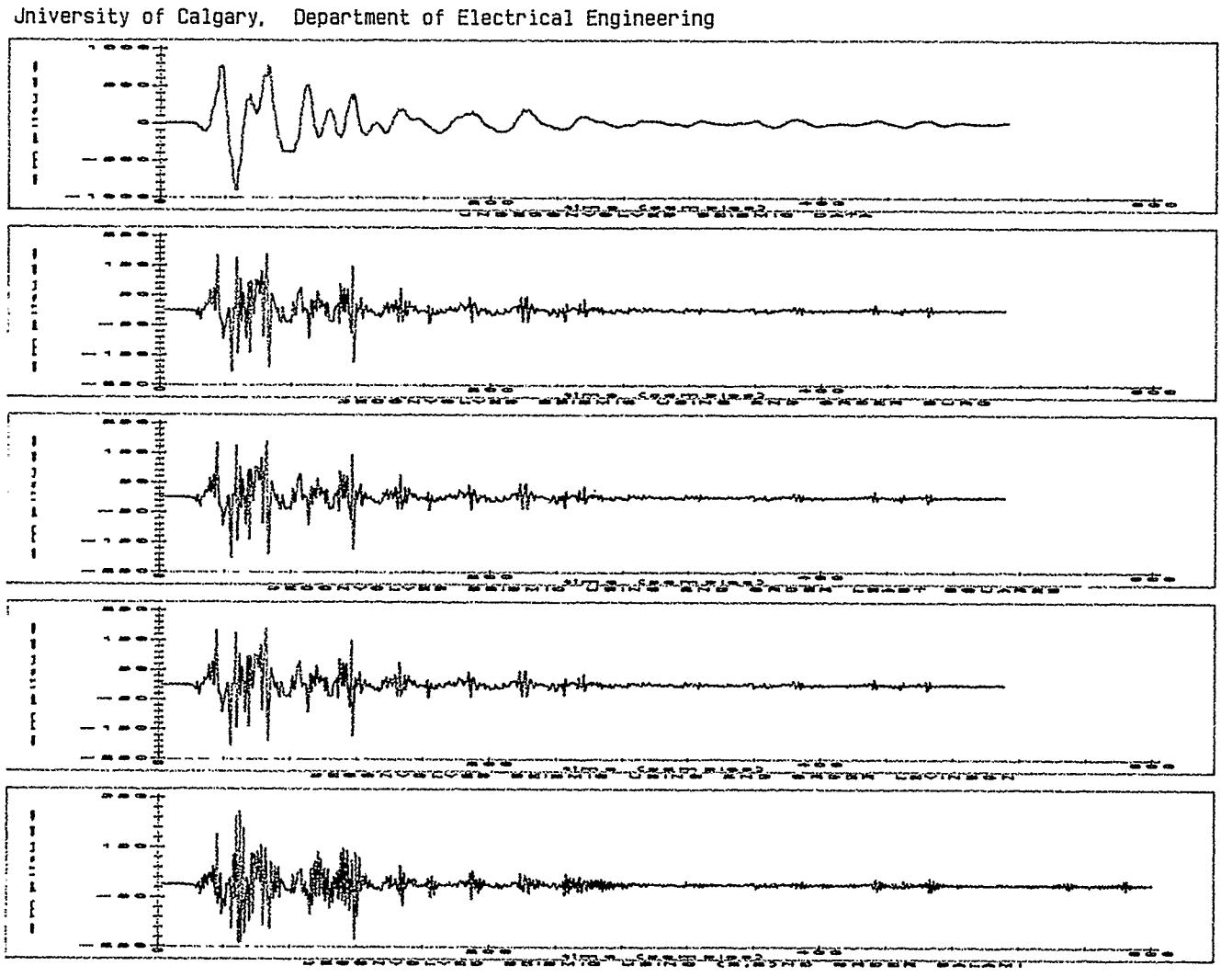

Figure 5.22 SALAMI DECONVOLUTION (2,2) COMPARED WITH AR (p) TECHNIQUES

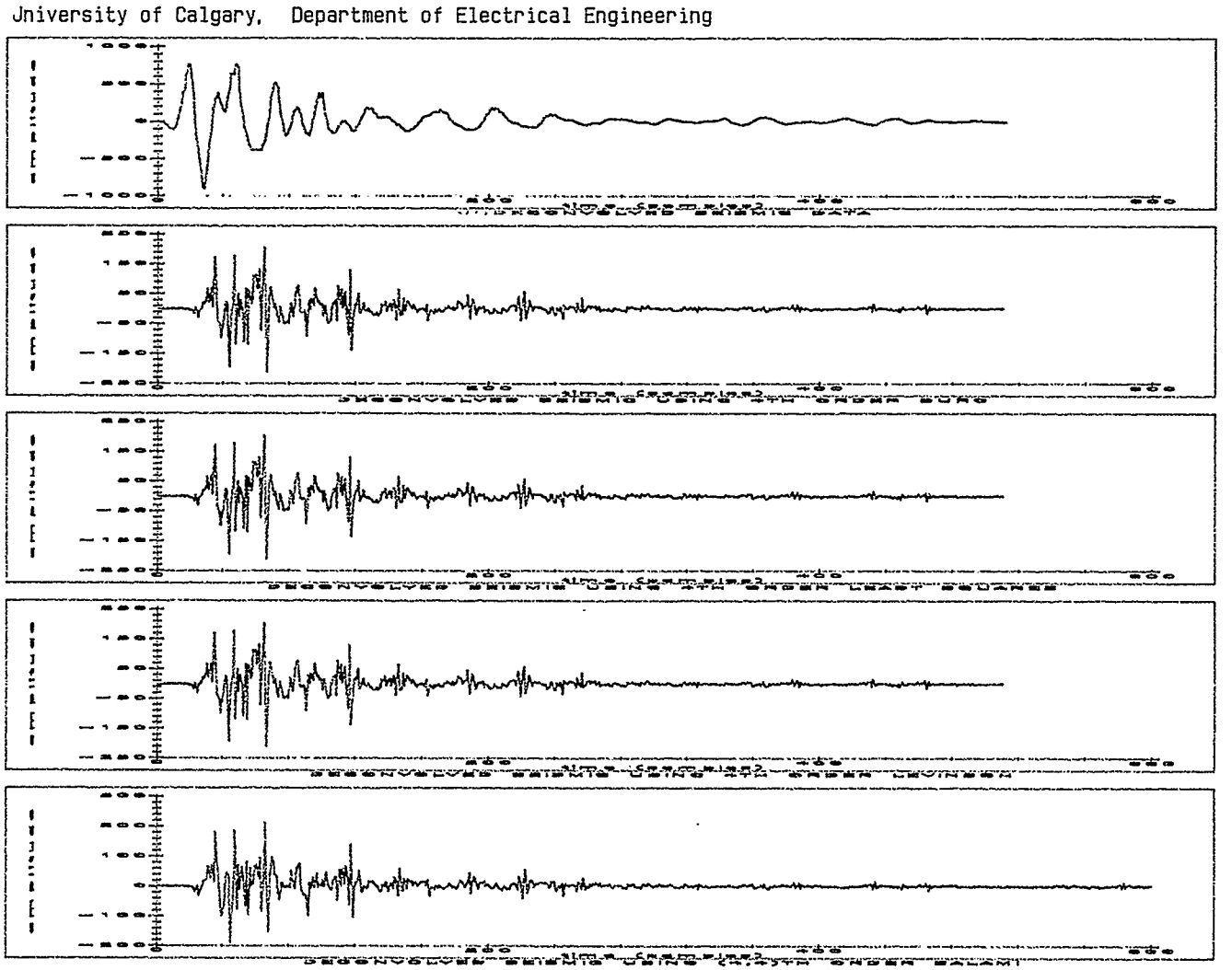

Figure 5.23 SALAMI DECONVOLUTION (4,4) COMPARED WITH AR (p) TECHNIQUES

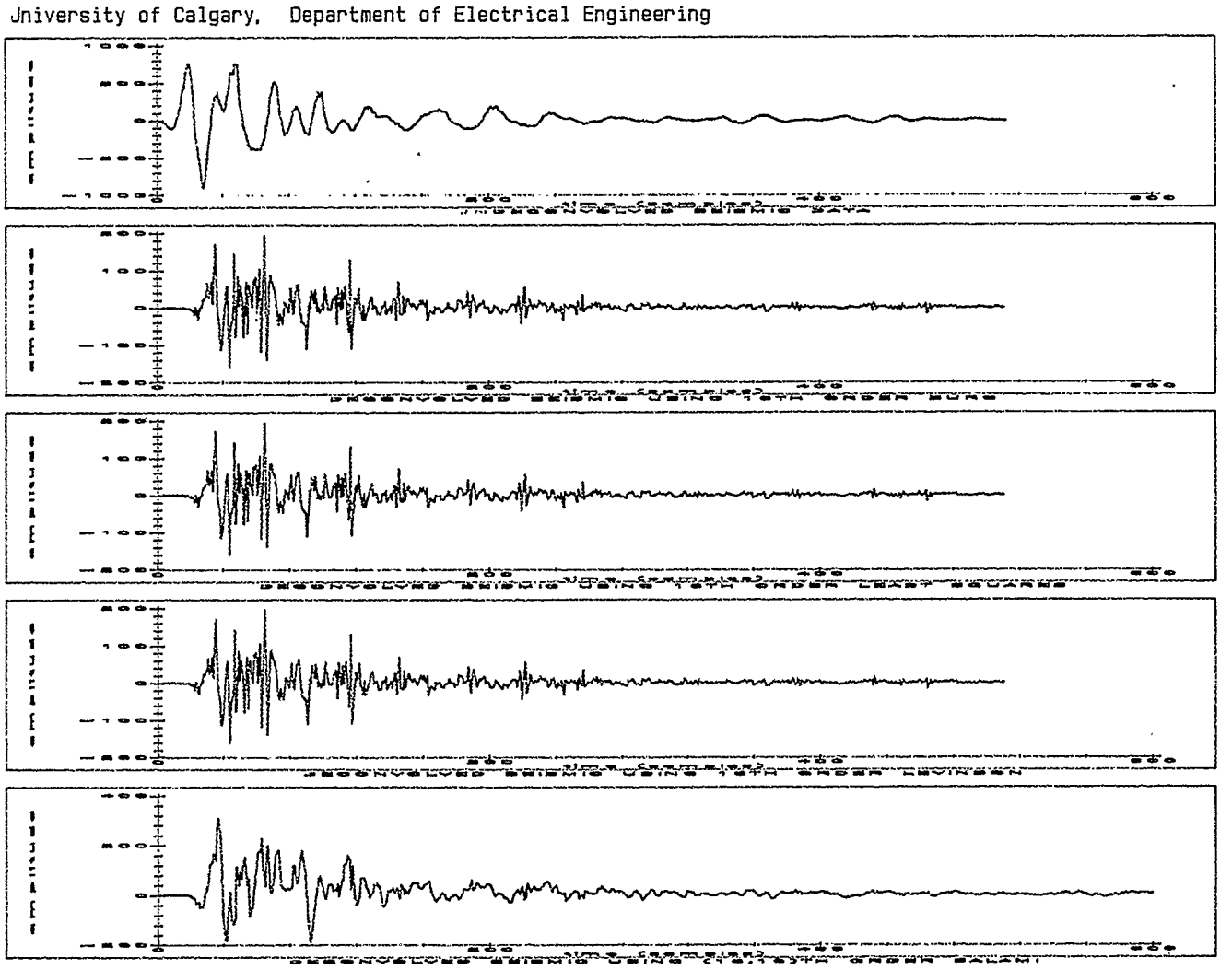

Figure 5.24 SALAMI DECONVOLUTION (16,16) COMPARED WITH AR (p) TECHNIQUES

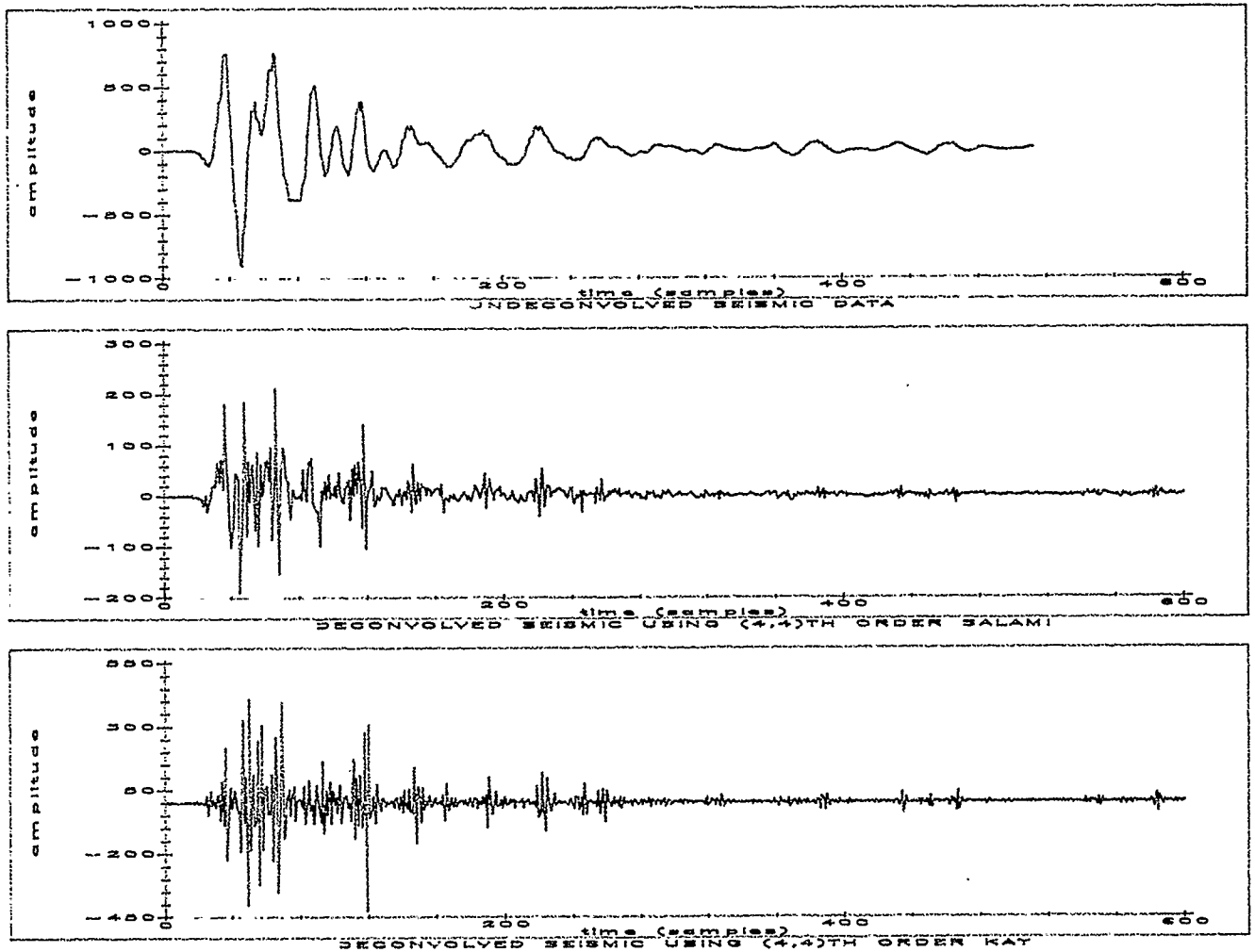

Figure 5.25 SALAMI AND KAYE DECONVOLUTIONS AT ORDER (4,4)

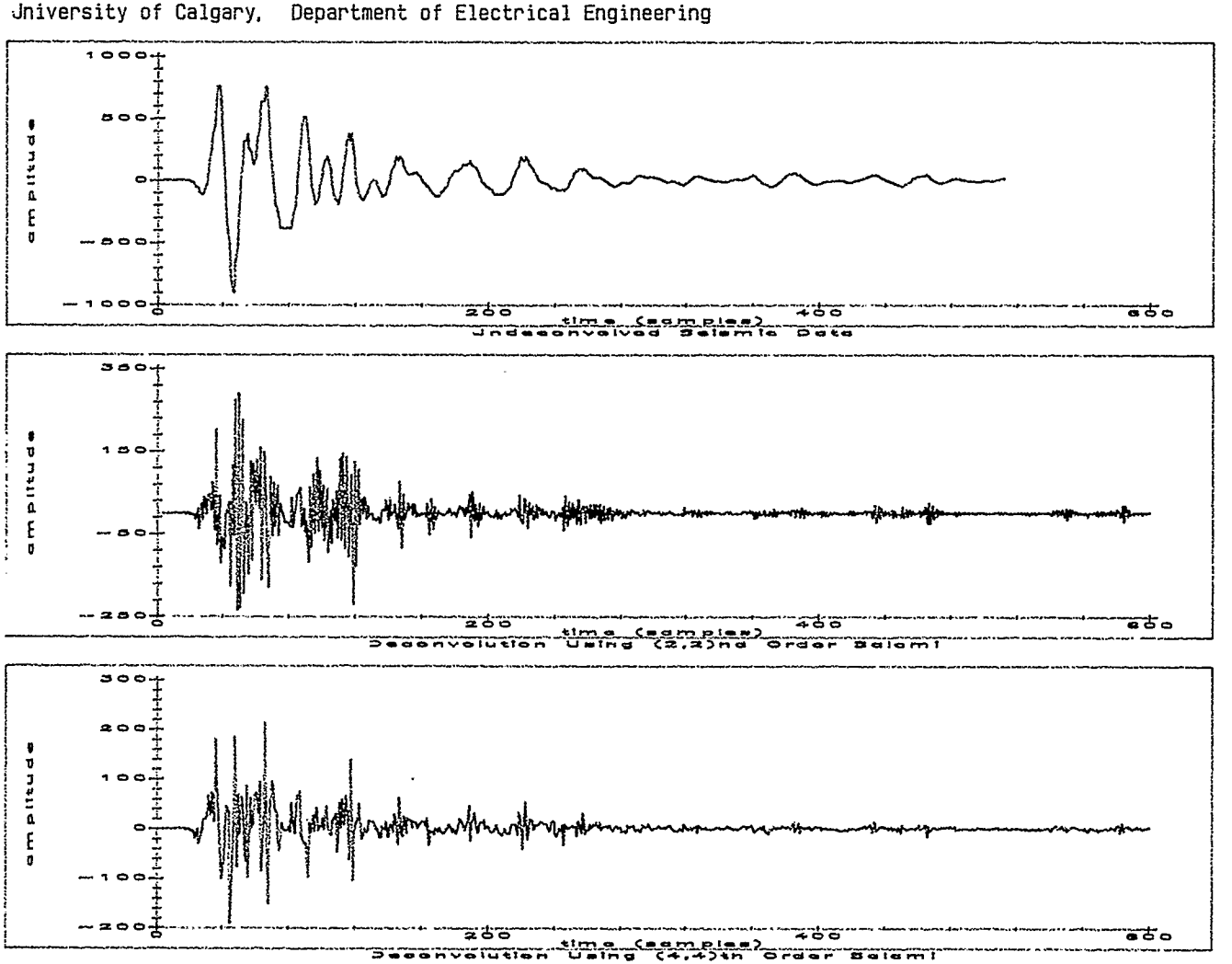

Figure 5.26 SALAMI DECONVOLUTION (2,2) AND (4,4)

Chapter 6. Conclusions

Arguments are developed for the preferred representation of seismic data by ARMA (p,q) models. ARMA (p,q) modelling techniques are applied to both real and synthetic seismic data and the results of spectral fitting and deconvolution compared with those of AR (p) techniques. The superiority of ARMA (p,q) representation is recognized in theory but not realized in practice, principally because the MA and AR components of the seismic signal cannot be separated in the modelling process. The improvement achieved by introducing MA (q) terms is negligible except in fitting the seismic spectrum where it rolls off to low to signal noise. Deconvolution with ARMA (p,q) models, therefore, yields noisy results without otherwise improving on AR (p) techniques. Oversampling is found to necessitate higher order models; the consequences of decimation and demodulation are demonstrated.

Seismic data is shown to be ARMA (p,q) with the AR (p) component comprising reverberatory (multiple) information and the MA (q) component comprising primary reflection information and earth filtering effects. The AR (p) nature of the reverberations and the MA (q) nature of the primary reflections are developed in Chapter 2 from the work of Silvia and Robinson on the communication theory description of wave propagation in layered media [1].

The MA (q) nature of the earth filtering process is developed in Chapter 4 from the work of Ricker on wave propagation in visco-elastic media [43]. The ARMA (p,q) description of seismic data has serious implications on the viability of deconvolution. Necessarily the convolutional model of the seismic trace as a wavelet convolved with a primary reflection coefficient series is inadequate; either the wavelet or the primary reflectivity series must incorporate reverberations. Deconvolution as practiced in the geophysical industry fails to accomplish realization of the primary reflection coefficients because traditional methods target wavelet spiking and dereverberation independently.

Recognizing the problem posed by ARMA (p,q) representation, however, is not the same as resolving it. In practise, the seismic data is not found to be separable into its AR (p) and MA (q) components, consequently, ARMA (p,q) models fit the composite seismic data in much the same way as the traditional methods, with AR (p) contributions dominating. The problem is the complex nature of the reverberatory AR (p) part which has the appearance of randomness and is therefore not distinguished from the white noise excitation series. Furthermore, the MA (q) component is expected to be long and decaying such that it is well represented by a low order AR process.

The inseparability of MA (q) and AR (p) components and recognized AR (p) dominance renders the supposed benefit of finite wavelet phase specification conferred by ARMA (p,q) models essentially ineffective. Meaningful phase modification through finite options is only achievable if the MA (q) contribution is strong and has sufficient roots. Swapping roots out of the unit circle can still be accomplished with the AR (p) components when they are inverted for deconvolution, but such is true of traditional techniques.

Results in Chapter 5 illustrate that spectral fitting seismic data with ARMA (p,q) models yields marginally improved fits at lower orders when compared with AR (p) methods, particularly at the low and high ends of the seismic spectrum where signal rolls off to noise. Because of lower signal to noise ratios in these areas the improved fit proves to be a mixed blessing; deconvolutions based on ARMA (p,q) fits provide a strong, theoretically correct, compensatory boost to the low S/N portions of the spectrum. The poorer fit of the AR (p) methods has the consequence of limiting boost to these frequencies.

The ARMA (p,q) techniques of both Kay and Salami are fairly robust for seismic data. Both methods are sensitive with increasing model orders, however, and badly overspike the data

yielding ringing time domain responses unsuitable for seismic interpretation. The Transient Error Method of Nichols [62, 70] does not share this problem, and is the most robust of the techniques tested. The tendency to overspike is also characteristic of the Burg and Least Squares AR (p) techniques. The Cadzow ARMA (p,q) procedure fails at all orders yielding negative spectral estimates.

Levinson provides the closest spectral fits in good signal areas and makes least attempt at fitting noise, making it the winner and still champion of seismic modelling methods. An earlier comparison of deconvolution techniques (not including ARMA (p,q) methods) resulted in a similar conclusion [55].

Oversampling of seismic data forces the models to fit the roll off to the non-signal portion of the spectrum. Since the roll off is the dominant magnitude contrast of the spectrum, the models preferentially expend order in characterizing it.

Much higher orders are required, therefore, to yield fits comparable with those on minimally sampled data. High orders not only overspike data in the signal portion of the spectrum, they overfit the noise. The problem of overfitting noise is particularly acute with ARMA (p,q) methods.

Seismic data is typically oversampled. To alleviate oversampling effects both decimation and decimation followed by demodulation were applied to the oversampled seismic data. As expected, lower model orders were found to yield better spectral fits with less overspiking. Demodulation was particularly effective in allowing better low order fits.

1. Silvia, M.T., and Robinson, E.A., 1979, *Deconvolution of Geophysical Time Series in the Exploration for Oil and Natural Gas*: Elsevier Scientific Publishing Company, Amsterdam, 251 pages.

2. Sheriff, R.E., and Geldart, L.P., 1982, *Exploration Seismology Volume I*: Cambridge University Press, Cambridge, 253 pages.

3. Jans, K. (I.B.M. Sales), pers. comm.

4. Robinson, E.A., 1985, Seismic time-invariant convolutional model, *Geophysics* 50, 2742-2751.

5. Childers, D.G., (ed.), 1978, *Modern Spectrum Analysis*: John-Wiley & Sons, New York, 334 pages.

6. Kay, S.M., and Marple, S.L., 1981, Spectrum Analysis - A Modern Perspective: *Proc. IEEE* 69, 1380-1419.

7. Box, G.E.P., and Jenkins, G.M., 1976, *Time Series Analysis: Forecasting and Control*: Holden-Day, San Francisco, 575 pages.

8. Cadzow, J.A., 1980, High Performance Spectral Estimation - A New ARMA Method: *IEEE Trans. ASSP* 28, 524-529.

9. Gutowski, P.R., Robinson, E.A., and Treitel, S., 1978, Spectral Estimation: Fact or Fiction: *IEEE Trans. GE* 16, 80-84.

10. Salami, M.J.E., 1984, Improved ARMA Spectral Estimation, Method: Unpublished paper, Department of Electrical Engineering, University of Calgary, Calgary.

11. Robinson, E.A., and Treitel, S., 1980, *Geophysical Signal Analysis*: Prentice-Hall, Inc., Englewood Cliffs, N.J., 466 pages.

12. Waters, K.H., 1978, *Reflection Seismology*: John Wiley & Sons, New York, 377 pages.

13. Grant, F.S., and West, G.F., 1965, *Interpretation Theory in Applied Geophysics*: McGraw-Hill, New York, 584 pages.

14. Ewing, W.M., Jardetzky, W.S., and Press, F., 1959, *Elastic Waves In Layered Media*: McGraw-Hill, New York.

15. Aki, K., and Richards, P.G., 1980, *Quantitative Seismology Theory and Methods, Vol. I*: W.H. Freeman, San Francisco.

16. Robinson, E.A., 1954, Predictive Decomposition of Time Series with Application to Seismic Exploration: Ph.D. Thesis, Massachusetts Institute of Technology, Cambridge, Mass., Reprinted 1967 in *Geophysics* 32, 418-484.

17. Wuenschel, P.C., 1960, Seismogram Synthesis Including Multiples and Transmission Coefficients: *Geophysics* 25, 106-129.

18. Sherwood, J.W.C., and Trorey, A.W., 1965, Minimum Phase and Related Properties of the response of a Horizontally Stratified Absorptive Earth to Plane Acoustive Waves: *Geophysics* 30, 191-197.

19. Peterson, R.A., Fillipone, W.R., and Coker, F.B., 1955, The Synthesis of Seismograms from Well Log Data: *Geophysics* 27, 516-538.

20. Geoquest, 1979, *Seismic Data Processing: Course Notes*: Geoquest, Houston.

21. Treitel, S., And Robinson, E.A., 1966, Seismic Wave Propagation in Layered Media in Terms of Communication Theory: *Geophysics* 31, 17-32.

22. Kanasewich, E.R., 1975, *Time Sequence Analysis in Geophysics*: The University of Alberta Press, Edmonton, 364 pages.

23. Graul, M., 1985, *Seismic Processing Deconvolution*: Exploration Education Consultants, Houston, unnumbered.

24. White, R.E., and O'Brien, P.M.S., 1974 Estimation of the Primary Seismic Pulse: *Geophysical Prospecting* 22, 627-651.

25. Vaage, S., Haugland, K., and Utheim, T., 1983, Signatures from Single Airguns: *Geophysical Prospecting* 31, 87-97.

26. Carrol, P., 1972, Signature Deconvolution for Marine Seismic Reflection Surveys: *CSEG Journal* 8, 41-51.

27. Stone, D.G., 1979, Pulse Shaping Methods, in Fitch, A.A. (ed.), *Developments in Geophysical Exploration Methods - 1*: Applied Science Publishers Ltd., London, 239-270.

28. Lindsey, P., Niedell, N., and Hilterman, F., 1975, Interpretative Uses of Seismic Modelling with Emphasis on Stratigraphy and Seismic Resolution: *SEG Preprint*, Tulsa, OK.

29. Hampson, D., and Galbraith, M., 1981, Wavelet Extraction by Sonic Log Correlation: *CSEG Journal* 17, 24-42.

30. Oppenheim, A.V., and Schafer, R.W., 1975, *Digital Signal Processing*: Prentice-Hall, Inc., Englewood Cliffs, N.J., 585 pages.

31. Ulrych, T.J., 1971, Application of Homomorphic Deconvolution to Seismology: *Geophysics* 36, 650-660.

32. Stoffa, P.L., 1974, The Application of Homomorphic Deconvolution to Shallow Water Marine Seismology Part I: *Geophysics* 39, 401-416.

33. Tribolet, J.M., 1978, *Seismic Applications of Homomorphic Signal Processing*: Prentice-Hall, Englewood Cliffs, N.J.

34. Tribolet, J.M., 1978, Application of Short-Time Homomorphic Signal Analysis to Seismic Wavelet Estimation in Chen, C.H. (ed.), *Computer-Aided Seismic Analysis and Discrimination: Geoexploration* 16, 76-96.

35. Mendel, J.M., 1983, *Optimal Seismic Deconvolution*: Academic Press, Inc., New York, N.Y., 407 pages.

36. Robinson, E.A., 1976, Dynamic Predictive Deconvolution, *Geophysical Prospecting* 23, 780-798.

37. Robinson, E.A., 1978, Iterative Identification of Non-Invertible Autoregressive Moving-Average Systems with Seismic Applications in Chen, C.H. (ed.), *Computer-Aided Seismic Analysis and Discrimination: Geoexploration* 16, 1-19.

38. Gutowski, P.R., and Frisillo, A.L., 1981, ARMA Processing of Ultrasonic Data for Absorption Measurements: *Geophysical Prospecting* 29, 241-259.

39. Hubral, P., Treitel, S., And Gutowski, P.R., 1980, A Sum Autoregressive Formula for the Reflection Response: *Geophysics* 45, 1697-1705.

40. Ricker, N., 1940, The Form and Nature of Seismic Waves and the Structure of Seismograms: *Geophysics* 5, 348-366.

41. Ricker, N., 1944, Wavelet Functions and their Polynomials: *Geophysics* 9, 314-323.

42. Ricker, N., 1953, The Form and Laws of Propagation of Seismic Wavelets: *Geophysics* 18, 10-40.

43. Ricker, N.H., 1977, *Transient Waves in Visco-Elastic Media*: Elsevier Scientific Publishing Co., New York, 278 pages.

44. Cadzow., J.A., 1980, ARMA Spectral Estimation: A Model Equation Error Procedure: *Proc. IEEE ASSP ICASSP* 80, Denver, CO., 589-602.

45. Cadzow, J.A., and Moses, R.L., 1981, A Superresolution Method of ARMA Spectral Estimation: *Proc. IEEE ASSP ICASSP* 81, Atlanta, GA., 484-487.

46. Cadzow, J.A., 1983, ARMA Time Series Modelling: An Effective Method: *IEEE Trans. AES* 19, 49-58.

47. Moses, R.L., 1980, *An Iterative Algorithm for ARMA Spectral Estimation*: M.Sc. Thesis, Virginia Polytechnic Institute and State University, Blacksburg, VA., 75 pages.

48. Pao, Y-H., and Lee, D.T., 1981, Additional Results on the Cadzow ARMA Method for Spectrum Estimation: *Proc. IEEE ASSP ICASSP* 81, Atlanta, GA., 480-483.

49. Ogino, K., 1981, *Computationally Fast Algorithms for ARMA Spectral Estimation*: Ph.D. Thesis, Virgina Polytechnic Institute and State University, Blacksburg, VA., 181 pages.

50. Cadzow, J.A. and Ogino, K., 1981, Adaptive ARMA Spectral Estimation: *Proc. IEEE ASSP ICASSP* 81, Atlanta, GA., 475-479.

51. Kay, S.M., 1980, A New ARMA Spectral Estimator: *IEEE Trans. ASSP* 28, 585-588.

52. Treitel, S., Gutowski, P.R., and Robinson, E.A., 1977, Empirical Spectral Analysis Revisited, in Miller, J.J.H. (ed.), *Topics in Numerical Analysis* III: Academic Press, London, 429-446.

53. Robinson, E.A., 1979, Iterative Least-Squares Procedure for ARMA Spectral Estimation, in Haykin, S. (ed.), *Topics in Applied Physics Volume 34: Nonlinear Methods of Spectral Analysis*: Springer-Verlag, Berlin.

54. Rabiner, L.R. and Gold, B., 1975, *Theory and Application of Digital Signal Processing*: Prentice-Hall, Inc., Englewood Cliffs, N.J., 762 pages.

55. Jerkevics, A. and Wiggins, R., 1984, A Critique of Seismic Deconvolution Methods: *Geophysics* 49, 2109-2116.

56. Powers, D.W., 1984, Order and Randomness in Sedimentary Sequences (abstract only): *AAPG Bulletin* 68, 519.

57. Bendat, J.S., and Piersol, A.G., 1971, *Random Data: Analysis and Measurement Procedures*: Wiley-Interscience, New York, N.Y., 407 pages.

58. Jenkins, G.M. and Watts, D.G., 1968, *Spectral Analysis and its Applications*: Holden-Day, Inc., San Francisco, 525 pages.

59. Schoenberger, M. and Levin, F.K., 1979, *The Effect of Subsurface Sampling on One-Dimensional Synthetic Seismograms:* Geophysics 44, 1813-1829.

60. Hosken, J.W.J., 1980, A Stochastic Model of Seismic Reflections: *SEG Preprint*, Tulsa, OK.

61. Rietsch, E., 1983, What is the Color of Reflection Coefficient Series? (abstract only): *Geophysics* 49, 648

62. Nichols, S.T., Smith, M.R., and Salami, M.J.E., 1985 in Barker, H.A., and Young, P.C., (eds.), *IFAC Identification and System Parameter Estimation,* 1985, York, U.K., 1473-1478.

63. Sheriff, R. E., and Geldart, L.P., 1982, *Exploration Seismology Volume II:* Cambridge University Press, Cambridge, 221 pages.

64. Claerbout, J.F., 1976, *Fundamentals of Geophysical Data Processing:* McGraw-Hill, New York, N.Y., 274 pages.

65. Ziolkowski, A., 1984, *Deconvolution:* IHRDC Publishers, Boston, MA., 175 pages.

66. Salami, M.J.E., 1985, *Application of ARMA Models in Multicomponent Signal Analysis,* Ph.D. Thesis, University of Calgary, Calgary, Alberta.

67. Ziolkowski, A., 1987, *The Determination of the Far-Field Signature of an Interacting Array of Marine Seismic Sources from Near-Field Measurements - Results from the Delft Air-Gun Experiment,* First Break Vol. 5, No. 1, 15-29.

68. Buttkus, B., 1975, *Homomorphic Filtering - Theory and Practice,* Geophysical Prospecting 23, 712-748.

69. Wiggins, R., 1985, *Entropy Guided Deconvolution,* Geophysics 50, 2720-2726.

70. Smith, N.R., Nichols, S.T., Henkelman, R.M., and Wood, M.L., 1986, *Application of Autoregressive Moving Average Parametric Modelling in Magnetic Resonance Image Reconstruction,* IEEE Trans. on Medical Imaging, Vol. MI-5, No. 3, 132-139.

Appendix A. Statistics of Reflection Coefficient Series

A.1 Introduction

The assumption that reflection coefficient series are stationary with randomly occurring amplitudes conforming to a Gaussian probability density distribution is implicit in many deconvolution routines - including the ARMA deconvolution routines described in this report [55]. Measurements from well log data, however, indicate that reflection coefficients are neither Gaussian distributed nor random [56]. This appendix illustrates some statistics of reflection coefficient series and considers the implications of deviation from the Gaussian-random assumption on deconvolution routines.

A.2 Theory

Recall the convolutional model for seismic data

$$s(n) = w(n)*r(n)$$

$$= \sum_{k=-\infty}^{\infty} r(k)w(n-k)$$

The convolutional model is obviously a linear time-invariant system. Seismic data is therefore a statistical time series generated by a linear operation on the reflection coefficient series r(n), which can be written as follows

$$s(n) = A\{r(n)\}$$

where A is the linear time invarient operator acting on the term inside the brackets { }.

If r(n) is a random process then the process of taking expected values is commutative with the linear operation [57]. That is

$$E\{s(n)\} = E\{A\{r(n)\}\} = A\{E\{r(n)\}\}$$

where E{ } denotes the expectation operation.

This commutative property fosters two important results [57]:

1. If r(n) is a stationary random process then s(n) will also be a stationary random process.

2. If r(n) exhibits a Gaussian distribution then s(n) will also exhibit a Gaussian distribution.

Two further results from probability theory are pertinent to the discussion:

3. A stochastic time series can be completely characterized by its autocovariance and mean if and only if the series is stationary and has a Gaussian probability density function [57, 58].

4. A stochastic time series which is the output of a linear process can be described by the parameters of the linear process if and only if the series is Gaussian-stationary [58].

Result 3 requires that all deconvolution routines based on the auto-correlation of seismic data pre-suppose stationary Gaussian data. Result 4 is merely a corollary to 3 specific to explicit linear modelling deconvolution techniques such as AR, MA, and ARMA.

Given, therefore, that most of the deconvolution routines described herein require that the seismic data s(n) be Gaussian and stationary it follows from results 1 and 2 that the reflection coefficient series r(n) be Gaussian and stationary.

A further requirement of most deconvolution routines is that the spectrum of the reflection coefficient series be white.

$$S(f) = W(f)R(f)$$

If R(f) is white, that is R(f) = k where k is some constant, then

$$S(f) = W(f)k \qquad \text{A.1}$$

The spectral shape of the seismic data, therefore, can be attributed to the filtering effect of the seismic wavelet alone. Deconvolution, then, attempts to whiten the spectrum of the seismic data assuming that in doing so only the wavelet spectrum is modified.

That is, the deconvolution operator g(n) is designed such that

$$S(f)G(f) = k \; ; \; G(f) = [W(f)]-1$$

where S(f) is as defined in equation A.1.

A.3 Measurements

Reflection coefficients were determined from eighteen wells in Northern Alberta in the vicinity from which the seismic data used in this report were collected. Velocity logs from each well were digitized at .3 m and then mapped from depth to time and resampled at .002 s. Reflection coefficients were then calculated using equation 2.20 in time and ignoring density variations.

That is

$$r(n) = \frac{v(n) - v(n-1)}{v(n) + v(n-1)}$$

The choice of .002 s time sampling was arbitrary. The .3 m depth sampling maps to .0002 s time sampling in even the slowest sedimentary rock. Schoenberger and Levin [59] argue for finest possible sampling of reflection coefficient series (<.0005 s) based on their observations of the sensitivity of calculated earth transmission filters to sample rate. Hosken [60] and Rietsch [61], however, report that the statistics of reflection coefficient series appear to be scale invariant.

The reflection coefficients in time for the eighteen wells are shown in figure A.1. Their corresponding power spectra are shown in figure A.2.

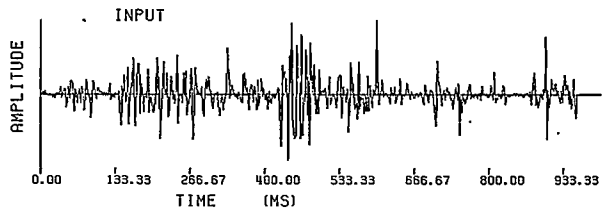

1

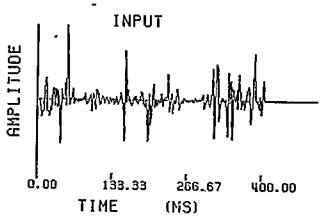

2

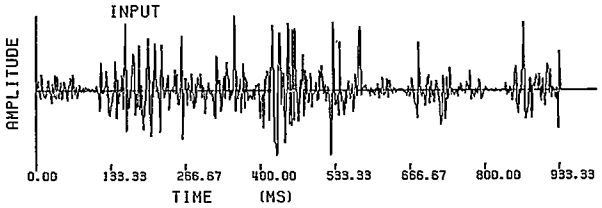

3

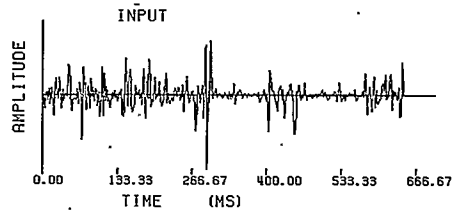

4

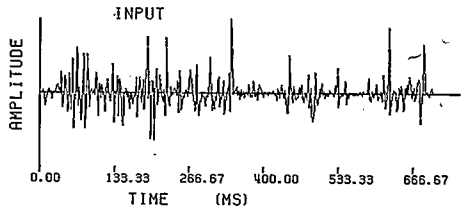

5

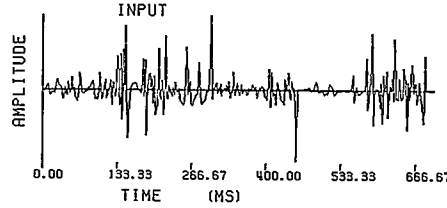

6

Figure A.1 REFLECTION COEFFICIENTS IN TIME

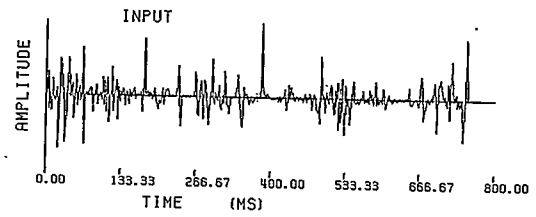

7

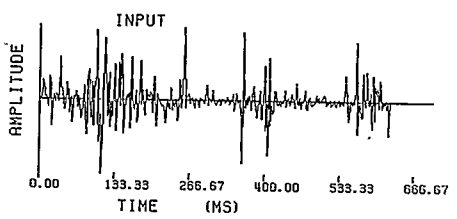

10

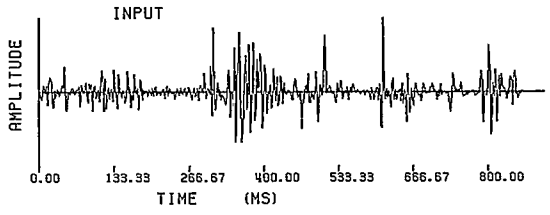

8

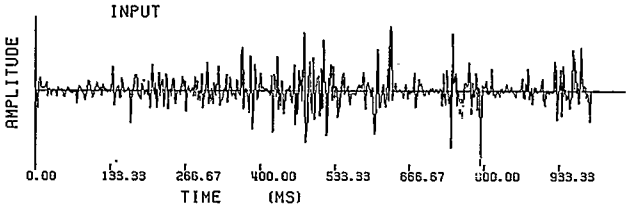

11

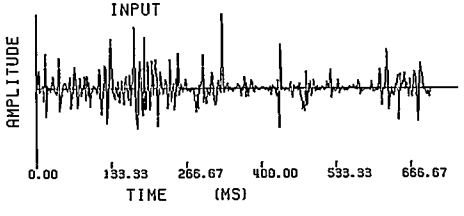

9

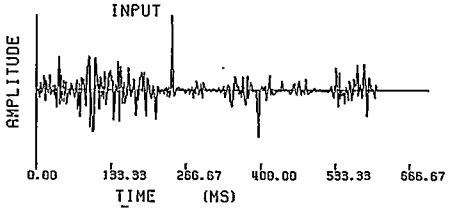

12

Figure A.1 (cont.)

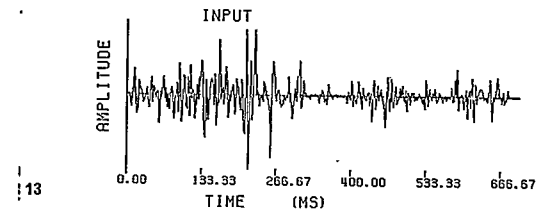

13

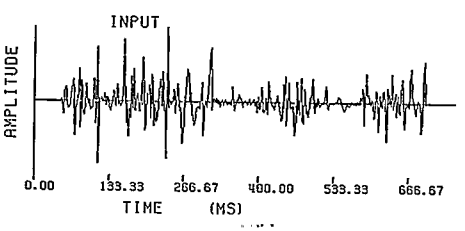

14

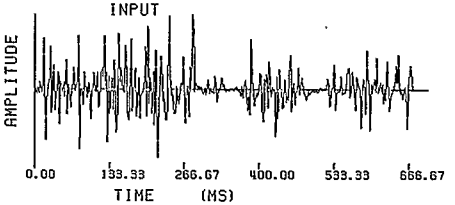

15

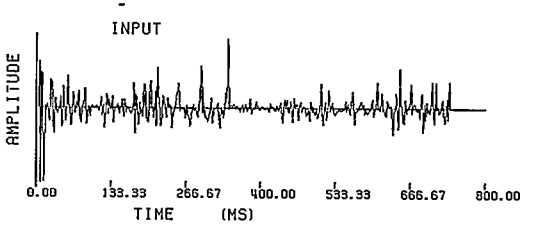

16

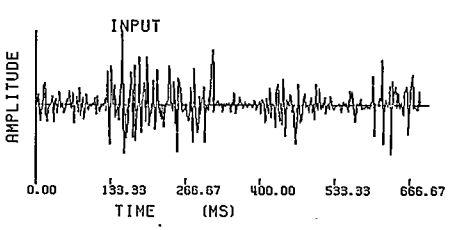

17

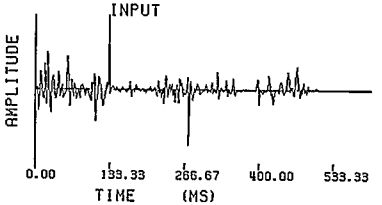

18

Figure A.1 (cont. 2)

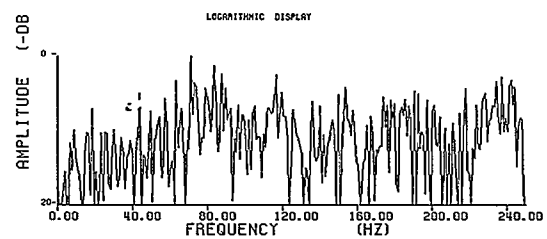

1

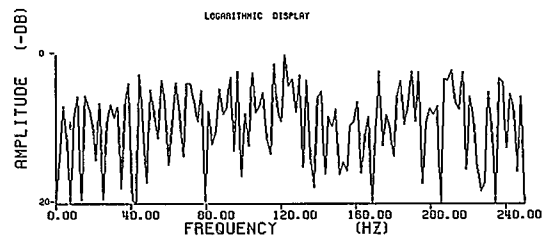

2

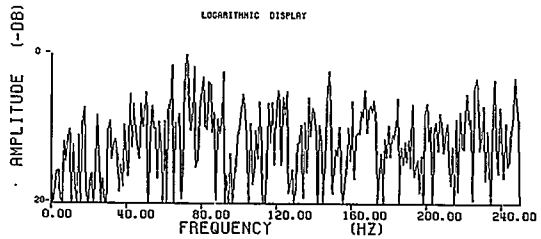

3

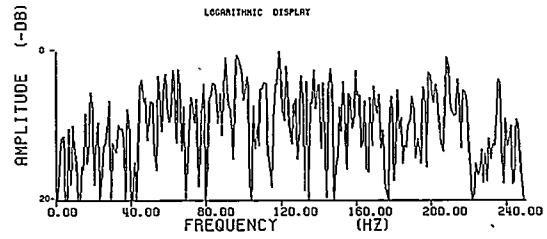

4

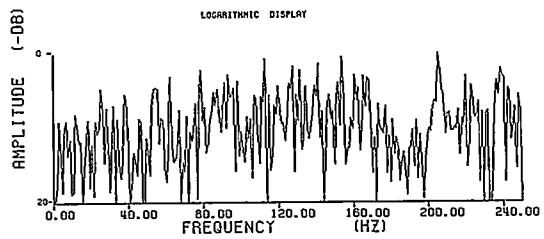

5

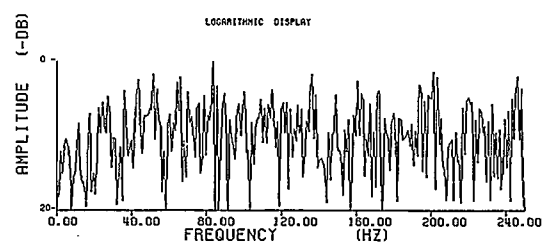

6

Figure A.2 POWER SPECTRA OF REFLECTION COEFFICIENTS

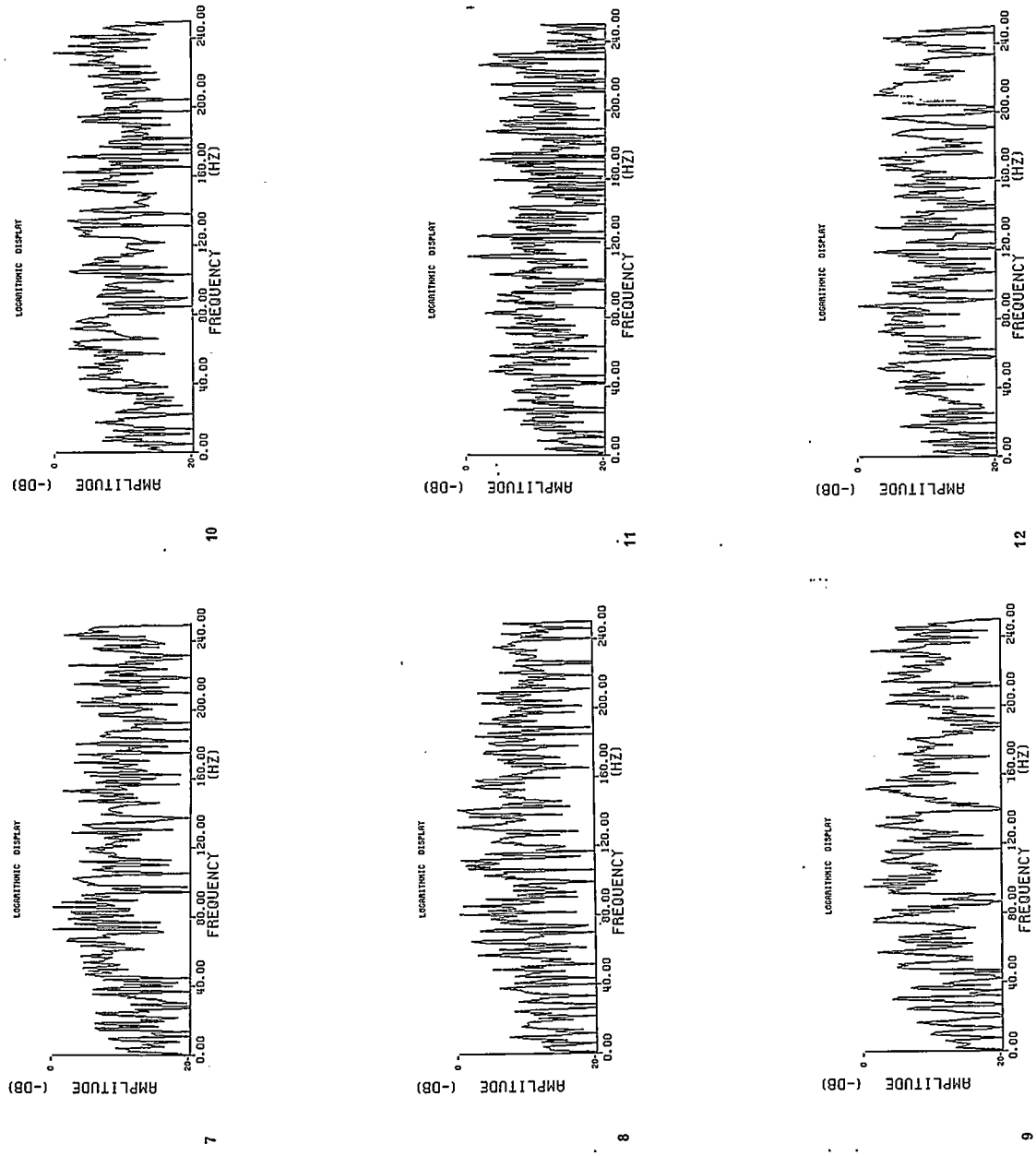

Figure A.2 (cont.)-

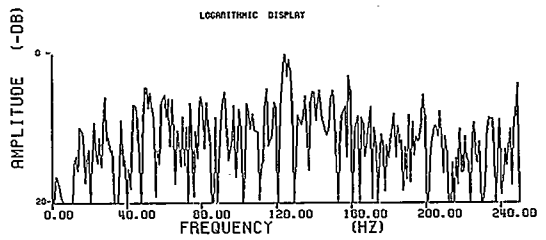

13

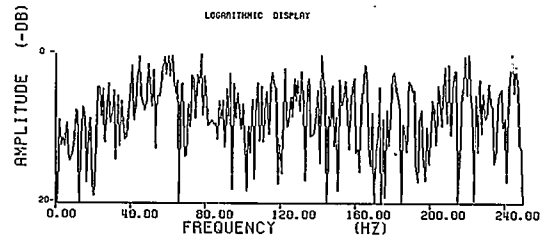

14

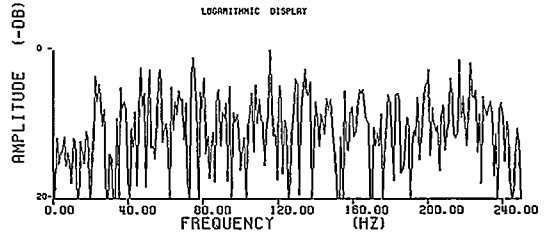

15

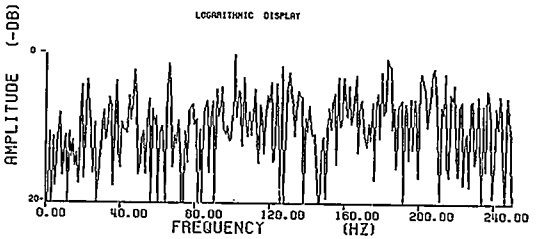

16

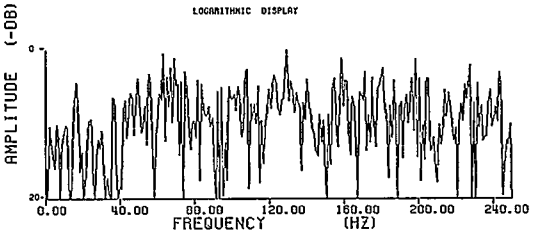

17

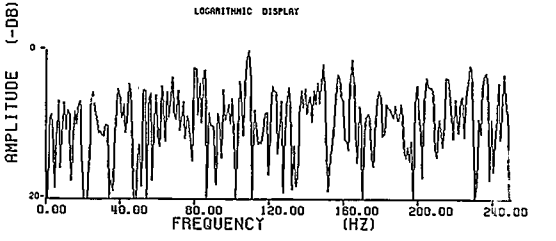

18

Figure A.2 (cont. 2)

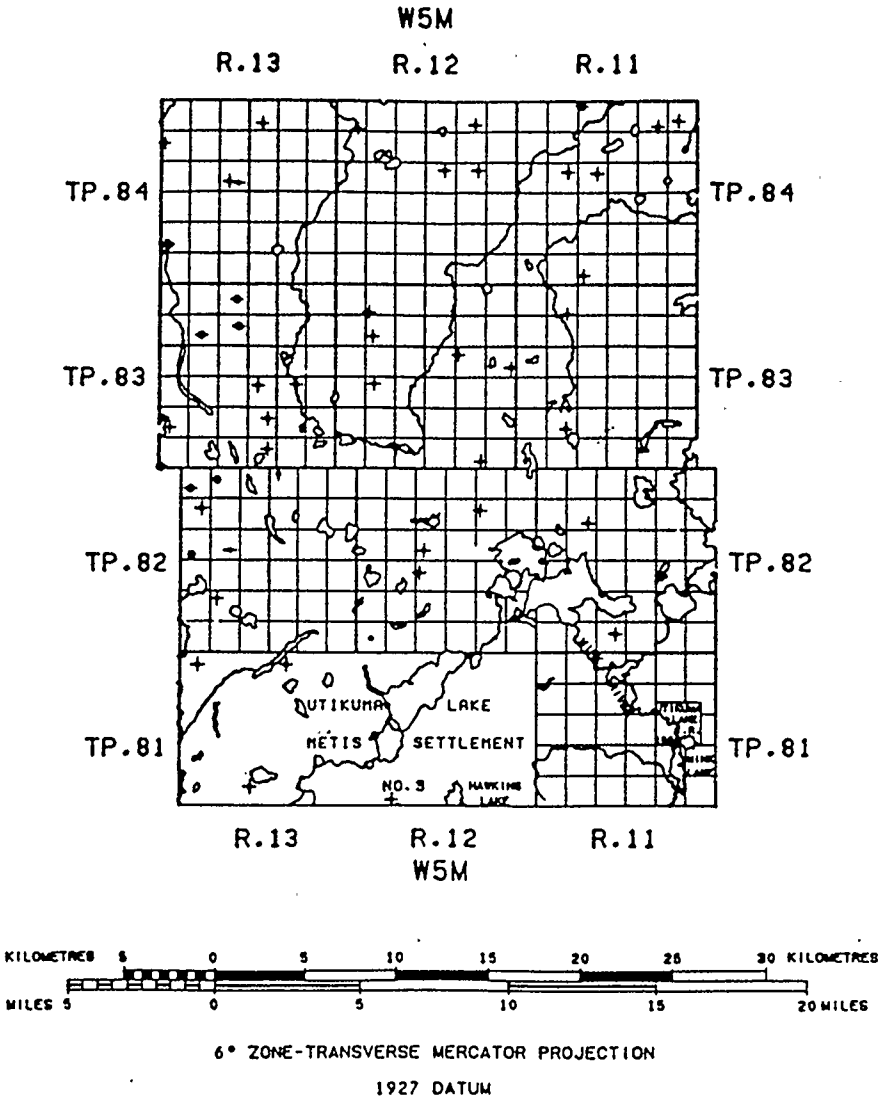

Figure A.3 LOCATION MAP FOR WELLS USED IN MEASUREMENTS